Stability of Periodic Waves in Nonlocal Dispersive Equations

By

Kyle Claassen

Submitted to the Department of Mathematics and the
Faculty of the Graduate School of the University of Kansas
in partial fulfillment of the requirements for the degree of

Doctor of Philosophy

Committee members

Mathew Johnson, Chairperson

Dionyssios Mantzavinos

Agnieszka Międlar

Milena Stanislavova

Timothy Jackson

Date defended: May 8, 2018

The Dissertation Committee for Kyle Claassen certifies
that this is the approved version of the following dissertation:

Stability of Periodic Waves in Nonlocal Dispersive Equations

Mathew Johnson, Chairperson

Date approved: May 8, 2018

# Abstract

In this work consisting of joint projects with my advisor, Dr. Mathew Johnson, we study the existence and stability of periodic waves in equations that possess *nonlocal dispersion*, i.e. equations in which the dispersion relation between the temporal frequency $\omega$ and wavenumber $k$ of a plane wave $(x,t) \mapsto e^{i(kx-\omega t)}$ is *not* of the form $\omega(k) = p(ik)$ where $p$ is a polynomial. In models that involve only classical derivative operators (known as *local* equations), the behavior of the system at a point is influenced solely by the behavior in an arbitrarily small neighborhood. In contrast, equations involving nonlocal operators incorporate long-range interactions as well. Such operators appear in numerous applications, including water wave theory and mathematical biology.

Specifically, we establish the existence and nonlinear stability of a special class of periodic bound state solutions of the *Fractional Nonlinear Schrödinger Equation*, where the nonlocality of the fractional Laplacian presents formidable analytical challenges and elicits the development of functional-analytic tools to complement the absence of more-understood techniques commonly used to analyze local equations.

Further, we use numerical methods to survey the existence and spectral stability of small- and large-amplitude periodic wavetrains in *Bidirectional Whitham water wave models*, which implement the exact (nonlocal) dispersion relation of the incompressible Euler equations and are thus expected to better capture high-frequency phenomena than the unidirectional Whitham and Korteweg-de Vries (KdV) equations.

# Acknowledgements

As I conclude my career as a graduate student, I find myself reflecting on the abundance of people who have positively influenced my life and without whom I never would have gotten this far. They are simply too numerous to adequately recognize here. Nevertheless, I want to acknowledge a small handful of individuals who significantly shaped my development during my time at the University of Kansas.

First, I wish to thank my dissertation committee for taking the time to review my work in addition to their many other responsibilities. In particular, I owe a great debt of gratitude to my Ph.D. advisor, Dr. Mathew Johnson. I am proud to be his first Ph.D. student, and I truly cannot imagine a more patient and supportive guide through the rigors of academia. I look up to him as a model scholar, teacher, and all-around good person. (He never even made me wash his car!) I am also thankful for his financial support as a research assistant during summers and for travel funding to conferences, which would have been difficult to attend otherwise. He was also instrumental in my successful academic job search, which ultimately makes my efforts feel all the more worthwhile.

I also want to thank the KU Department of Mathematics for its financial support and the opportunity to be a graduate teaching assistant every semester. I have grown a great deal through these teaching experiences–professionally, personally, and in my understanding of mathematics.

I am sincerely appreciative of Bennet Goeckner and Peter Lewis, my friends and fellow graduate students, for all the helpful discussions and friendly banter over the years. We weathered the trials of graduate school together, made it out alive, and I hope we keep in touch as we go our separate ways. Additional thanks to Bennet for sharing his pop tarts.

Most of all, I am incredibly blessed to have a stable and supportive family. I am especially indebted to my parents, Robert and Shelley, my brother, Kevin, and sister-in-law, Michelle, for enduring my frequent despairing and venting of frustrations. I very well may have given up altogether if not for their constant reassurance. I love them all very much. They are partially to blame for supporting my questionable life choice to attend graduate school in the first place, but I suppose they're off the hook now that things are finally coming together. :)

# Contents

# Chapter 1

# Background and Overview

As an overarching theme, in this work we will examine the stability of periodic waves in nonlocal dispersive equations. Here, *dispersion* refers to the phenomenon in which waves of different frequencies travel at different speeds. For example, consider the classical linear *transport equation*

$$u_t + cu_x = 0, \quad u = u(x,t),$$

which provides a simple translational model of mass transport. One can easily verify that this system admits *plane wave* solutions of the form

$$u(x,t) = Ae^{i(kx-\omega t)}, \quad A \in \mathbb{R} \tag{1.1}$$

when $c = \omega/k$, which is interpreted as the wave speed of (1.1). This is readily seen when (1.1) is expressed in traveling wave form:

$$u(x,t) = Ae^{ik(x-ct)}, \quad c = \frac{\omega}{k}.$$

In this example, we write $\omega(k) = ck$, where this relationship between the plane wave's temporal frequency $\omega$ as a function of its wavenumber $k$ is referred to as the *dispersion*

*relation* of the PDE. Moreover, we define the *linear phase speed* $c(k) := \omega(k)/k$. Per these relationships, we see that waves of different wavenumber $k$ (in correspondence with the frequency of the wave) will indeed propagate at different speeds $c(k)$.

The dispersion relation varies from equation to equation. For example, upon substituting the plane wave ansatz (1.1) into the linearized *Korteweg-de Vries* equation

$$u_t + u_x + \frac{1}{6}u_{xxx} = 0,$$

we obtain the following dispersion relation and linear phase speed, respectively:

$$\omega(k) = k - \frac{1}{6}k^3, \quad c(k) = k - \frac{1}{6}k^2.$$

We say that an equation has *local dispersion* if the dispersion relation is of the form $\omega(k) = p(k)$, where $p$ is a polynomial. This is often the case, as equations involving only classical derivative operators $\partial_x^j$ will possess polynomial dispersion relations. However, equations involving *nonlocal* operators (e.g. integral operators) that incorporate long-range interactions across the entire spatial domain will have non-polynomial dispersion relations. We will examine a few such equations.

In particular, in Chapter 2 we study the existence and nonlinear, *orbital stability*, i.e. stability modulo translation and phase symmetries, of $T$-antiperiodic *standing waves* $(x,t) \mapsto e^{i\omega t}\phi(x)$ in the *Fractional Nonlinear Schrödinger Equation* (fNLS)

$$iu_t - \Lambda^\alpha u + \gamma |u|^{2\sigma} u = 0, \quad x,t \in \mathbb{R}$$

where $u = u(x,t)$ is generally complex-valued and $\Lambda^\alpha := (-\partial_x^2)^{\alpha/2}$ is the nonlocal *fractional Laplacian* operator defined through Fourier multipliers:

$$\widehat{\Lambda^\alpha f}(n) = \left|\frac{\pi n}{T}\right|^\alpha \widehat{f}(n), \quad n \in \mathbb{Z}.$$

Guided by what is known in the local case $\alpha = 2$ (where fNLS becomes the *Classical Nonlinear Schrödinger Equation*), we roughly follow a standard program of demonstrating the existence and stability of constrained energy minimizers, where existence is obtained through variational methods and stability is shown as a consequence of the *nondegeneracy* of the Hessian of the Lagrangian functional; that is, we show that the kernel of the Hessian evaluated at the antiperiodic standing wave profile is spanned precisely by eigenfunctions obtained by differentiating with respect to translation and phase symmetries in the governing PDE. The techniques typically used to show nondegeneracy of the Hessian do not apply in the genuinely nonlocal setting $\alpha \in (1,2)$, hence suitable replacement theories must be developed. In Section 1.1.1, we review the variational methods used to find solutions of the classical Nonlinear Schrödinger Equation as constrained minimizers of an energy functional, and in Section 1.1 we review the definitions and techniques relevant to the stability of waves in Hamiltonian systems.

In Chapter 3, we numerically survey the existence and spectral stability of a class of periodic traveling waves in several *Bidirectional Whitham* shallow water models, e.g.

$$\begin{cases} u_t &= -\eta_x - uu_x \\ \eta_t &= -\mathcal{K}u_x - (\eta u)_x, \end{cases}$$

where $u$ is a fluid velocity (more specifically, the trace of the velocity potential at the free surface of the wave), $\eta$ is the wave surface's displacement from the undisturbed water

depth, and the nonlocal operator $\mathcal{K}$ is defined through Fourier multipliers as

$$\widehat{\mathcal{K}f}(n) := \frac{\tanh(n)}{n}\,\widehat{f}(n), \quad n \in \mathbb{Z}.$$

In contrast with other popular shallow water models such as the *Korteweg-de Vries equation* (KdV) and the *unidirectional Whitham equation* (see Section 1.2.1), these Bidirectional Whitham models possess the exact (non-dimensionalized) dispersion relation

$$(\omega(k))^2 = k\tanh(k)$$

of the extremely general *incompressible Euler equations* and are thus expected to better capture high-frequency phenomena than the KdV and the unidirectional Whitham models, whose dispersion relations approximate but do not match those of the full water wave model. Numerical approximations of solutions in the bidirectional Whitham models are obtained through continuation methods seeded by their local bifurcation theory, which is sketched in Section 1.2.2, and *Floquet's theorem* (see Section 1.2.3) forms the foundation for the numerical methods used to approximate the spectrum of the linearized equation about an equilibrium background wave.

## 1.1 Existence and Stability in Hamiltonian Systems

### 1.1.1 Variational Methods

In local equations, where equilibria possess an ODE structure, it is generally convenient to establish existence of equilibria via phase plane analysis. However, such structure is absent in the *Fractional Schrödinger Equation*, which will be studied in depth in Chapter 2. Here, we outline the process of establishing existence of solutions to a PDE through *variational*

*methods*, where solutions are found as critical points of a functional subject to constraint(s). Fortunately, this procedure does not rely on ODE structure and will be used heavily in the analysis of Chapter 2.

To illustrate such methods, consider the cubic, defocusing *Classical Nonlinear Schrödinger Equation* (NLS)

$$iu_t + u_{xx} - |u|^2 u = 0, \quad x,t \in \mathbb{R} \tag{1.2}$$

where $u$ is generally complex-valued, posed on the $L^2$-based Sobolev space

$$H^1(0,2T) := \left\{ u \in L^1_{\text{loc}}(0,2T) : \|u\|^2_{H^1(0,2T)} := \int_0^{2T} \left( |u|^2 + |u_x|^2 \right) dx < \infty \right\},$$

where $u_x$ is to be interpreted in the weak sense. Further, ansatz a spatially periodic *bound state* solution of the form

$$u(x,t) = e^{i\omega t}\phi(x), \quad \omega \in \mathbb{R}, \tag{1.3}$$

where the *profile* $\phi(x)$ is $2T$-periodic. Substituting (1.3) into (1.2), we obtain the *profile equation*

$$-\phi'' + \omega\phi + |\phi|^2 \phi = 0. \tag{1.4}$$

Now, NLS possesses the following conserved quantities, referred to as the *Hamiltonian energy* and *charge*, respectively:

$$\mathcal{H}(u) := \frac{1}{2}\int_0^{2T} \left( |u_x|^2 + \frac{1}{2}|u|^4 \right) dx, \quad Q(u) := \frac{1}{2}\int_0^{2T} |u|^2 \, dx.$$

Using these conserved quantities, consider the following minimization problem over real-valued functions in which the Hamiltonian energy is minimized subject to fixed charge

$\mu > 0$:

$$\phi = \operatorname*{argmin}_{u \in \mathcal{A}_\mu} \mathcal{H}(u), \quad \mathcal{A}_\mu := \{u : Q(u) = \mu\}. \tag{1.5}$$

We will use the following theorem regarding constrained minimizers:

**Theorem 1.1.1** (Lagrange multiplier theorem)**.** *Suppose that $\phi \in \mathcal{A}_\mu := \{u \in X : Q(u) = \mu\}$ is a local minimum (or maximum) of $\mathcal{H}|_{\mathcal{A}_\mu}$. If the Gâteaux derivative $d\mathcal{H}[\phi]$ exists at $\phi$ and is linear, and the Fréchet derivative $DQ(\phi)$ is not the zero map, then there exist $\omega \in \mathbb{R}$ such that*

$$d\mathcal{H}[\phi]v + \omega DQ(\phi)v = 0 \quad \textit{for all } v \in X.$$

So, provided such a $\phi$ exists per (1.5), then by the Lagrange multiplier theorem there exists $\omega \in \mathbb{R}$ such that

$$\delta\mathcal{H}(\phi) + \omega\,\delta Q(\phi) = 0, \tag{1.6}$$

which, when $c = 0$, is equivalent the profile equation (1.4). See Appendix A for a discussion of the *variational derivatives* $\delta\mathcal{H}$, $\delta Q$ in the generally fractional setting. In particular, $\alpha = 2$ corresponds to the classical case discussed here.

In order to show that such a $\phi$ exists in (1.5), first note that $\mathcal{H}$ is clearly bounded below (by zero), hence $\lambda := \inf_{u \in \mathcal{A}_\mu} \mathcal{H}(u)$ is well-defined and there exists a minimizing sequence $\{u_k\} \subset \mathcal{A}_\mu$ such that $\lim_{k\to\infty} \mathcal{H}(u_k) = \lambda$. Further, $\mathcal{H}$ and the constraint $Q \equiv \mu$ control the $H^1(0, 2T)$ norm for the sequence $\{u_k\}$:

$$\frac{1}{2}\|u_k\|^2_{H^1(0,2T)} \leq Q(u_k) + \mathcal{H}(u_k) = \mu + \mathcal{H}(u_k) \to \mu + \lambda \quad \text{as } k \to \infty,$$

hence $\{u_k\}$ is bounded in $H^1(0, 2T)$. Since the unit ball is not compact in $H^1(0, 2T)$, an infinite dimensional (Hilbert) space, we cannot a-priori extract a convergent subsequence

in $H^1(0,2T)$. However, the following theorem allows one to extract a convergent subsequence in the weak topology:

**Theorem 1.1.2** (Banach-Alaoglu)**.** *Let $\{u_k\}$ be a bounded sequence in a reflexive Banach space $X$. Then there exists $\phi \in X$ and a subsequence $\{u_{k_j}\} \subset X$ that converges to $\phi$ weakly in $X$.*

Since $H^1(0,2T)$ is a Hilbert space, it is reflexive, and we use the Banach-Alaoglu theorem to extract a candidate minimizer $\phi \in H^1(0,2T)$ which is the weak limit of a subsequence $\{u_{k_j}\}$. It is yet unclear whether $\phi \in \mathcal{A}_\mu$, i.e that $Q(u) = \mu$. However, by the following theorem, one can extract a further subsequence that converges strongly (i.e. in norm) to $\phi$ in $L^2(0,2T)$:

**Theorem 1.1.3** (Rellich-Kondrachov)**.** *If $s_1 > s_0$, then $H^{s_1}((0,T);\mathbb{C})$ is compactly embedded in $H^{s_0}((0,T);\mathbb{C})$.*

*(The statement given here is a special case of [1, Theorem 5.1] with $n = 1$, $p_0 = p_1 = 2$, $E_0 = E_1 = \mathbb{C}$, and $X = (0,T) \subset \mathbb{R}$.)*

Now, since strong convergence implies weak convergence and weak limits are unique, there exists a further subsequence $\{u_{k_j}\}$ such that $\|u_{k_j} - \phi\|^2_{L^2(0,2T)} \to 0$, which implies that $Q(u_{k_j}) \to Q(\phi)$. Thus $\phi \in \mathcal{A}_\mu$ is a *candidate* constrained minimizer of $\mathcal{H}$, and it remains to show that $\mathcal{H}(\phi) = \lambda := \inf_{u \in \mathcal{A}_\mu} \mathcal{H}(u)$. Since $H^1(0,T)$ is compactly embedded in $L^4(0,2T)$ by Sobolev embedding, there exists a further subsequence such that $P(u_{k_j})$ converges, and by the weak lower semicontinuity of the $L^4(0,2T)$ norm and the weak lower semicontinuity of the functional $u \mapsto \int_0^{2T} |u_x|^2 \, dx$, we have that

$$\lambda = \liminf_{j \to \infty} \mathcal{H}(u_{k_j}) \geq \mathcal{H}(\phi) \geq \lambda,$$

hence $\mathcal{H}(\phi) = \lambda$, and we have that $\phi$ is a minimizer of $\mathcal{H}$ with respect to fixed charge, hence by the previous discussion $\phi$ and the corresponding Lagrange multiplier $\omega$ form a bound state solution $u(x,t) = e^{i\omega t}\phi(x)$ of (1.2).

We remark that the bound state solution (1.3) constructed above with real-valued profile is embedded in a family of complex-valued *traveling waves*

$$u(x,t) = e^{i\omega t}\psi(x - ct; c),$$

with a generally complex-valued profile $\psi$ which satisfies the profile equation

$$-\psi'' + \omega\psi + ic\psi' + |\psi|^2\psi = 0. \tag{1.7}$$

This embedding is due to the *Galilean invariance*

$$\mathcal{G}_c u(x,t) = e^{\frac{icx}{2} - \frac{ic^2 t}{4}} u(x - ct, t) \tag{1.8}$$

which smoothly maps a real-valued standing wave solutions to complex-valued traveling wave solutions. In proving the stability of standing waves, it will be important to differentiate the profile equation (1.7) with respect to the wave speed $c$, which is justified by this Galilean invariance.

In Proposition 2.2.2, we use a similar approach as above to construct a class of spatially periodic traveling waves $(x,t) \mapsto e^{i\omega t}\phi(x - ct)$ in the fractional case, solving an adapted minimization problem to account for the lack of an exact Galilean invariance.

### 1.1.2 Nondegeneracy and Orbital Stability

In addition to the question of existence, one is often also interested in the *stability* of solutions, which essentially addresses whether an equilibrium will persist for long times even when slightly perturbed. Continuing with the discussion of the Classical Nonlinear Schrödinger Equation, we will examine the nonlinear stability of the constrained energy minimizers $\phi$ constructed in Section 1.1.1. In a co-rotating frame, such $\phi$ are equilibria of the PDE

$$iu_t + u_{xx} - \omega u - |u|^2 u = 0. \tag{1.9}$$

We say that $\phi$ is *stable* (in the sense of Lyapunov) if for every $\varepsilon > 0$ there exists $\delta > 0$ such that if $\|v\| < \delta$, then the solution of (1.9) with initial data $u(x,0) = \phi + v$ satisfies $\|u(\cdot,t) - \phi\| < \varepsilon$ for all time, where $\|\cdot\|$ is an appropriate norm.

Now, note that (1.2) has translation and trivial-phase invariances; i.e. if $u(\cdot,t)$ is a solution, then so is

$$e^{i\beta}u(\cdot - x_0, t), \quad \text{for all } x_0, \beta \in \mathbb{R}.$$

So, we can only expect that a time-evolved solution of (1.9) remains close to its initial data *modulo invariances*. This leads us to define the notion of *orbital stability*, where we classify an initial datum $\phi$ as *orbitally* stable if the time-evolved solution $u(\cdot,t)$ with initial data $u(\cdot,0) = \phi + v$ for a small perturbation $v$ remains close to $\phi$ for all time, where "close" is measured in the semidistance

$$\rho(u(\cdot,t),\phi) := \inf_{x_0,\beta\in\mathbb{R}} \left\| e^{i\beta}u(\cdot - x_0, t) - \phi \right\|.$$

That is, the time-evolved solution is translated and rotated for "best fit" before measuring its norm-difference from $\phi$.

To proceed, consider the Lagrangian functional

$$\mathcal{E}(u) := \mathcal{H}(u) + \omega Q(u).$$

Then (1.9) can be written as the *Hamiltonian system*

$$u_t = J\,\delta\mathcal{E}(u) \tag{1.10}$$

with symplectic form $J = -i$. Then, per (1.6), a solution of the profile equation (1.4) is a critical point of $\mathcal{E}$, i.e. $\delta\mathcal{E}(\phi) = 0$. Perturbing $\phi$ by a complex-valued, co-periodic perturbation $v$ and expanding in a Taylor series, we have

$$\mathcal{E}(\phi + v) - \mathcal{E}(\phi) = \frac{1}{2}\left\langle \delta^2\mathcal{E}(\phi)v, v\right\rangle + \mathcal{O}(\|v\|^3).$$

As is known from the theory of finite dimensional Hamiltonian systems, the stability of $\phi$ follows if $\left\langle \delta^2\mathcal{E}(\phi)v, v\right\rangle$ is uniformly positive for all $v$, i.e. that the *Hessian* $\delta^2\mathcal{E}(\phi)$ of the Lagrangian is *positive-definite*. A-priori, this is too much to hope for due to the symmetries present in NLS. Indeed, $\delta^2\mathcal{E}(\phi)$ has a nontrivial kernel: writing $v = \mathrm{Re}(v) + i\,\mathrm{Im}(v)$ and decomposing the action of $\delta^2\mathcal{E}(\phi)$ into real and imaginary parts, due to the reality of $\phi$ we can represent $\delta^2\mathcal{E}(\phi)$ as a diagonal matrix operator

$$\delta^2\mathcal{E}(\phi)v \sim \begin{bmatrix} L_+ & 0 \\ 0 & L_- \end{bmatrix} \begin{bmatrix} \mathrm{Re}(v) \\ \mathrm{Im}(v) \end{bmatrix},$$

where

$$L_+ := -\partial_x^2 + 3\phi^2 + \omega, \quad L_- := -\partial_x^2 + \phi^2 + \omega.$$

It is easy to verify that, due to the profile equation (1.4), $\phi \in \ker(L_-)$ and $\phi' \in \ker(L_+)$, hence $\delta^2\mathcal{E}(\phi)$ is *not* positive definite, as $\phi' + i\phi \in \ker(\delta^2\mathcal{E}(\phi))$.

However, not all hope is lost–an appropriate positive-definiteness can be recovered if $\delta^2\mathcal{E}(\phi)$ can be shown to be *nondegenerate*, i.e. that its kernel is precisely spanned by symmetry eigenfunctions. Here, this means showing that

$$\ker(L_+) = \operatorname{span}\{\phi'\}, \quad \ker(L_-) = \operatorname{span}\{\phi\}.$$

The proof of nondegeneracy relies on a ground state and oscillation theory for the $L_+$ and $L_-$ operators, which is traditionally addressed via *Sturm-Liouville Theory*:

**Theorem 1.1.4** (Periodic Sturm-Liouville Theory)**.** *Consider the eigenvalue problem*

$$\mathcal{L}u = \lambda u, \quad \mathcal{L} := -\partial_x^2 + V(x) \tag{1.11}$$

*where $V$ is $T$-periodic. There exists a real sequence*

$$\lambda_0 < \lambda_1 \leq \lambda_2 < \lambda_3 \leq \lambda_4 < \lambda_5 \leq \cdots$$

*such that:*

1. *The eigenvalue problem (1.11) has a $T$-periodic solution $u$ if and only if $\lambda = \lambda_{4j-1}$ or $\lambda = \lambda_{4j}$ for some $j \geq 0$. The $T$-periodic eigenfunction corresponding to $\lambda_0$ has no zeros in $[0,T)$, and the $T$-periodic eigenfunctions corresponding to $\lambda_{4j-1}, \lambda_{4j}$ for $j \geq 1$ have $2j$ zeros on $[0,T)$.*

2. *The eigenvalue problem (1.11) has a $T$-*antiperiodic *solution (i.e. $u(x+T) = -u(x)$) if and only if $\lambda = \lambda_{4j-3}$ or $\lambda = \lambda_{4j-2}$ for some $j \geq 1$. Such $T$-antiperiodic eigenfunctions have $2n-1$ zeros in $[0,T)$.*

*(See [63, Theorem 5.37], [49, Theorem 2.1].)*

Analyzing $L_+$ and $L_-$ on subspaces of odd and even functions and applying Sturm-Liouville theory in conjunction with monotonicity and parity properties of $\phi$ and $\phi'$, it is possible through proof by contradiction with the Fredholm alternative to rule out the existence of further non-trivial eigenfunctions in the kernels of $L_\pm$. For these Fredholm alternative arguments, knowledge of a few elements in the range of $L_\pm$ will be needed, some of which are obtained by differentiating (1.7) with respect to parameters. The ability to do this is justified in the classical case by the Galilean invariance (1.8), but smoothness assumptions will be needed in the fractional case. Moreover, the classical Sturm-Liouville Theory stated in Theorem 1.1.4, whose proof depends on ODE techniques (e.g. Wronskian determinant, Prüfer variables in phase space) does not apply in the fractional setting, hence a similar ground state and oscillation theory must be developed to replace it. This is done through semigroup theory and applying rearrrangement inequalities to a variational characterization of a linear operator's the principal eigenvalue. See Section 2.3.1 and Section 2.3.2.

Lastly, we remark that the Hessian $\delta^2\mathcal{E}(\phi)$ considered as an operator acting on $2T$-antiperiodic functions a-priori has at most two negative eigenvalues, which is too unwieldy to establish stability. This difficulty was encountered in [3], where the proof of stability of cnoidal waves required an additional assumption that the wave profile be *$T$-antiperiodic*, i.e. that $\phi(x+T) = -\phi(x)$. In addition to the fact that phase-plane analysis in the local case yields the existence of antiperiodic solutions (see the introductory discussion of Section 2.2), this difficulty motivates incorporating $T$-antiperiodic function spaces directly into the existence and stability theories for the fractional setting.

## 1.2 Dispersive Shallow Water Wave Models

### 1.2.1 Korteweg-de Vries and Unidirectional Whitham Equations

To set the stage for an exploration of bidirectional Whitham shallow water models as presented in Chapter 3, consider the *Incompressible Euler Equations*

$$\begin{cases} \mathbf{u}_t + \mathbf{u}\cdot\nabla\mathbf{u} &= -\frac{1}{\rho}\nabla P - g\mathbf{j}, \\ \nabla\cdot\mathbf{u} &= 0, \end{cases} \tag{1.12}$$

which are a very general model of an inviscid, incompressible fluid. Here, $\mathbf{u}$ is the fluid velocity vector (which will be assumed to be irrotational), $-g\mathbf{j}$ is a constant gravitational field, $\rho$ is the density of the fluid, and $P$ is the pressure of the fluid. Since $\mathbf{u}$ is irrotational, we can express $\mathbf{u} = \nabla\varphi$ in terms of a *velocity potential* $\varphi$, and the incompressibility condition leads to the velocity potential satisfying Laplace's equation in the fluid. Then by continuity of pressure in the fluid, the role of pressure is reduced to a boundary condition at the wave surface, where the pressure is taken to be the constant, undisturbed air pressure. Under these assumptions, it is shown in [66, Chapter 13], that waves in water of constant mean depth $h_0$ possess the dispersion relation

$$\omega^2 = gk\tanh(kh_0). \tag{1.13}$$

*Remark* 1.2.1. That the dispersion relation (1.13) does not depend on the pressure $P$ in the Incompressible Euler Equations (1.12) can be intuited from the fact that the external forcing (including $\nabla P$) drops out of the linearized system.

Making a further assumption that the fluid depth $h_0$ is small relative to the wavelength $2\pi/\kappa$ leads to the one-dimensional *shallow water equations* [66, (13.79)]

$$\begin{cases} \eta_t + h_0 u_x + (u\eta)_x &= 0 \\ u_t + u u_x + g\eta_x &= 0, \end{cases} \tag{1.14}$$

which is *not* dispersive since the linear part of (1.14) can easily be checked to have constant linear phase speed $\omega/k = \pm\sqrt{gh_0}$. To introduce dispersion into the shallow water equations, note that since $kh_0 \ll 1$ by the shallow water hypothesis, the dispersion relation (1.13) can be expanded in a Maclaurin series to obtain

$$\omega^2 = gh_0k^2\left(1 - \frac{1}{3}(kh_0)^2 + \mathcal{O}((kh_0)^4\right).$$

Taking the square root of both sides, keeping the positive branch (which corresponds to unidirectional waves propagating to the right), and expanding the square root in a Maclaurin series yields, to third order,

$$\omega = \sqrt{gh_0}\left(k - \frac{h_0^2}{6}k^3\right). \tag{1.15}$$

This is the dispersion relation for the linear equation

$$\eta_t + \sqrt{gh_0}\,\eta_x + \frac{h_0^2}{6}\eta_{xxx} = 0,$$

and combining this linear equation with the shallow water nonlinearity $\eta\eta_x$ leads to the dimensional *Korteweg-de Vries* (KdV) equation

$$\eta_t + \sqrt{gh_0}\,\eta_x + \frac{h_0^2\sqrt{gh_0}}{6}\eta_{xxx} + \frac{3}{2h_0}\eta\eta_x = 0. \tag{1.16}$$

Due to the truncation of the full Euler dispersion relation in (1.15), we expect (1.16) to be a poor model for waves of large wavenumber (i.e. high frequency). In an effort to more closely capture the behavior of the full Euler equations, Whitham [66] suggested a correction of the KdV model in which its linear phase speed is replaced with the (positive) Euler phase speed. To do this, first observe that one can express (1.16) as

$$\eta_t + \mathcal{F}_k^{-1}(c_{\text{KdV}}(k)) * \eta_x + \frac{3}{2h_0}\eta\eta_x = 0, \tag{1.17}$$

where $c_{\text{KdV}}(k) = \sqrt{gh_0}\left(1 - \frac{h_0^2}{6}k^2\right)$ is the linear phase speed obtained from (1.15). Note that the linear phase speed of the full Euler equations is given by

$$(c_{\text{Euler}}(k))^2 = \frac{g\tanh(kh_0)}{k},$$

hence waves propagating to the right have phase speed

$$c_{\text{Euler},+}(k) = \sqrt{\frac{g\tanh(kh_0)}{k}}. \tag{1.18}$$

Replacing the KdV linear phase speed in (1.17) with the positive Euler phase speed, we obtain

$$\eta_t + \mathcal{F}_k^{-1}(c_{\text{Euler},+}(k)) * \eta_x + \frac{3}{2h_0}\eta\eta_x = 0. \tag{1.19}$$

In contrast with cnoidal periodic traveling waves in KdV, which are always spectrally stable [6], numerical studies [60] show that periodic traveling waves in (1.19) possess spectral instabilities. This difference of behavior indicates that stability/instability in the full water wave model depends sensitively on both dispersion and nonlinearity. In Chapter 3, we numerically study the spectral stability of *bidirectional Whitham models* whose linear phase speed matches (1.18), permitting waves that travel the left or to the right. One such model

is given by

$$\begin{cases} u_t &= -\eta_x - uu_x \\ \eta_t &= -\mathcal{K}u_x - (\eta u)_x \end{cases} \tag{1.20}$$

where the operator $\mathcal{K}$ incorporates the full-Euler dispersion and is defined via its symbol

$$\widehat{\mathcal{K}f}(n) = \widehat{\mathcal{K}}(n)\widehat{f}(n) := \frac{\tanh(n)}{n}\,\widehat{f}(n), \quad n \in \mathbb{Z}. \tag{1.21}$$

Here, $\eta$ represents the fluid height and $u = \phi_x$, where $\phi(x,t) = \phi(x,\eta(x,t),t)$ denotes the trace of the velocity potential at the free surface.

Due to accurate dispersion, we will find that traveling waves in bidirectional Whitham equations such as (1.20) capture a high frequency instability that is found in neither of the KdV nor unidirectional Whitham equations.

### 1.2.2 Local Bifurcation Theory and Continuation

In Chapter 3, we will find traveling wave solutions of bidirectional Whitham water wave models such as (1.20) by seeking equilibrium wave profiles $\phi$ and their corresponding wave speeds $c$ that satisfy a profile equation of the form

$$F(c,\phi) := \mathcal{K}\phi - g(c,\phi) = 0, \tag{1.22}$$

where the operator $\mathcal{K}$ defined in (1.21) encodes the full Euler dispersion and the function $g$ depends on the specific model and implicitly relates the profile $\phi$ and the wave speed $c$. It will be especially convenient to seek *constant* solutions and their corresponding wave speeds. Though constant solutions are not interesting in their own right, under appropriate conditions there could be non-trivial solutions of very small amplitude "nearby". So, we

ask the question: which constant solutions $\phi_0$ and corresponding wave speeds $c_0$ could possibly experience a *bifurcation* into small-amplitude periodic solutions?

By the implicit function theorem, a constant solution $(c_0, \phi_0)$ of (1.22) can possibly bifurcate into a nonconstant one if the kernel of the Fréchet derivative $\delta_\phi F(c_0, \phi_0)$ is nontrivial; i.e. if

$$\delta_\phi F(c_0, \phi_0)(v) := \lim_{\varepsilon \to 0} \frac{F(c_0, \phi_0 + \varepsilon v) - F(c_0, \phi_0)}{\varepsilon} = 0.$$

for some nontrivial $v$. That is, if the above Fréchet derivative vanishes at $v$, then the curve $\{(c, \phi) : F(c, \phi) = 0\}$ is not guaranteed to be uniquely parameterized by $c$ in a neighborhood of $(c_0, \phi_0)$, which potentially allows nontrivial solutions $(c, v)$ to satisfy $F(c, v) = 0$ in a neighborhood of $(c_0, \phi_0)$.

We now endeavor to find such nontrivial $v$ and corresponding $c$. For this example discussion, we will use

$$\begin{aligned} F(c, \phi) &:= \mathcal{K}\phi - \frac{1}{2}\phi^3 + \frac{3}{2}c\phi^2 - c^2\phi, \\ \implies \delta_\phi F(c, \phi) &:= \mathcal{K} - \frac{3}{2}\phi^2 + 3c\phi - c^2 \operatorname{Id} \end{aligned}$$

corresponding to the traveling wave profile equation of (1.20). See (3.24) and the surrounding discussion for further details. Restricting to even, real-valued $2\pi$-periodic functions, we express $v$ in its Fourier series as $v(x) = \sum_{n=0}^{\infty} \widehat{v}(n) \cos(nx)$. We want constant $\phi_0$, $c_0$, and nontrivial $v$ to simultaneously satisfy

$$\begin{cases} F(c_0, \phi_0) &= \mathcal{K}\phi_0 - \frac{1}{2}\phi_0^3 + \frac{3}{2}c_0\phi_0^2 - c_0^2\phi_0 = 0 \\ \delta_\phi F(c_0, \phi_0)(v) &= \mathcal{K}v - \frac{3}{2}\phi_0^2 v + 3c_0\phi_0 v - c_0^2 v = 0. \end{cases} \tag{1.23}$$

Taking the Fourier transform of the second equation in (1.23), we have

$$\left(\widehat{\mathcal{K}}(n) - \frac{3}{2}\phi_0^2 + 3c_0\phi_0 - c_0^2\right)\widehat{v}(n) = 0, \quad \forall n \in \mathbb{Z}.$$

When $n = 1$ (corresponding to fundamental period $2\pi$), we see that if

$$\widehat{\mathcal{K}}(1) - \frac{3}{2}\phi_0^2 + 3c_0\phi_0 - c_0^2 = 0,$$

then $\widehat{v}(1)$ can be any real number, hence

$$\ker\left(\delta_\phi F(c_0, \phi_0)\right) = \operatorname{span}\{\cos(x)\}. \tag{1.24}$$

So, any $c_0$ and *constant* $\phi_0$ satisfying

$$\begin{cases} \mathcal{K}\phi_0 - \frac{1}{2}\phi_0^3 + \frac{3}{2}c_0\phi_0^2 - c_0^2\phi_0 = 0 \\ \widehat{\mathcal{K}}(1) - \frac{3}{2}\phi_0^2 + 3c_0\phi_0 - c_0^2 = 0. \end{cases}$$

will yield a solution that can likely be continued to a branch of nontrivial $2\pi$-periodic solutions. Taking $\phi_0 = 0$ (as is done in Section 3.3.1), we have that $c_0 := \sqrt{\widehat{\mathcal{K}}(1)}$ yields a point where a bifurcation from the trivial solution $\phi \equiv 0$ is possible. To *continue* the branch of nontrivial solutions from $(c_0, 0)$, for $|a| \ll 1$ we seek $(c(a), v(\cdot; a))$ of the form

$$\begin{aligned} c(a) &= c_0 + ac_1 + a^2c_2 + a^3c_3 + \mathcal{O}(a^4) \\ v(x; a) &= 0 + a\cos(x) + a^2v_2 + a^3v_3 + \mathcal{O}(a^3) \end{aligned}$$

such that $F(c(a), v(\cdot; a)) = 0$, where $v_2$ and $v_3$ are even, $2\pi$-periodic functions. (The above expansion is justified by the *Lyapunov-Schmidt reduction*.) Computing $F(c(a), v(\cdot; a))$ and

grouping the $\mathcal{O}(a)$, $\mathcal{O}(a^2)$, and $\mathcal{O}(a^3)$ terms yields[1]

$$\begin{aligned}0 = &\left(\mathcal{K}\cos(x) - c_0^2\cos(x)\right)a \\ &+ \left(\mathcal{K}v_2 - c_0 v^2 + \frac{3c_0}{4} - 2c_0c_1\cos(x) + \frac{3}{4}c_0\cos(2x)\right)a^2 \\ &+ \left(\mathcal{K}v_3 - c_0^2 v_3 - \left(\frac{3}{8} + 2c_0c_2\right)\cos(x) + 3c_0v_2(x)\cos(x) - \frac{1}{8}\cos(3x) + \mathcal{O}(c_1)\right)a^3 \\ &+ \mathcal{O}(a^4).\end{aligned}$$

The coefficient of $a$ above vanishes since $\cos(x) \in \ker(\mathcal{K} - c_0^2\,\mathrm{Id})$ by (1.24). We also want the coefficient of $a^2$ to vanish. Taking the Fourier transform of the coefficient of $a^2$ yields

$$\left(\widehat{\mathcal{K}}(n) - c_0^2\right)\widehat{v}_2(n) - 2c_0c_1\delta_{n,1} + \frac{3c_0}{4}(\delta_{n,0} + \delta_{n,2}) = 0, \tag{1.25}$$

where $\delta_{n,k}$ is the Kronecker delta. When $n = 1$, (1.25) becomes $-2c_0c_1 = 0$, which implies that $c_1 = 0$. When $n = 0$ (and now $c_1 = 0$) in (1.25), we immediately obtain

$$\widehat{v}_2(0) = \frac{3c_0}{4(c_0^2 - 1)}.$$

Similarly, with $n = 2$ in (1.25) we obtain

$$\widehat{v}_2(2) = \frac{3c_0}{4(c_0^2 - \widehat{\mathcal{K}}(2))}.$$

Finally, analyzing the Fourier transform of the $\mathcal{O}(a^3)$ terms with $c_1 = 0$ and $n = 1$ yields

$$\begin{aligned}c_2 &= \frac{3}{2}\widehat{v}_2(0) + \frac{3}{4}\widehat{v}_2(2) - \frac{3}{16c_0} \\ &= \frac{9c_0}{8(c_0^2 - 1)} + \frac{9c_0}{8(c_0^2 - \widehat{K}(2))} - \frac{3}{16c_0}.\end{aligned}$$

[1] This is very tedious, and Mathematica can help a lot here.

Putting it all together, we finally have

$$c(a) = c_0 + \left( \frac{9c_0}{8(c_0^2 - 1)} + \frac{9c_0}{8(c_0^2 - \widehat{K}(2))} - \frac{3}{16c_0} \right) a^2 + \mathcal{O}(a^3)$$
$$v(x;a) = a\cos(x) + \mathcal{O}(a^2),$$

where $c_0 = \widehat{\mathcal{K}}(1) = \tanh(1)$. Such *local bifurcation formulas* will be sufficient to seed a numerical continuation method that successively solves for solutions of larger and larger amplitude; see Section 3.2.2.

### 1.2.3 Spectral Stability and Floquet's Theorem

In studying the bidirectional Whitham models, we will numerically approximate the spectrum of the linearization of the system about an equilibrium background wave. In particular, we concern ourselves with the following notion of stability, known as *spectral stability*, which is defined as follows:

*Definition* 1.2.2 (Spectral Stability). An equilibrium solution $\phi$ of an autonomous system $u_t = F(u)$ is *spectrally stable* if the linear operator $\mathcal{L}[\phi]$ obtained by linearizing system about $\phi$ has no spectrum with strictly positive real part.

We will be interested in studying the stability of an equilibrium $\phi$ with respect to *localized* perturbations $v(\cdot, t) \in L^2(\mathbb{R})$, which satisfy to first order

$$v_t = \mathcal{L}[\phi]v.$$

Separating variables, we write $v(x,t) = e^{\lambda t}V(x)$, which yields the eigenvalue problem

$$\mathcal{L}[\phi]V = \lambda V \tag{1.26}$$

on $L^2(\mathbb{R})$. Clearly if any eigenpair $V$, $\lambda$ is such that $\mathrm{Re}(\lambda) > 0$, then the perturbation grows exponentially forward in time, leading to (spectral) instability.

Floquet's theorem provides a convenient representation of bounded solutions to the eigenvalue problem (1.26):

**Theorem 1.2.3** (Floquet)**.** *Consider the linear homogeneous differential equation $y' = A(x)y$ for some square matrix $A(x)$ of complex continuous functions such that $A(x+L) = A(x)$. Then any fundamental matrix $\Phi(x)$ of this system may be decomposed as*

$$\Phi(x) = \widetilde{\Phi}(x)e^{Rx},$$

*where $R$ is a constant matrix and $\widetilde{\Phi}(x)$ is $L$-periodic and nonsingular. The eigenvalues of $R$ are known as* Floquet exponents*, and bounded solutions on $\mathbb{R}$ correspond to purely imaginary Floquet exponents. Thus every bounded solution of* (1.26) *is of the form*

$$V(x) = e^{i\mu x}\widetilde{V}(x), \tag{1.27}$$

*where $\widetilde{V}(x)$ is $L$-periodic and $\mu \in [0, 2\pi/L)$.*

In implementing the Fourier-Floquet-Hill Method (FFHM) [16] for approximating the spectrum of a linear operator with periodic coefficients, the decomposition (1.27) of the eigenfunction in (1.26) is advantageous since the periodic function $\widetilde{V}$ can be expanded in a (truncated) Fourier series, which leads to a finite dimensional eigenvalue problem on the Fourier coefficients for each $\mu \in [0, 2\pi/L)$ that can be solved using standard numerical techniques and software packages [43].

A further important consequence of Floquet's theorem is that the $L^2(\mathbb{R})$-spectrum of a linear operator with periodic coefficients is purely essential. Indeed, by Floquet's theorem, any nontrivial $V \in L^2(\mathbb{R})$ satisfying (1.26) is either unbounded on $\mathbb{R}$ or is of the form

(1.27); regardless, $\|V\|_{L^2(\mathbb{R})} = +\infty$, hence

$$\sigma_{L^2(\mathbb{R})}(\mathcal{L}[\phi]) = \sigma_{L^2(\mathbb{R}),\text{ess}}(\mathcal{L}[\phi]).$$

Moreover, given that every eigenfunction of (1.26) is of the form (1.27), we have for each *Bloch parameter* $\mu \in [0, 2\pi/L)$ that

$$\begin{aligned} &\lambda e^{i\mu x}\widetilde{V} = \mathcal{L}[\phi]\left(e^{i\mu x}\widetilde{V}\right) \\ \implies &\lambda\widetilde{V} = \left(e^{-i\mu x}\mathcal{L}[\phi]e^{i\mu x}\right)\widetilde{V} =: \mathcal{L}^{\mu}[\phi]\widetilde{V}, \end{aligned}$$

where $\mathcal{L}^{\mu}[\phi]$ is a linear operator with periodic coefficients acting on a bounded domain with periodic boundary conditions. Hence for each $\mu \in [0, 2\pi/L)$ the spectrum of $\mathcal{L}^{\mu}[\phi]$ is purely point spectrum, which leads to the following convenient characterization of the spectrum of $\mathcal{L}[\phi]$:

$$\sigma_{L^2(\mathbb{R})}(\mathcal{L}[\phi]) = \sigma_{L^2(\mathbb{R}),\text{ess}}(\mathcal{L}[\phi]) = \bigcup_{\mu\in[0,2\pi/L)} \sigma_{L^2_{\text{per}}(0,L),\text{pt}}(\mathcal{L}^{\mu}[\phi]).$$

In the spectral computations of Chapter 3 (and in the more general discussion of Appendix C) we will capitalize on this characterization to numerically approximate the spectrum of the linearization of a bidirectional Whitham models by expanding the periodic eigenfunctions for each $\mathcal{L}^{\mu}[\phi]$ in Fourier series.

Lastly, we remark that Floquet's theorem as stated above applies to purely differential operators. This theorem can be extended to a nonlocal setting (see [42, Proposition 3.1], for instance), which will be of interest in the bidirectional Whitham equations we consider.

# Chapter 2

# The Fractional Nonlinear Schrödinger Equation

## 2.1 Introduction

In this chapter, we consider the existence and stability properties of a class of spatially periodic solutions to the fractional nonlinear Schrödinger equations (fNLS) of the form

$$iu_t - \Lambda^\alpha u + \gamma |u|^{2\sigma} u = 0, \quad x, t \in \mathbb{R}, \tag{2.1}$$

where subscripts denote partial differentiation. Here and throughout, $u = u(x,t)$ is a generally complex-valued function, and the pseudodifferential operator $\Lambda^\alpha := (-\partial_x)^{\alpha/2}$ acting on $2T$-periodic functions is defined by Fourier multipliers via

$$\widehat{\Lambda f}(n) = \left|\frac{\pi n}{T}\right|^\alpha \widehat{f}(n), \quad n \in \mathbb{Z}.$$

Further, $\gamma = 1$, $\gamma = -1$ distinguishes between focusing (attracting) and defocusing (repulsive) nonlinearities, respectively.

The parameter $\alpha \in (0, 2]$ describes the fractional dispersive nature of the equation. When $\alpha = 2$, the operator $\Lambda^2 = -\partial_x^2$ is the classical (local) Laplacian having positive, discrete point spectrum. In this case, (2.1) reduces to the well-studied classical nonlinear

Schrödinger equation (NLS), which serves as a canonical model for weakly nonlinear wave propagation in dispersive media; see, for example, [61]. When $\alpha \in (0,2)$, $\Lambda^\alpha$ denotes the so-called *fractional Laplacian*, which arises naturally in a variety of applications including the continuum limit of discrete models with long range interaction [46], dislocation dynamics in crystals [11], mathematical biology [51], water wave dynamics [41], and modeling waves in lossy media [62]. See also [9] for a recent discussion on applications.

Throughout our analysis, we will study solutions of the form

$$u(x,t) = e^{i\omega t}\phi(x-ct;c), \tag{2.2}$$

where $\omega, c \in \mathbb{R}$ are parameters and $\phi$ is a bounded solution to the (generally) nonlocal profile equation

$$\Lambda^\alpha \phi + \omega\phi + ic\phi' - \gamma|\phi|^{2\sigma}\phi = 0.$$

When $c = 0$, the focusing fNLS is known to admit standing solitary waves that are asymptotic to zero at spatial infinity; see [25]. Among such solitary wave solutions, specific attention is often paid to the positive, radially symmetric solutions typically referred to as "ground states". The stability of such ground states dates back to the work of Cazenave and Lions [13] and Weinstein [64, 65] on the classical case $\alpha = 2$, using the method of concentration compactness along with the construction of appropriate Lyapunov functionals. For $\alpha \in (1,2]$, such ground states are known to be orbitally stable provided the nonlinearity is energy sub-critical, i.e. if $0 < \sigma < \alpha$; see [32, 65], for example. While no nontrivial localized solutions exist in the defocusing case $\gamma = -1$, it is known in the classical case $\alpha = 2$ to admit so-called black solitons of the form (2.2) corresponding to monotone front-like solutions asymptotic to constants as $x \to \pm\infty$. The dynamics and stability of black solitons has been studied in numerous works; see, for example, [5, 28, 29].

The stability of periodic standing waves of (2.1) is considerably less understood than their asymptotically constant counterparts, even in the classical case. For the classical cubic NLS, Rowlands [59] formally demonstrated that all periodic standing waves in the focusing case are modulationally unstable (i.e. spectrally unstable to long-wavelength perturbations), while periodic standing waves are modulationally stable in the defocusing case. These results were rigorously established later by Gallay and Haragus [27] for small amplitude waves, and for arbitrary amplitude waves by Gustafson, Le Coz, and Tsai [33] and Deconinck and Segal [15]. The spectral stability to arbitrary bounded perturbations of periodic standing waves in the defocusing NLS ($\alpha = 2$) was later shown by Gallay and Haragus [27] for small amplitude waves and by Bottman, Deconinck, and Nivala [7], for waves of arbitrary amplitude by using complete integrability. These results give the impression that the *defocusing* NLS demonstrates better stability properties, hence we restrict our attention to the defocusing case for the nonlocal fNLS as well. As for the local case, we expect that periodic waves in the nonlocal fNLS will also be modulationally unstable, though this has not been verified; to our knowledge there has been no rigorous study into the dynamics of such waves in the fractional case.

In this work, we will study the *nonlinear stability* of periodic standing waves of (2.1) in the genuinely nonlocal case $\alpha \in (0, 2)$. Since (2.1) is invariant under phase rotation and spatial translation, i.e. if $u(x,t)$ solves (2.1), then so does $e^{i\beta}u(x - x_0, t)$, we should only expect stability up to these invariances. Thus, we will measure stability with the semidistance

$$\rho(u, v) := \inf_{x_0, \beta \in \mathbb{R}} \left\| u(\cdot, t) - e^{i\beta} v(\cdot - x_0, t) \right\|_X,$$

where $X$ is a suitably-chosen function space. Such an *orbital stability* result for solutions of (2.1) was first obtained in the classical, focusing, periodic case by Angulo-Pava [3], where the orbital stability of dnoidal type (hence strictly positive) standing waves was

established to co-periodic perturbations. Pava's analysis relied on a direct adaptation of the classical approach to orbital stability by Grillakis, Shatah, and Strauss [30, 31] and could not be extended to cnoidal type (sign changing) solutions in either of the focusing or defocusing cases. This issue was later resolved by Gallay and Haragus in [26], which demonstrated the stability of cnoidal waves in the defocusing cubic NLS ($\alpha = 2$, $\sigma = 1$) to perturbations with the same period as the *modulus* of the underlying wave. This restrictive class of perturbations is essential to employ the techniques of [30, 31] since, as noted by Pava, the Hessian of the Lagrangian associated with such a cnoidal wave has two negative eigenvalues when acting on co-periodic functions, invalidating the structural hypotheses of [30, 31].

Here, per the analysis in [26], we study the existence and nonlinear stability of periodic standing waves of the fNLS (2.1) with fractional dispersion $\alpha \in (0, 2)$ to an appropriately restricted class of perturbations. We concentrate on the defocusing case, and in Section 2.2 we construct a three-parameter family of real-valued $T$-*antiperiodic* standing waves, i.e. $2T$-periodic waves with

$$\phi(x+T) = -\phi(x),$$

as local minima of the Hamiltonian energy subject to conservation of charge and angular momentum: see Proposition 2.2.2 and Lemma 2.2.6. Then we establish the nonlinear orbital stability of these standing waves to small $T$-antiperiodic perturbations: see Theorem 2.4.1.

A key step in the stability analysis is to demonstrate that the Hessian of the Hamiltonian energy is *nondegenerate* at such an antiperiodic, local constrained minimizer of the defocusing fNLS; i.e. that the kernel is generated only by spatial translations and phase rotations. The nondegeneracy of the linearization is known to play an important role in the stability of traveling and standing waves (see [65], [48], and [26]) and in the blowup

analysis (see [45], [61], for instance) of the related dynamical equation. In the case of the classical NLS with cubic nonlinearity, the nondegeneracy at such antiperiodic standing wave solutions was established by Gallay and Haragus [26, Proposition 3.2]. Their proof, however, fundamentally relies on ODE techniques, particularly the Sturm-Liouville theory for ODEs and a-priori bounds on the number of linearly independent solutions to the linearized equations. These methods are not directly applicable to the nonlocal case $\alpha \in (0,2)$. Nevertheless, Frank and Lenzmann [25] recently established the nondegeneracy of *solitary* waves for a family of nonlocal evolution equations, including the focusing fNLS. Their analysis develops a nonlocal analog of Sturm-Liouville theory using the characterization of the fractional Laplacian as a Dirichlet-to-Neumann operator for a *local* elliptic problem in the upper half-plane. Then, via topological nodal domain arguments, they obtain an upper bound on the number of sign changes achieved by eigenfunctions of fractional linear Schrödinger operators acting on the line. This oscillation theory was recently extended to the periodic setting in [39], which considers the orbital stability of periodic traveling waves of the fractional gKdV equation.

Considerable modification is needed in the defocusing case to account for the incongruity of the $T$-*periodic* potential in the associated linear Schrödinger operators acting on $T$-*antiperiodic* function spaces. Indeed, even in the classical case, antiperiodic ground states for linear Schrödinger operators *need not be simple*, and there are examples of potentials for which the associated Schrödinger operator will have an antiperiodic ground state of multiplicity two; see [49] for instance. We handle this difficulty by demonstrating that the associated linear semigroup is positivity improving when restricted to antiperiodic subspaces of even and odd functions, which ultimately yields a characterization of the antiperiodic ground states of such fractional linear Schrödinger operators restricted to these even and odd subspaces: see Theorem 2.3.8. Further, using antiperiodic rearrangement inequalities developed in Appendix B, we demonstrate that the ordering of the even and

odd antiperiodic ground states for a fractional linear Schrödinger operator depends explicitly on the monotonicity properties of the real-valued periodic potential: see Proposition 2.3.9. Once the appropriate ground state theory is developed, a suitable oscillation theory for higher antiperiodic eigenfunctions follows by the arguments in [25, 39]: see Lemma 2.3.10.

We emphasize that the realness of the $T$-antiperiodic solutions $\phi$ discussed above is *absolutely crucial* to our analysis, guaranteeing that the Hessian of the Lagrangian functional (whose critical points are solutions of the fNLS profile equation (2.3)) acts as a diagonal operator on $L^2_{\mathrm{a}}(0,T) \times L^2_{\mathrm{a}}(0,T)$ upon decomposing into real and imaginary parts. This diagonal property reduces the nondegeneracy analysis to the study of two scalar linear fractional Schrödinger operators, which is precisely the setting where our techniques from Section 2.3 apply. In the "nontrivial phase" case where solutions $\phi$ are genuinely complex-valued, the Hessian operator couples the real and imaginary parts of the perturbations, invalidating the strategy and techniques contained in this chapter: see equation (2.21) below. The corresponding nondegeneracy and stability analysis for the nontrivial phase solutions is completely open in the nonlocal case and is an interesting direction for future research. To our knowledge, the only nondegeneracy result known in the nontrivial phase case was provided by in [26] using ODE techniques that are not applicable to the nonlocal setting.

The outline of the chapter is as follows. In Section 2.2 we use variational arguments to establish the existence of antiperiodic solutions of the profile equation (2.3) in the defocusing case. We then consider the nondegeneracy of these antiperiodic solutions in Section 2.3, followed by a proof of their orbital stability in Section 2.4. Appendix B contains proofs of the relevant rearrangement inequalities used in the development of the antiperiodic ground state theory used in Section 2.3, and Appendix A gives an account of the functional derivatives used in the existence and stability theories.

## 2.2 Existence of Constrained Local Minimizers in the Defocusing Case

We begin our analysis by establishing the existence of periodic waves of the form (2.2) of the *defocusing* ($\gamma = -1$) fNLS (2.1). Substituting the standing wave ansatz (2.2) into (2.1) yields the nonlocal *profile equation*

$$\Lambda^\alpha \phi + \omega\phi + ic\phi' + |\phi|^{2\sigma}\phi = 0, \quad \omega, c \in \mathbb{R}, \tag{2.3}$$

where $\phi$ is generally a complex-valued function and $\sigma > 0$; further restrictions will be placed on $c$, $\omega$, $\sigma$, and $\alpha$ later. Here and throughout, given a finite period $T > 0$ we consider for each $\alpha > 0$ the operator $\Lambda^\alpha$ as a closed operator on

$$L^2_{\text{per}}([0,2T];\mathbb{C}) := \left\{ f \in L^2_{\text{loc}}(\mathbb{R};\mathbb{C}) : f(x+2T) = f(x) \ \ \forall x \in \mathbb{R} \right\}$$

with dense domain $H^\alpha_{\text{per}}([0,2T];\mathbb{C})$, defined via its Fourier series as

$$\Lambda^\alpha f(x) = \sum_{n \in \mathbb{Z}\setminus\{0\}} \left|\frac{\pi n}{T}\right|^\alpha e^{\pi i n x/T} \hat{f}(n), \quad \alpha \geq 0.$$

We will be interested primarily in *standing* wave solutions of (2.1) with *real-valued* profiles, in which case $c = 0$. To motivate the expected structure of such solutions, we note that when $\alpha = 2$ and $c = 0$ the profile equation (2.3) is integrable and, upon integration, can be expressed as

$$\frac{1}{2}\left(\phi'\right)^2 = \mathcal{H} - V(\phi;\omega)$$

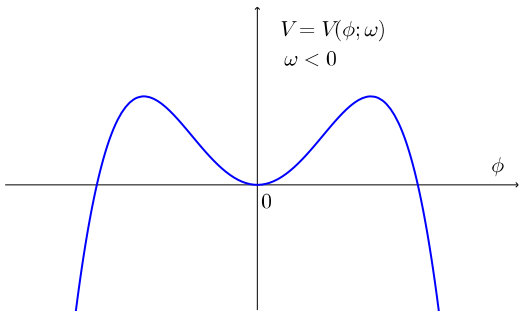


Figure 2.1: The effective potential $V(\phi;\omega)$ for the defocusing NLS with $\omega < 0$.

where $\mathcal{H} \in \mathbb{R}$ denotes the ODE energy and

$$V(\phi;\omega) := -\frac{\omega}{2}\phi^2 - \frac{1}{2\sigma+2}\phi^{2\sigma+2}$$

denotes the effective potential energy. Observe that the potential $V$ is even for every $\omega \in \mathbb{R}$ and, possesses a unique local minimum when $\omega < 0$, yielding the existence of a one-parameter family, of periodic orbits[1] parameterized by $\mathcal{H}$ that oscillate symmetrically about the equilibrium solution $\phi = 0$; see Figure 2.1. Further, up to translations these waves can be chosen to be even and *antiperiodic*, i.e. they satisfy

$$\phi(x+T) = -\phi(x)$$

where $2T > 0$ denotes the fundamental period of $\phi$. While such solutions can be expressed explicitly in terms of the Jacobi elliptic function $\mathrm{cn}$ when $\alpha = 2$, we are unaware of such an explicit solution formula for $\alpha \in (0,2)$. Nevertheless, for each $\alpha \in (1,2)$ and $T > 0$ we expect to be able to construct a three-parameter family of real-valued, $T$-antiperiodic solutions of the profile equation (2.3).

[1] When $\omega > 0$, the potential $V$ is strictly decreasing on $(0,\infty)$ and hence no nontrivial bounded solutions exist in this case.

Through a constrained minimization argument, we will construct real-valued, antiperiodic solutions of (2.3) with $c = 0$ as a member of a larger family of complex-valued, traveling waves with $c \neq 0$. See Remark 2.3.12. In the local case, the existence of such a family is apparent from an exact Galilean invariance; that is, if $u(x,t)$ solves (2.1) with $\alpha = 2$, then so does

$$\mathcal{G}_c u(x,t) = e^{\frac{icx}{2} - \frac{ic^2 t}{4}} u(x - ct, t) \tag{2.4}$$

for each wave speed $c \in \mathbb{R}$. However, when $\alpha \neq 2$ no such exact Galilean invariance exists, so the variational arguments below will construct a general class of antiperiodic traveling wave solutions of (2.1) of the form (2.2) with $|c|$ sufficiently small. With appropriate smoothness assumptions, the resulting wave at $c = 0$ can be taken to be real-valued, even, and decreasing on $(0,T)$ by applying rearrangement arguments.

To this end, for a fixed $T > 0$ we will use $L^2$-based Lebesgue and Sobolev spaces over the antiperiodic interval $[0,T]$. Define the *real* vector space

$$L^2_{\mathrm{a}}([0,T];\mathbb{C}) := \left\{ f \in L^2_{\mathrm{loc}}(\mathbb{R};\mathbb{C}) : f(x+T) = -f(x) \ \ \forall x \in \mathbb{R} \right\}$$

equipped with inner product $\langle u, v \rangle = \mathrm{Re} \int_0^T u\bar{v}\, dx$, and for each $\alpha \in (0,2)$ define

$$H^{\alpha/2}_{\mathrm{a}}([0,T];\mathbb{C}) := \left\{ f \in H^{\alpha/2}_{\mathrm{loc}}(\mathbb{R};\mathbb{C}) : f \in L^2_{\mathrm{a}}([0,T];\mathbb{C}) \right\} \tag{2.5}$$

considered as a *real* vector space with inner product

$$(u,v) := \mathrm{Re} \int_0^T (u\bar{v} + \Lambda^{\alpha/2} u \, \overline{\Lambda^{\alpha/2} v})\, dx.$$

Unless otherwise indicated, throughout this chapter we will denote

$$H^s_*(0,T) := H^s_*([0,T];\mathbb{C}),$$

where $*$ could be either "per", or "a". At times we may work with the subspace of *real-valued* functions $H^{\alpha/2}_{\text{a}}([0,T];\mathbb{R})$ in $H^{\alpha/2}_{\text{per}}(0,T)$; when the choice of scalar field is irrelevant or obvious from context, we will simply write $H^{\alpha/2}_{\text{a}}(0,T)$ for these spaces.

In applying machinery from functional analysis, it will be important that (2.5) is a Hilbert space, which we show here.

**Lemma 2.2.1.** *$H^{\alpha/2}_a(0,T)$ is a Hilbert space for all $\alpha > 1$.*

*Proof.* The space $H^{\alpha/2}_{\text{a}}(0,T)$ is clearly a subspace of $H^{\alpha/2}_{\text{per}}(0,T)$, so it only remains to show that $H^{\alpha/2}_{\text{a}}(0,T)$ is closed. Let $\{u_n\} \subset H^{\alpha/2}_{\text{a}}(0,T)$ be a convergent sequence in $H^{\alpha/2}_{\text{per}}(0,T)$ with limit $u_* \in H^{\alpha/2}_{\text{per}}(0,T)$. We will show that $u_* \in H^{\alpha/2}_{\text{a}}(0,T)$. Since $H^{\alpha/2}_{\text{a}}(0,T)$ $\subset H^{\alpha/2}_{\text{per}}(0,T) \Subset L^\infty(0,T)$, there exists a convergent subsequence $\{u_{n_j}\}$ in $L^\infty(0,T)$. By the above embedding, for $\alpha > 1$ there exists constant $C > 0$ such that

$$\|v\|_{L^\infty(0,T)} \leq C \|v\|_{H^{\alpha/2}_{\text{a}}(0,T)}$$

for all $v \in H^{\alpha/2}_{\text{a}}(0,T)$, hence

$$\left\|u_{n_j} - u_*\right\|_{L^\infty(0,T)} \leq C \left\|u_{n_j} - u_*\right\|_{H^{\alpha/2}_{\text{a}}(0,T)} \to 0 \quad \text{as } j \to \infty.$$

Now examine

$$|u_*(x+T) + u_*(x)| = \Bigg| u_*(x+T) \underbrace{-u_{n_j}(x+T) - u_{n_j}(x)}_{=0 \text{ since } u_{n_j} \text{ is } T\text{-antiperiodic}} + u_*(x) \Bigg|$$

$$
\begin{aligned}
&\leq \left|u_*(x+T)-u_{n_j}(x+T)\right| + \left|u_*(x)-u_{n_j}(x)\right| \\
&\leq 2\left\|u_*-u_{n_j}\right\|_{L^\infty(0,T)} \\
&\to 0 \quad \text{as } j\to\infty.
\end{aligned}
$$

Therefore $u_*(x+T)+u_*(x)=0$ for all $x\in(0,T)$, i.e. $u_*\in H_{\mathrm{a}}^{\alpha/2}(0,T)$. So, $H_{\mathrm{a}}^{\alpha/2}(0,T)$ is a closed subspace of the Hilbert space $H_{\mathrm{per}}^{\alpha/2}(0,T)$, which implies that $H_{\mathrm{a}}^{\alpha/2}(0,T)$ is itself a Hilbert space. □

Furthermore, we identify the dual space $H_{\mathrm{a}}^{\alpha/2}(0,T)^*$ with $H_{\mathrm{a}}^{-\alpha/2}(0,T)$ via the pairing

$$
\ell(v)=\langle w,v\rangle := \mathrm{Re}\int_0^T w\bar{v}\,dx, \quad \ell\in H_{\mathrm{a}}^{\alpha/2}(0,T)^*, \quad v\in H_{\mathrm{a}}^{\alpha/2}(0,T), \tag{2.6}
$$

where $w=w(\ell)\in H^{-\alpha/2}(0,T)$ is the unique element such that (2.6) holds for all $v\in H_{\mathrm{a}}^{\alpha/2}(0,T)$.

To begin the existence theory, we consider $\alpha>1$ and define the functionals

$$
K(u):=\frac{1}{2}\int_0^T |\Lambda^{\alpha/2}u|^2\,dx, \quad P(u):=\frac{1}{2\sigma+2}\int_0^T |u|^{2\sigma+2}\,dx
$$

on $H_{\mathrm{a}}^{\alpha/2}(0,T)$, which we refer to as the *kinetic* and *potential* energies, respectively. Then the fNLS (2.1) admits the conserved quantities

$$
\mathcal{H}(u):=K(u)+P(u)=\frac{1}{2}\int_0^T\left(\left|\Lambda^{\alpha/2}u\right|^2+\frac{1}{\sigma+1}|u|^{2\sigma+2}\right)dx, \tag{2.7}
$$

$$
Q(u):=\frac{1}{2}\int_0^T |u|^2\,dx, \tag{2.8}
$$

$$
N(u):=\frac{i}{2}\int_0^T \overline{\Lambda^{1/2}u}\,H\Lambda^{1/2}u\,dx, \tag{2.9}
$$

which we refer to as the *Hamiltonian (energy)*, *charge*, and *(angular) momentum*, respectively. By Noether's theorem, conservation of $\mathcal{H}$ is due to the fact that (2.1) is autonomous in time, while conservation of $Q$ and $N$ follow from the phase and translational invariance of (2.1), respectively. For smooth solutions, the momentum functional (2.9) is typically defined as $N(u) := \frac{i}{2}\int_0^T \bar{u}u_x\,dx$, but we may consider $u_x$ to be well-defined on $H_{\mathrm{a}}^{\alpha/2}(0,T)$ in the sense of distributions via integration by parts and the identity $\partial_x = H\Lambda$, where $H$ is the Hilbert transform, a bounded linear map from $L^2_{\mathrm{a}}(0,T) \to L^2_{\mathrm{a}}(0,T)$ with $\|Hf\|_{L^2} \leq \|f\|_{L^2}$, defined through Fourier multipliers as

$$\widehat{Hf}(\xi) := -i\,\mathrm{sgn}(\xi)\widehat{f}(\xi).$$

For a general $\alpha \in (1,2]$, the functionals $\mathcal{H}$, $Q$, and $N$ are smooth on $H_{\mathrm{a}}^{\alpha/2}(0,T)$, and their first order variational derivatives are smooth maps from $H_{\mathrm{a}}^{\alpha/2}(0,T)$ into $H_{\mathrm{a}}^{\alpha/2}(0,T)^*$ with the dual elements in $H_{\mathrm{a}}^{-\alpha/2}(0,T)$ given explicitly by

$$\delta\mathcal{H}(u) = \Lambda^\alpha u + |u|^{2\sigma}u, \quad \delta Q(u) = u, \quad \delta N(u) = iu_x.$$

(See Appendix A.) Then the fNLS profile equation (2.3) can be written in terms of these variational derivatives as

$$\delta\mathcal{H}(\phi) + \omega\,\delta Q(\phi) + c\delta N(u) = 0,$$

hence $T$-antiperiodic standing waves of (2.1) arise as critical points of the Lagrangian functional

$$H_{\mathrm{a}}^{\alpha/2}(0,T) \ni u \mapsto \mathcal{H}(u) + \omega Q(u) + cN(u)$$

for some $\omega, c \in \mathbb{R}$. Thus it would be natural to seek solutions of (2.3) as critical points of $\mathcal{H}$ subject to the conservation of $Q$ and $N$, treating both $\omega$ and $c$ as Lagrange multipliers. However, in the existence theory we will need precise information on the range of values of $c$ for which such a critical point exists, so it will be more appropriate to treat the wave speed as a free parameter and to attempt to construct solutions of (2.3) for a *fixed* $c$ as critical points of the functional

$$F_c(u) := \mathcal{H}(u) + cN(u) \tag{2.10}$$

subject to fixed $Q$.

**Proposition 2.2.2.** *Let $\alpha \in (1,2)$ and $T, \sigma > 0$ be fixed in the defocusing ($\gamma = -1$) fNLS (2.1). For each $\mu > 0$ define the constraint space*

$$\mathcal{A}_\mu := \left\{ u \in H_{\mathrm{a}}^{\alpha/2}(0,T) : Q(u) = \mu \right\}.$$

*Then for each $\mu > 0$ and $|c| < c_* := \left(\frac{\pi}{T}\right)^{\frac{\alpha-1}{2}}$ there exists a nontrivial $\phi = \phi(\cdot; c, \mu) \in \mathcal{A}_\mu$ such that*

$$F_c(\phi) = \min_{u \in \mathcal{A}_\mu} F_c(u)$$

*where $F_c$ is as in (2.10), and $\phi(\cdot; c, \mu)$ satisfies (2.3) for some $\omega = \omega(c, \mu) \in \mathbb{R}$ in the sense of distributions. Moreover, the function $\phi$ belongs to $H_{\mathrm{a}}^{\infty}(0,T)$ and minimizes the Lagrangian functional*

$$\mathcal{E}(u; c, \mu) := \mathcal{H}(u) + \omega(c, \mu) Q(u) + cN(u) \tag{2.11}$$

*over $H_{\mathrm{a}}^{\alpha/2}(0,T)$ subject to the fixed $Q \equiv \mu$ and $N \equiv N(\phi)$, specifically*

$$\mathcal{E}(\phi; c, \mu) = \inf \left\{ \mathcal{E}(\psi; c, \mu) : \psi \in \mathcal{A}_\mu, \;\; N(\psi) = N(\phi) \right\}.$$

To prove this proposition, we will first need the following technical lemmas:

**Lemma 2.2.3.** $|N(u)| \leq \left(\frac{T}{\pi}\right)^{\frac{\alpha-1}{2}} K(u)$ *for all* $u \in H^{\alpha/2}([0,T];\mathbb{C})$ *and* $\alpha > 1$.

*Proof.* Let $u \in H_a^{\alpha/2}([0,T];\mathbb{C})$. Then

$$\begin{aligned}
|N(u)| &\leq \frac{1}{2}\int_0^T \left|\Lambda^{1/2}u\right|\left|H\Lambda^{1/2}u\right| dx \\
&\leq \frac{1}{2}\left\|\Lambda^{1/2}u\right\|_{L^2(0,T)}\left\|H\Lambda^{1/2}u\right\|_{L^2(0,T)} \quad \text{by Cauchy-Schwarz} \\
&\leq \frac{1}{2}\left\|\Lambda^{1/2}u\right\|^2_{L^2(0,T)} \quad \text{since } H : L^2(0,T) \to L^2(0,T) \text{ is bounded with constant } 1 \\
&= \frac{T}{2}\cdot\left(\frac{\pi}{T}\right)^{1/2}\sum_{n\in\mathbb{Z}} |n|^{1/2}\,|\widehat{u}(n)|^2 \quad \text{by Parseval} \\
&\leq \frac{T}{2}\cdot\left(\frac{\pi}{T}\right)^{1/2}\sum_{n\in\mathbb{Z}} |n|^{\alpha/2}\,|\widehat{u}(n)|^2 \quad \text{for } \alpha > 1 \\
&= \frac{T}{2}\left(\frac{T}{\pi}\right)^{\frac{\alpha-1}{2}}\sum_{n\in\mathbb{Z}} \left|\frac{n\pi}{T}\right|^{\alpha/2}|\widehat{u}(n)|^2 \\
&= \frac{1}{2}\left(\frac{T}{\pi}\right)^{\frac{\alpha-1}{2}}\left\|\Lambda^{\alpha/2}u\right\|^2_{L^2(0,T)} \quad \text{by Parseval} \\
&= \left(\frac{T}{\pi}\right)^{\frac{\alpha-1}{2}} K(u).
\end{aligned}$$

□

**Lemma 2.2.4.** *Let* $u_k \to u$ *be a strongly convergent (i.e. in norm) sequence* $H^{1/2}(0,T)$. *Then* $\lim_{k\to\infty} N(u_k) = N(u)$.

*Proof.* Since $u_k \to u$ in norm in $H^{1/2}(0,T)$, there exists $M > 0$ such that $\|u_k\|_{H^{1/2}(0,T)} \leq M$ for all $k$. Recall that the Hilbert transform $H : L^2(0,T) \to L^2(0,T)$ is defined by $\widehat{Hf}(\xi) = -i\,\mathrm{sgn}(\xi)\widehat{f}(\xi)$. Now examine

$$-2i\left(N(u_k) - N(u)\right) = \left\langle H\Lambda^{1/2}u_k, u_k\right\rangle_{L^2(0,T)} - \left\langle H\Lambda^{1/2}u, u\right\rangle_{L^2(0,T)}$$

$$= \left\langle H\Lambda^{1/2}(u_k - u), u_k \right\rangle_{L^2(0,T)} - \left\langle H\Lambda^{1/2}u, u_k - u \right\rangle_{L^2(0,T)}$$
$$= \left\langle u_k - u, -H\Lambda^{1/2}u_k \right\rangle_{L^2(0,T)} - \left\langle H\Lambda^{1/2}u, u_k - u \right\rangle_{L^2(0,T)}.$$

Thus by Cauchy-Schwarz and the fact that $H : L^2(0,T) \to L^2(0,T)$ is bounded with sharp constant 1, we have

$$\begin{aligned} 2|N(u_k) - N(u)| &\leq \|u_k - u\|_{L^2(0,T)} \left\|\Lambda^{1/2}u_k\right\|_{L^2(0,T)} + \left\|\Lambda^{1/2}u\right\|_{L^2(0,T)} \|u_k - u\|_{L^2(0,T)} \\ &\leq \left(M + \left\|\Lambda^{1/2}u\right\|_{L^2(0,T)}\right) \|u_k - u\|_{L^2(0,T)} \\ &\to 0 \end{aligned}$$

as $k \to \infty$. Thus $N(u_k) \to N(u)$ as $k \to \infty$. □

**Lemma 2.2.5.** *$K$ is weakly lower semicontinuous on $H^{\alpha/2}(0,T)$.*

*Proof.* Let $u_k \rightharpoonup u$ weakly in $H^{\alpha/2}(0,T)$ and note that $u_k \mapsto \left\langle \Lambda^{\alpha/2}u_k, \Lambda^{\alpha/2}u \right\rangle_{L^2(0,T)}$ is a bounded linear functional on $H^{\alpha/2}(0,T)$ for fixed $u$. By Cauchy-Schwarz we have

$$\begin{aligned} \left\langle \Lambda^{\alpha/2}u_k, \Lambda^{\alpha/2}u \right\rangle_{L^2(0,T)} &\leq \left\|\Lambda^{\alpha/2}u_k\right\|_{L^2(0,T)} \left\|\Lambda^{\alpha/2}u\right\|_{L^2(0,T)} \\ &= 2K(u_k)^{1/2}K(u)^{1/2}, \end{aligned} \tag{2.12}$$

hence we have by weak convergence that

$$\begin{aligned} 2K(u) &= \lim_{k\to\infty} \left\langle \Lambda^{\alpha/2}u_k, \Lambda^{\alpha/2}u \right\rangle_{L^2(0,T)} \\ &= \liminf_{k\to\infty} \left\langle \Lambda^{\alpha/2}u_k, \Lambda^{\alpha/2}u \right\rangle_{L^2(0,T)} \\ &\leq 2K(u)^{1/2} \liminf_{k\to\infty} K(u_k)^{1/2} \quad \text{by (2.12)} \\ \implies K(u) &\leq \liminf_{k\to\infty} K(u_k). \end{aligned}$$

Thus $K$ is weakly lower semicontinuous on $H^{\alpha/2}(0,T)$. $\square$

*Proof of Proposition 2.2.2.* Fix $\mu > 0$ and consider the functional

$$F_c(u) := \mathcal{H}(u) + cN(u) = K(u) + cN(u) + P(u).$$

For $u \in \mathcal{A}_\mu$ we have

$$\begin{aligned} F_c(u) &= K(u) + cN(u) + P(u) \\ &\geq K(u) + cN(u) \\ &\geq K(u) - |c| \left(\frac{T}{\pi}\right)^{\frac{\alpha-1}{2}} K(u) \quad \text{by Lemma 2.2.3} \\ &= \left(1 - |c| \left(\frac{T}{\pi}\right)^{\frac{\alpha-1}{2}}\right) K(u). \end{aligned}$$

So, if $|c| < \left(\frac{T}{\pi}\right)^{\frac{\alpha-1}{2}} =: c_*$, then $F_c$ is bounded below (by zero) on $\mathcal{A}_\mu$, hence $\lambda := \inf_{u \in \mathcal{A}_\mu} F(u)$ is well-defined and there exists a minimizing sequence $\{u_k\} \subset \mathcal{A}_\mu$ such that $\lim_{k\to\infty} F(u_k) = \lambda$. Now examine

$$\begin{aligned} \frac{1}{2} \|u_k\|^2_{H^{\alpha/2}(0,T)} &= K(u_k) + Q(u_k) \\ &= F_c(u_k) - cN(u_k) - P(u_k) + \mu \\ &\leq F_c(u_k) + |c| \left(\frac{T}{\pi}\right)^{\frac{\alpha-1}{2}} K(u_k) - P(u_k) + \mu \quad \text{by Lemma 2.2.3} \\ &\leq F_c(u_k) + \frac{1}{2} |c| \left(\frac{T}{\pi}\right)^{\frac{\alpha-1}{2}} \|u_k\|^2_{H^{\alpha/2}(0,T)} + \mu, \end{aligned}$$

hence

$$\frac{1}{2} \left(1 - |c| \left(\frac{T}{\pi}\right)^{\frac{\alpha-1}{2}}\right) \left\|u_{k_j}\right\|^2_{H^{\alpha/2}(0,T)} \leq F_c(u_k) + \mu,$$

where the right-hand side of the above inequality is bounded since $\{F_c(u_k)\}$ is a convergent real sequence. Thus if $|c| < c_*$, then $\{u_k\}$ is bounded in $H^{\alpha/2}(0,T)$. By Banach-Alaoglu, there exists a subsequence $\{u_{k_j}\}$ converging weakly in $H^{\alpha/2}(0,T)$ to some $\phi \in H_{\mathrm{a}}^{\alpha/2}(0,T)$. Now, by Rellich-Kondrachov, there exists a further subsequence[2] such that $u_{k_j} \to \phi$ strongly (in norm) in $H^{1/2}(0,T)$. Moreover, since strong convergence implies weak convergence and weak limits are unique, there exists a further subsequence converging to $\phi$ strongly in $L^2(0,T)$. For this subsequence, we have

$$Q(\phi) = \frac{1}{2}\|\phi\|^2_{L^2(0,T)} = \lim_{j\to\infty} \frac{1}{2}\left\|u_{k_j}\right\|_{L^2(0,T)} = \lim_{j\to\infty} Q(u_{k_j}) = \mu,$$

thus $u \in \mathcal{A}_\mu$.

Now, since $u_{k_j} \rightharpoonup \phi$ (weak limits are unique) with $P$ compact on $H^{\alpha/2}(0,T)$ due to the compact Sobolev embedding $H_{\mathrm{a}}^{\alpha/2}(0,T) \Subset L^{2\sigma+2}(0,T)$ for $\sigma > 0$, there exists a further subsequence $\{u_{k_j}\}$ such that $\{P(u_{k_j})\}$ converges in $\mathbb{R}$. Also, by Lemma 2.2.4, we have

$$\liminf_{j\to\infty} N(u_{k_j}) = \lim_{j\to\infty} N(u_{k_j}) = N(\phi).$$

Since $K$ is weakly lower semicontinuous on $H^{\alpha/2}(0,T)$ by Lemma 2.2.5 and $P(\cdot)$ is the $L^{2\sigma+2}(0,T)$ norm (which is weakly lower semicontinuous), we have that

$$\liminf_{j\to\infty} F_c(u_{k_j}) \geq K(\phi) + cN(\phi) + P(\phi) = F_c(\phi).$$

Now, since $\phi \in \mathcal{A}$, we have by the definition of infimum that

$$\lambda \leq F_c(\phi) \leq \liminf_{j\to\infty} F_c(u_{k_j}) = \lim_{j\to\infty} F_c(u_{k_j}) = \lambda.$$

[2]To avoid the burden of excessive subscripts, going forward we will abuse notation by continuing to use $\{u_{k_j}\}$ to denote further subsequences.

Therefore $F_c(\phi) = \lambda$, so $\phi \in \mathcal{A}$ satisfies $F_c(\phi) = \inf_{u\in\mathcal{A}} F_c(u)$, hence by Lagrange multipliers there exists $\omega(c,\mu) \in \mathbb{R}$ such that

$$0 = \delta F_c(\phi) + \omega(c,\mu)\delta Q(\phi) = \Lambda^\alpha \phi + ic\phi' + |\phi|^{2\sigma}\phi + \omega\phi,$$

i.e. $\phi = \phi(\cdot; c, \mu)$ solves the profile equation (2.3), and we have that $u(x,t) = e^{i\omega t}\phi(x - ct)$ is a traveling wave solution of (2.1).

It remains to establish the $H^\infty$ smoothness of the solution $\phi \in H_{\mathrm{a}}^{\alpha/2}(0,T)$, which we will demonstrate via a bootstrap argument. To show that $\phi \in H_{\mathrm{a}}^{\alpha}(0,T)$, i.e. that it actually has twice its a-priori regularity, notice that for any $|c| < c_*$ the profile equation (2.3) can be written as

$$-\phi = (\Lambda^\alpha + ic\partial_x)^{-1}\left(\omega\phi + |\phi|^{2\sigma}\phi\right), \tag{2.13}$$

where the operator $(\Lambda^\alpha + ic\partial_x)^{-1}$ is guaranteed to be well-defined on $H_{\mathrm{a}}^{\alpha/2}(0,T)$ since the $T$-antiperiodic function $\phi$ has zero mean. Specifically, for $u \in H_{\mathrm{a}}^{\alpha/2}(0,T)$, the function $v = (\Lambda^\alpha + ic\partial_x)^{-1}u$ solves

$$(\Lambda^\alpha + ic\partial_x)v = u,$$

where $u$ is orthogonal to $\ker(\Lambda^\alpha + ic\partial_x) = \mathrm{span}\{1\}$ by antiperiodicity, hence such a $v$ exists by the Fredholm alternative. Moreover, note that if an operator $L$ has symbol $\widehat{L}(n)$, then $\widehat{L^{-1}}(n) = \left(\widehat{L}(n)\right)^{-1}$ since

$$\widehat{u}(n) = \widehat{L^{-1}Lu}(n) = \widehat{L^{-1}}(n)\widehat{L}(n)\widehat{u}(n) \implies \widehat{L^{-1}}(n) = \left(\widehat{L}(n)\right)^{-1}. \tag{2.14}$$

Applying $\Lambda^\alpha$ to both sides of (2.13), we have

$$-\Lambda^\alpha\phi = \Lambda^\alpha(\Lambda^\alpha + ic\partial_x)^{-1}(\omega\phi + |\phi|^{2\sigma}\phi),$$

and taking the $L^2(0,T)$ norm of both sides yields, by Parseval and (2.14),

$$\begin{aligned}\|\Lambda^\alpha \phi\|_{L^2(0,T)} &= \sqrt{T}\left\| \frac{|n|^\alpha}{|n|^\alpha - \left(\frac{T}{\pi}\right)^{\alpha-1} cn} \left(\omega\hat{\phi}(n) + \widehat{|\phi|^{2\sigma}\phi}(n)\right)\right\|_{\ell^2_n(\mathbb{Z}\setminus\{0\})} \\ &\lesssim \|\phi\|_{L^2(0,T)} + \||\phi|^{2\sigma}\phi\|_{L^2(0,T)} \\ &\lesssim \|\phi\|_{L^2(0,T)} + \|\phi\|^{2\sigma}_{L^\infty(0,T)}\|\phi\|_{L^2(0,T)} \\ &< \infty,\end{aligned} \tag{2.15}$$

where $\lesssim$ denotes less than or equal to, up to multiplication by a constant independent of $\phi$. The last inequality is due to the Sobolev embedding $H^{\alpha/2}_{\mathrm{a}}(0,T) \subset L^\infty(0,T)$.

So, $\phi \in H^\alpha_{\mathrm{a}}(0,T)$. We claim that $\Lambda^{2\alpha}\phi \in L^2(0,T)$ as well. Indeed,

$$\begin{aligned}\left\|\Lambda^{2\alpha}\phi\right\|_{L^2(0,T)} &= \|\Lambda^\alpha(\Lambda^\alpha\phi)\|_{L^2(0,T)} \\ &\lesssim \|\Lambda^\alpha\phi\|_{L^2(0,T)} + \left\|\Lambda^\alpha(|\phi|^{2\sigma}\phi)\right\|_{L^2(0,T)} \quad \text{by (2.15).}\end{aligned} \tag{2.16}$$

By the fractional Leibniz rule [14, Proposition 3.3], we have

$$\begin{aligned}\left\|\Lambda^\alpha(|\phi|^{2\sigma}\phi)\right\|_{L^2(0,T)} &\lesssim \|\phi\|^{2\sigma}_{L^\infty(0,T)} + \|\phi\|_{L^\infty(0,T)}\left\|\Lambda^\alpha|\phi|^{2\sigma}\right\|_{L^2(0,T)} \\ &\le \|\phi\|^{2\sigma}_{L^\infty(0,T)} + \|\phi\|_{L^\infty(0,T)}\left\|\Lambda^\alpha\phi^{2\sigma}\right\|_{L^2(0,T)} \quad \text{by Lemma (B.0.3).}\end{aligned}$$

By the fractional chain rule [34, (3.3)],

$$\left\|\Lambda^\alpha\phi^{2\sigma}\right\|_{L^2(0,T)} \lesssim \|\phi\|^{2\sigma-1}_{L^\infty(0,T)}\|\Lambda^\alpha\phi\|_{L^2(0,T)},$$

hence

$$\left\|\Lambda^\alpha(|\phi|^{2\sigma}\phi)\right\|_{L^2(0,T)} \lesssim \|\phi\|^{2\sigma}_{L^\infty(0,T)} + \|\phi\|_{L^\infty(0,T)}\|\phi\|^{2\sigma-1}_{L^\infty(0,T)}\|\Lambda^\alpha\phi\|_{L^2(0,T)}$$

$$= \|\phi\|_{L^\infty(0,T)}^{2\sigma} + \|\phi\|_{L^\infty(0,T)}^{2\sigma} \|\Lambda^\alpha \phi\|_{L^2(0,T)}$$
$$< \infty,$$

hence in (2.16) we finally have $\left\|\Lambda^{2\alpha}\phi\right\|_{L^2(0,T)} < \infty$, so $\phi \in H_{\mathrm{a}}^{2\alpha}(0,T)$. Iterating, we achieve $\phi \in H_{\mathrm{a}}^{\infty}(0,T)$.

Lastly, we show that $\phi(\cdot;c,\mu)$ minimizes $\mathcal{E}(u;c,\mu)$ with respect to fixed $Q \equiv \mu$ and $N \equiv N(\phi)$. Simply examine

$$\begin{aligned}
\inf_{\substack{Q(u)=\mu \\ N(u)=N(\phi)}} \mathcal{E}(u;c,\mu) &= \inf_{\substack{Q(u)=\mu \\ N(u)=N(\phi)}} (\mathcal{H}(u) + cN(u) + \omega Q(u)) \\
&= \inf_{\substack{Q(u)=\mu \\ N(u)=N(\phi)}} F_c(u) + \omega\mu \\
&= F_c(\phi) + \omega Q(\phi) \\
&= \mathcal{E}(\phi;c,\mu),
\end{aligned}$$

as claimed. □

To recap, for each $\alpha \in (1,2)$, $\sigma > 0$, $T > 0$, $|c| < c_*$ and $\mu > 0$, Proposition 2.2.2 produces a generally complex-valued function $\phi(\cdot;c,\mu) \in H_{\mathrm{a}}^{\infty}(0,T)$ and a $\omega(c,\mu) \in \mathbb{R}$ such that

$$\Lambda^\alpha \phi + \omega(c,\mu)\phi + ic\phi' + |\phi|^{2\sigma}\phi = 0, \quad Q(\phi) = \mu.$$

In particular, incorporating phase and translation invariances, for each half-period $T > 0$ we have constructed a four-parameter family of generally complex-valued $T$-antiperiodic smooth solutions of the defocusing fNLS (2.1):

$$u(x,t;c,\mu,\theta,\zeta) = e^{i(\omega(c,\mu)t-\theta)}\phi(x-ct+\zeta;c,\mu)$$

where $|c| < c_*$, $\mu > 0$, $\theta \in [0, 2\pi)$ and $\zeta \in \mathbb{R}$ are constants. These solutions are parameterized by the wave speed $c$, the charge $Q(u)$ of the wave, and the parameters $\theta$ and $\zeta$ with the phase and translation symmetries of the PDE (2.1). The remainder of this chapter focuses on the *standing* wave solutions of (2.1), which correspond to the above solutions with $c = 0$. Some important properties of and assumptions on the minimizer $\phi$ and the temporal frequency (Lagrange multiplier) $\omega$ at $c = 0$ are provided here.

**Lemma 2.2.6.** *The function $\omega = \omega(c, \mu) : (-c_*, c_*) \times \mathbb{R}_+ \to \mathbb{R}$ constructed in Proposition 2.2.2 is smooth in $c$, $\mu$ provided the minimizer $\phi(\cdot; c, \mu)$ and the functionals depend smoothly on $c, \mu$. Further, for each $\mu > 0$, the profile $\phi(\cdot; 0, \mu) \in H_a^\infty((0,T); \mathbb{C})$ satisfies the constrained variational problem*

$$\mathcal{E}(\phi; 0, \mu) = \inf \left\{ \mathcal{E}(\psi; 0, \mu) : \psi \in H_{\mathrm{a}}^{\alpha/2}(0,T),\ \ Q(\psi) = Q(\phi),\ \ N(\psi) = 0 \right\}, \tag{2.17}$$

*and there exists a real-valued profile $\phi_{\mathbb{R}}(\cdot; 0, \mu) \in H_a^\infty((0,T); \mathbb{R})$ that is even and strictly decreasing on $(0,T)$ which we will* assume *also satisfies (2.17).*

*Outside the proof of this lemma, we abuse notation and use $\phi(\cdot; 0, \mu)$ to denote the* real-valued *minimizer $\phi_R(\cdot; 0, \mu)$ at $c = 0$.*

*Proof.* A minimizer $\phi = \phi(\cdot, c, \mu)$ and a corresponding Lagrange multiplier $\omega(c, \mu)$ constructed per Proposition 2.2.2 satisfy the Euler-Lagrange equation

$$\Lambda^\alpha \phi + \omega(c, \mu)\phi + ic\phi' + |\phi|^{2\sigma} \phi = 0. \tag{2.18}$$

Since $\phi(\cdot; c, \mu)$ is such that $Q(\phi) = \mu > 0$, multiplying through (2.18) by $\bar{\phi}$ and integrating yields

$$2K(\phi(; c, \mu)) + 2\mu\omega(c, \mu) + 2cN(\phi(; c, \mu)) + \int_0^T |\phi(x; c, \mu)|^{2\sigma} \phi(x; c, \mu)\, dx = 0$$

$$\implies \omega(c,\mu) = -\frac{1}{\mu}\left[\mathcal{H}(\phi(\cdot;c,\mu)) + cN(\phi(\cdot;c,\mu)) + 2\sigma P(\phi(\cdot;c,\mu))\right].$$

Due to the smoothness of the functionals $\mathcal{H}$, $N$, and $P$, it follows that $\omega(c,\mu)$ depends smoothly on $c,\mu$ so long as $\phi(\cdot;c,\mu)$ depends smoothly on $c,\mu$.

The real-valued profile $\phi_{\mathbb{R}}(\cdot;0,\mu)$ at $c=0$ is obtained through the exact same minimization program as in Proposition 2.2.2, except working over the space $H_{\mathrm{a}}^{\alpha/2}((0,T);\mathbb{R})$ of real-valued functions instead of the space $H_{\mathrm{a}}^{\alpha/2}((0,T);\mathbb{C})$ of complex-valued functions. Since $H_{\mathrm{a}}^{\alpha/2}((0,T);\mathbb{R}) \subset H_{\mathrm{a}}^{\alpha/2}((0,T);\mathbb{C})$, the minimizer of $F_c$ over the space of real-valued functions may a-priori not be a minimizer of $F_c$ over the space of complex-valued functions. Nevertheless, going forward we will assume that

$$F_c(\phi_{\mathbb{R}}(\cdot;0,\mu)) = \min_{\substack{u\in H_{\mathrm{a}}^{\alpha/2}((0,T);\mathbb{R}) \\ Q(u)=\mu}} F_c(u) = \min_{\substack{u\in H_{\mathrm{a}}^{\alpha/2}((0,T);\mathbb{C}) \\ Q(u)=\mu}} F_c(u) = F_c(\phi(\cdot;0,\mu)) \tag{2.19}$$

in order to apply rearrangement inequalities to obtain the desired parity and monotonicity properties for later analysis. See Remark 2.2.7 for further discussion.

Outside this lemma, we will abuse notation and use $\phi(\cdot;0,\mu)$ to denote the *real-valued* minimizer $\phi_{\mathbb{R}}(\cdot;0,\mu)$ at $c=0$, and the parity and monotonicity of $\phi(\cdot;0,\mu) := \phi_{\mathbb{R}}(\cdot;0,\mu)$ now follow from the $2T$-periodic rearrangement arguments outlined in Appendix B. □

*Remark* 2.2.7. In the nonlocal case, it is a difficult open problem to prove the smoothness of minimizers and the Lagrange multiplier on parameters $c$ and $\mu$ without an a-priori convexity (positive-definiteness) assumption on the energy functional. So, we make such smoothness assumptions for our analysis, which depends on differentiating with respect to parameters $c$ and $\mu$.

As evidence that complex-valued minimizers may be taken to be real at $c=0$, i.e. that (2.19) holds, we claim that $N(\phi(\cdot;0,\mu)) = 0 = N(\phi_{\mathbb{R}}(\cdot;0,\mu))$. That is, the complex-valued

minimizer has zero angular momentum, same as any real-valued minimizer. To this end, observe that since $\phi(\cdot;c,\mu)$ minimizes $F_c$ subject to fixed $Q \equiv \mu$, we have

$$\begin{aligned} & F_c(\phi(\cdot;c,\mu)) \leq F_c(\overline{\phi}(\cdot;c,\mu)) \\ \implies & cN(\phi(\cdot;c,\mu)) \leq cN(\overline{\phi}(0;c,\mu)) = -cN(\phi(0;c,\mu)), \end{aligned}$$

hence

$$cN(\phi(\cdot;c,\mu)) \leq 0 \quad \text{for all } |c| < c_*.$$

Then

$$N(\phi(\cdot;c,\mu)) \leq 0 \quad \text{if } c > 0 \quad \text{and} \quad N(\phi(\cdot;c,\mu)) \geq 0 \quad \text{if } c < 0,$$

and it must be that $N(\phi(\cdot;0,\mu)) = 0 = N(\phi_R(\cdot;0,\mu))$ provided $N(\phi(\cdot;c,\mu))$ is continuous at $c = 0$.

In conclusion, for fixed $\alpha \in (1,2)$ and $\sigma > 0$, we have constructed for each $T > 0$ a three-parameter family of *real-valued, $T$-antiperiodic, even* solutions of the profile equation (2.3) with $c = 0$. These profiles lead to a three-parameter family of *standing wave* solutions of (2.1) of the form

$$u(x,t;\mu,\beta,x_0) = e^{i(\omega(0,\mu)t+\beta)}\phi(x-x_0;0,\mu)$$

Going forward, we will restrict our attention to these real-valued profiles with $c = 0$. However, as stated previously, the fact that such solutions belong to a larger class of complex-valued traveling waves will be used heavily in the upcoming analysis; see Remark 2.3.12. For notational simplicity, we will also suppress the dependence of $\omega$ and $\phi$ on the wave speed $c$ whenever it is clear from context that $c = 0$.

## 2.3 Nondegeneracy of the Linearization in the Defocusing Case

Throughout this section, for each $\mu > 0$ we let $\phi(x;\mu)$ denote a real-valued, even, $T$-antiperiodic standing wave solution of the nonlocal profile equation (2.3) with $c = 0$ satisfying $Q(\phi) = \mu$, whose existence is guaranteed by Proposition 2.2.2 and Lemma 2.2.6, so that the function $u(x,t;\mu) = e^{i\omega(\mu)t}\phi(x;\mu)$ is a $T$-antiperiodic standing wave solution of the defocusing ($\gamma = -1$) fNLS (2.1) Moving to a co-rotating coordinate frame, the profile $\phi(\cdot;\mu)$ is thus a real-valued, $T$-antiperiodic equilibrium solution of the PDE

$$iu_t - \omega(\mu)u - \Lambda^\alpha u + \gamma|u|^{2\sigma}u = 0, \tag{2.20}$$

which can be rewritten as the Hamiltonian system

$$u_t = -i\,\delta\mathcal{E}(u;0,\mu)$$

acting on $L^2_{\text{per}}(0,2T)$, where here $\mathcal{E}$ is the modified energy functional defined in (2.11). For such Hamiltonian systems, it is well known that the local dynamics of (2.20) near $\phi$, in particular its orbital stability or instability, is intimately related to spectral properties of the second variation of the energy functional

$$\delta^2\mathcal{E}(\phi;c,\mu) = \Lambda^\alpha + \omega(\mu) + ic\partial_x - \gamma\,|\phi|^{2\sigma} - 2\gamma\sigma\,|\phi|^{2\sigma-2}\,\phi\,\text{Re}(\bar{\phi}\,\cdot) \tag{2.21}$$

acting on appropriate subspaces of $L^2_{\text{per}}(0,2T)$. See Appendix A for further details about computing the second variations of the component functionals of (2.21). Of particular importance, note that the operator $\delta^2\mathcal{E}(\phi)$ has $T$-periodic coefficients due to the $T$-antiperiodicity of $\phi$. As we will see below, however, the phase and translation symmetries of (2.20) gen-

erate elements of the kernel of $\delta^2\mathcal{E}(\phi)$ that are $T$-antiperiodic, hence zero is an isolated eigenvalue with finite multiplicity of $\delta^2\mathcal{E}(\phi)$ acting on $L^2_{\mathrm{a}}(0,T)$. We will restrict our attention to $T$-antiperiodic perturbations of the underlying wave $\phi$, which will necessitate a detailed spectral analysis of the operator $\delta^2\mathcal{E}(\phi)$ acting on $L^2_{\mathrm{a}}(0,T)$.

To aid in the analysis, it will be convenient to decompose the action of $\delta^2\mathcal{E}(\phi)$ into real and imaginary parts: for a real-valued, stationary background wave $\phi$ constructed in Lemma 2.2.6 when $c=0$, expressing a given $v \in H^\alpha_{\mathrm{a}}(0,T)$ as $v = a+bi$ for $a,b$ real-valued and applying (2.21) yields

$$\begin{aligned}\delta^2\mathcal{E}(\phi;0,\mu)(v) &= \left[\Lambda^\alpha a + \omega(0,\mu)a - \gamma(2\sigma+1)\phi^{2\sigma}a\right] + i\left[\Lambda^\alpha b + \omega(0,\mu)b - \gamma\phi^{2\sigma}b\right] \\ &=: L_+ a + iL_- b,\end{aligned}$$

where $L_\pm$ are linear operators acting on $L^2_{\mathrm{a}}([0,T];\mathbb{R})$ defined by

$$L_+ := \Lambda^\alpha - \gamma(2\sigma+1)\phi^{2\sigma} + \omega \tag{2.22}$$

$$L_- := \Lambda^\alpha - \gamma\phi^{2\sigma} + \omega. \tag{2.23}$$

Consequently, we can study $\delta^2\mathcal{E}(\phi)$ as the matrix operator $\mathrm{diag}(L_+, L_-)$ acting on the product space $L^2_{\mathrm{a}}([0,T];\mathbb{R}) \times L^2_{\mathrm{a}}([0,T];\mathbb{R})$. Concerning the spectrum of $\delta^2\mathcal{E}(\phi)$, observe that $\delta^2\mathcal{E}(\phi)$ is bounded below and self-adjoint on $L^2_{\mathrm{a}}(0,T)$ with compactly embedding domain $H^\alpha_{\mathrm{a}}(0,T)$. So, the spectrum of $\delta^2\mathcal{E}(\phi)$, and hence of the operators $L_\pm$, acting on $L^2_{\mathrm{a}}(0,T)$ is comprised of a countably infinite discrete set of real eigenvalues tending to $+\infty$ with no finite accumulation point. An important component in the stability analysis of $\phi$ will be to determine the number of negative $T$-antiperiodic eigenvalues of $\delta^2\mathcal{E}(\phi)$, as well as to enumerate its $T$-antiperiodic kernel. We now turn our attention to these matters.

Differentiating with respect to the symmetries of (2.20) yields eigenfunctions in the kernel of $\delta^2\mathcal{E}(\phi)$. To find the translation symmetry eigenfunction, note that if $(x,t) \mapsto e^{i\omega t}\phi(x)$ solves (2.1), then so does $(x,t) := e^{i\omega t}\phi(x + \Delta x)$. Taylor expanding

$$e^{i\omega t}\phi(x+\Delta x) = e^{i\omega t}(\phi(x)+\phi'(x)\Delta x+\mathcal{O}(\Delta x^2))$$

and substituting into (2.1) yields

$$\begin{aligned}(\Lambda^\alpha\phi+\gamma\phi^{2\sigma}\phi+\omega\phi)+(\Lambda^\alpha\phi'-\gamma(2\sigma+1)\phi^{2\sigma}\phi'+\omega\phi')\Delta x = \mathcal{O}(\Delta x^2)\\ \implies \Lambda^\alpha\phi'-\gamma(2\sigma+1)\phi^{2\sigma}\phi'+\omega\phi' = \mathcal{O}(\Delta x) \quad \text{by (2.3) at } c=0.\end{aligned}$$

Taking $\Delta x \to 0$, we have

$$L_+\phi' = 0, \tag{2.24}$$

hence $\operatorname{span}\{\phi'\} \subseteq \ker(L_+)$. To find the phase symmetry eigenfunction, note that if $(x,t) \mapsto e^{i\omega t}\phi(x)$ solves (2.1), then so does $u(x,t) := e^{i\omega t+\beta}\phi(x)$ for $\beta \in \mathbb{C}$, and substituting into (2.1) immediately yields

$$0 = \Lambda^\alpha\phi - \gamma|\phi|^{2\sigma}\phi+\omega\phi = L_-\phi,$$

hence $\operatorname{span}\{\phi'\} \subseteq \ker(L_-)$. Thus $\phi'$ and $\phi$ belong to the $T$-antiperiodic kernel of the $T$-periodic coefficient operators $L_+$ and $L_-$, respectively. In general, it is very difficult to determine whether these are the *only* nontrivial functions in the $T$-antiperiodic kernels, i.e. that $\ker(L_+) = \operatorname{span}\{\phi'\}$ and $\ker(L_-) = \operatorname{span}\{\phi\}$. Indeed, $T$-antiperiodic eigenvalues of a Schrödinger operator with $T$-periodic potential need not be simple, even in the local case. Hence standard Perron-Frobenius arguments fail to characterize the ground state eigenvalues of $\delta^2\mathcal{E}(\phi)$ on $L^2_{\text{a}}(0,T)$. Moreover, determining the number of $T$-antiperiodic

negative eigenvalues of $\delta^2\mathcal{E}(\phi)$ often involves classical Sturm-Liouville type arguments. Per the classical Sturm-Liouville theory of periodic functions in the local case, the fact that $\phi \in \ker(L_-)$ has one zero on $[0,T)$ implies that $\lambda = 0$ is either the first or second antiperiodic eigenvalue, so $L_-$ can have at most one negative antiperiodic eigenvalue. Similarly, since $\phi' \in \ker(L_+)$ has one zero on $[0,T)$, we have that $\lambda = 0$ is either the first or second antiperiodic eigenvalue of $L_+$, hence $L_+$ can have at most one negative antiperiodic eigenvalue. Altogether, $\delta^2\mathcal{E}(\phi)\Big|_{L^2_{\mathrm{a}}(0,T)}$ could potentially have at most *two* negative eigenvalues, which is typically an unfavorable configuration for orbital stability due to the overwhelming difficulty of controlling two negative directions. However, classical Sturm-Liouville arguments do not apply to the operators $L_\pm$ when $\alpha \in (1,2)$, so alternative methods will be necessary in order to determine the number of negative eigenvalues of $\delta^2\mathcal{E}(\phi)$, which we will handle in part by studying the action of $\delta^2\mathcal{E}(\phi)$ separately on the even and odd subspaces of $L^2_{\mathrm{a}}(0,T)$. We obtain the following nondegeneracy result:

**Proposition 2.3.1** (Nondegeneracy)**.** *Let $\alpha \in (1,2)$ and $\sigma > 0$ in the defocusing ($\gamma = -1$) fNLS (2.1). Let $\phi(\cdot;\mu) := \phi(\cdot, c = 0, \mu) \in H^{\alpha/2}_{\mathrm{a}}(0,T)$ be a real-valued local minimizer of $\mathcal{H}$ over $H^{\alpha/2}_{\mathrm{a}}(0,T)$ subject to fixed $Q(u) = \mu > 0$ and $N(u) = 0$, as constructed in Lemma 2.2.6, and assume that $\phi$ and the associated Lagrange multiplier $\omega$ depend on $c$ in a $C^1$ manner near $c = 0$. Then the associated Hessian operator $\delta^2\mathcal{E}(\phi)$ acting on $L^2_{\mathrm{a}}(0,T)$ is nondegenerate, i.e.*

$$\ker(\delta^2\mathcal{E}(\phi)) = \operatorname{span}\left\{\phi', i\phi\right\}$$

*and $n_-(\delta^2\mathcal{E}(\phi)) = 1$. Specifically, the operators $L_\pm$ are nondegenerate acting on $L^2_{\mathrm{a}}(0,T)$ with*

$$\ker\left(L_+\right) = \operatorname{span}\{\phi'\} \quad \textit{and} \quad \ker(L_-) = \operatorname{span}\{\phi\}.$$

*Moreover,* $n_-(L_+) = 0$ *and* $n_-(L_-) = 1$*, where the* Morse index *of a linear operator* $\mathcal{L}$ *is defined as* $n_-(\mathcal{L}) := \#\left\{\lambda \in \sigma_{L^2_a(0,T)}(\mathcal{L}) : \lambda < 0\right\}$.

*Remark* 2.3.2. In the above proposition, we must view the minimizer $\phi(\cdot;\mu)$ as a standing wave within larger family of traveling waves $\phi(\cdot;c,\mu)$, with $\phi(\cdot;c=0,\mu) = \phi(\cdot;\mu)$. In the local case when $\alpha = 2$, this embedding follows by an exact Galilean symmetry. Indeed, by (2.4), if $u(x,t) = e^{i\omega_0 t}\phi(x)$ for real-valued profile $\phi(x)$ and $\omega_0 \in \mathbb{R}$ solves NLS, then so does

$$\begin{aligned}\mathcal{G}_c u(x,t) &= e^{\frac{icx}{2} - \frac{ic^2 t}{4}} e^{i\omega_0 t}\phi(x-ct) \\ &= e^{i\omega(c)t}\,\widetilde{\phi}(x-ct),\end{aligned}$$

where $\widetilde{\phi}(x) := e^{icx/2}\phi(x)$ is complex-valued and $\omega(c) = \omega_0 + c^2/2$ is smooth in $c$. Furthermore, stability results for solitary and periodic waves in the local context fundamentally rely on the ability to differentiate $\phi$ and $\omega$ with respect to parameters, allowing one to connect the geometry and smoothness of the manifold of solutions to the associated stability theory; see, for example, the discussion immediately following the proof of Proposition 2.3.1 below. In this nonlocal context, however, we have yet to obtain this smoothness result, and we consider this an interesting direction for future research. Our methods depend heavily on $\phi$ and $\omega$ depending smoothly on $c$ near $c = 0$ (as in the analysis in the local case $\alpha = 2$), so we will take these as assumptions in the subsequent analysis; see Remark 2.3.12 below. Furthermore, it is important to note that even in cases where such smooth dependence is given a-priori, nondegeneracy is still represents a formidable problem. Finally, we note that while the smooth dependence of $\phi$ and $\omega$ on $\mu$ is not needed for this nondegeneracy theory, it will play a role in the upcoming stability theory. See Remark 2.4.2.

As noted in the introduction, Proposition 2.3.1 was established using ODE techniques in the local case $\alpha = 2$ by Gallay and Haragus [26]. Precisely, their proof uses Sturm-Liouville theory for (local) differential operators, together with a homotopy argument and a-priori control over the dimension of the $T$-antiperiodic kernels. While these ODE-based techniques are not directly available in the nonlocal setting $\alpha \in (0,2)$, Frank and Lenzmann [25] recently obtained the nondegeneracy of the linearization about solitary waves for a family of nonlinear nonlocal models that include the *focusing* ($\gamma = +1$) fNLS (2.1). Their idea was to find a suitable replacement for the Sturm-Liouville oscillation theory to control the number of sign changes in eigenfunctions for a fractional Schrödinger operator with real, localized potential. This theory, developed on the line, was then adapted to the periodic setting in [39], which studies the nonlinear orbital stability of $T$-periodic traveling wave solutions to the fractional gKdV equation.

The proof of Proposition 2.3.1 extends these previous nondegeneracy results to encompass the *$T$-antiperiodic spectra* of fractional Schrödinger operators with real, $T$-periodic potentials. As mentioned above, this extension is significant as, even in the classical $\alpha = 2$ case, the ground state antiperiodic eigenvalue of $T$-periodic linear Schrödinger type operators need not be simple. This is in stark contrast to the ground state $T$-periodic eigenvalues of such operators, which are *always simple* by Perron-Frobenius theory. While our proof follows the basic strategy in [25] and [39], substantial modifications are necessary to accommodate the antiperiodic structure of the admissible class of perturbations.

Two analytical results are key in establishing Proposition 2.3.1. First, we require an appropriate characterization of the ground state eigenfunctions of $L_\pm$ acting on $L^2_{\mathrm{a}}(0,T)$. A natural approach is to attempt a Perron-Frobenius argument, demonstrating that the semigroups $e^{-L_\pm t}$ are positivity improving on appropriate subspaces of $L^2_{\mathrm{a}}(0,T)$. Second, we require a nonlocal Sturm-Liouville type oscillation theory for the second antiperiodic eigenfunctions of $L_\pm$. Following the general ideas in [25] and [39], this is accomplished

by extending the antiperiodic eigenvalue problems for $L_{\pm}$ on $L^2_{\mathrm{a}}(0,T)$ to appropriate local problems on the upper half-space.

### 2.3.1 Ground State Theory for Antiperiodic Eigenfunctions

The goal of this section is to provide a characterization of the antiperiodic ground state eigenfunctions for linear, fractional Schrödinger operators of the form

$$L := \Lambda^{\alpha} + V(x), \tag{2.25}$$

where the potential $V(x)$ is even, real-valued, smooth and $T$-periodic for some finite $T > 0$. In particular, we will classify properties of the $T$-antiperiodic ground state for $L$, along with upper bounds on the number sign changes on higher $T$-antiperiodic eigenfunctions. As noted in the introduction, even in the local case $\alpha = 2$ such results are nontrivial, as $T$-antiperiodic ground states need not be simple. As we will see below, this comes from the fact that the semigroup generated by $L$ is not positivity improving when acting on $L^2_{\mathrm{a}}(0,T)$. To handle this difficulty, we will decompose the space $L^2_{\mathrm{a}}(0,T)$ of real-valued $T$-antiperiodic functions on $\mathbb{R}$ into the (invariant) even and odd subspaces, and develop ground state and oscillation theories for the operator $L$ in each subspace separately. As we will see, restricted to these subspaces, the semigroup generated by $L$ will indeed be positivity improving. Finally, using rearrangement properties we find an ordering between the antiperiodic odd and even ground state eigenvalues for $L$ in terms of monotonicity properties of the potential $V$ on $(0,T)$.

We begin by observing that the $T$-periodicity of the potential $V$ implies that the operator $L$ is well-defined as a closed, densely defined operator from $L^2_{\mathrm{a}}(0,T)$ into itself. Since $V$ is a bounded and smooth potential, the operator $L$ is a relatively compact perturbation of the operator $-\Lambda^{\alpha}$, hence Theorem XIII.44 from [55] implies that the ground state eigenvalues

of $L$ acting on an invariant subspace $\mathcal{Y}$ of $L^2_{\mathrm{a}}(0,T)$ is simple as an eigenvalue of $L|_{\mathcal{Y}}$ provided the fractional heat semigroup $\left\{e^{-\Lambda^\alpha t}\right\}_{t\geq 0}$ is positivity improving on $\mathcal{Y}$; that is, if

$$f \in \mathcal{Y},\ \ f \geq 0,\ \ f \neq 0 \quad \Longrightarrow \quad e^{-\Lambda^\alpha t} f > 0 \ \text{ on } \ \mathcal{Y}.$$

Thus, it is sufficient to study the semigroup generated by $-\Lambda^\alpha$ on $L^2_{\mathrm{a}}(0,T)$, which we study below by first considering the semigroup acting on $L^2(\mathbb{R})$ and appropriately periodizing its integral kernel.

The semigroup $e^{-\Lambda^\alpha t}$ acting on $L^2(\mathbb{R})$ is naturally understood via the Fourier transform

$$\mathcal{F}(f)(\xi) := \frac{1}{\sqrt{2\pi}} \int_{\mathbb{R}} e^{-i\xi x} f(x)\, dx,$$

which maps the Schwartz space $\mathcal{S}(\mathbb{R})$ to the space of tempered distributions $\mathcal{S}'(\mathbb{R})$ with inverse

$$\mathcal{F}^{-1}(f)(x) := \frac{1}{\sqrt{2\pi}} \int_{\mathbb{R}} e^{i\xi x} f(\xi)\, d\xi.$$

For all $t \geq 0$, the operators $e^{-\Lambda^\alpha t}$ acting on $\mathcal{S}(\mathbb{R})$ can be understood via

$$e^{-\Lambda^\alpha t} f(x) = \mathcal{F}^{-1}\left(e^{-|\cdot|^\alpha t} \widehat{f}(\cdot)\right)(x) = \frac{1}{\sqrt{2\pi}} \int_{\mathbb{R}} e^{-|\xi|^\alpha t} \widehat{f}(\xi) e^{i\xi x}\, d\xi, \tag{2.26}$$

which, using the convolution theorem, we may write

$$e^{-\Lambda^\alpha t} f(x) = \int_{\mathbb{R}} K(x-y,t) f(y)\, dy,$$

where $K$ is given by

$$K(x,t) := \mathcal{F}^{-1}\left(e^{-|\cdot|^\alpha t}\right)(x).$$

See Figure 2.2. Note that when $\alpha = 2$, the convolution kernel $K$ agrees with the standard

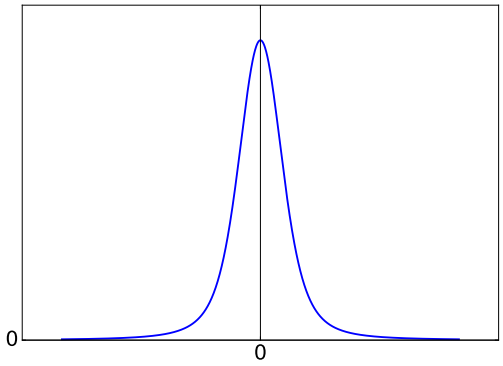


Figure 2.2: $K(x,t=0.3)$, with $\alpha = 3/2$. As expected, $K(\cdot,t)$ resembles a Gaussian.

Gauss-Weierstrass heat kernel and can be expressed explicitly as

$$K(x,t) = \frac{1}{\sqrt{2t}} e^{-x^2/(4t)}.$$

While such explicit formulas are not available in the nonlocal case $\alpha \in (0,2)$, in the recent work of Frank & Lenzmann [25, Appendix A] it was observed that, for all $t > 0$ and $\alpha \in (0,2)$, the kernel $K(\cdot,t)$ is even, strictly positive, and decays rapidly as $|x| \to \infty$ with $\partial_x K(x,t) < 0$ for all $x > 0$. Further, $K(\cdot,t) \in L^1(\mathbb{R})$ since, by the positivity of $K$,

$$\|K(\cdot,t)\|_{L^1(\mathbb{R})} = \int_{\mathbb{R}} K(x,t)\,dx = \mathcal{F}(K(\cdot,t))(\xi = 0) = 1.$$

Since we are interested in developing a $T$-antiperiodic oscillation theory for operators of the form (2.25), we now describe how $e^{-\Lambda^\alpha t}$ acts on periodic functions. Since $K(\cdot,t) \in L^1(\mathbb{R})$ for all $t > 0$, given any $2T$-periodic $f \in L^\infty(\mathbb{R})$ we can express the action of the semigroup $e^{-\Lambda^\alpha t}$ on $\mathbb{R}$ in terms of $K$ acting on $2T$-periodic cells:

$$e^{-\Lambda^\alpha t} f(x) = \int_{\mathbb{R}} K(x-y,t) f(y)\,dy$$

$$
\begin{aligned}
&= \sum_{n\in\mathbb{Z}} \int_{(2n-1)T}^{(2n+1)T} K(x-y,t) f(y)\, dy \\
&= \int_{-T}^{T} \left( \sum_{n\in\mathbb{Z}} K(x-y+2nT,t) \right) f(y)\, dy \\
&= \int_{-T}^{T} K_p(x-y,t) f(y)\, dy,
\end{aligned}
$$

where

$$
K_p(x,t) := \sum_{n\in\mathbb{Z}} K(x+2nT,t) \tag{2.27}
$$

represents the $2T$-periodic *periodization* of the integral kernel $K$. See Figure 2.3. Observe that the sum defining $K_p$ is absolutely convergent for each $t>0$ due to the rapid decay of $K(\cdot,t)$ at spatial infinity. Important properties of the periodized kernel $K_p$ are collected

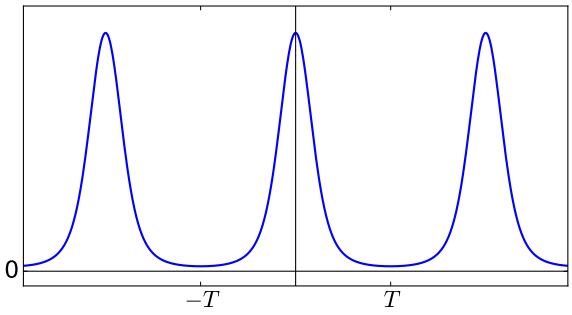


Figure 2.3: $K_p(x,t=0.3)$, with $\alpha = 3/2$.

here.

**Lemma 2.3.3.** *For all $t>0$ and $\alpha\in(0,2]$, $K_p(\cdot,t)$ is positive, even, $2T$-periodic, and strictly decreasing on $(0,T)$.*

*Proof.* The kernel $K(x,t)$ on $\mathbb{R}$ was shown by Frank & Lenzmann [25, Appendix A] to be even and positive for all $t>0$, $x\in\mathbb{R}$. Since $K(\cdot,t)\in L^1(\mathbb{R})$ for all $t>0$, the representation (2.27) implies that the periodization $K_p(\cdot,t)$ must also be even, positive and $2T$-periodic for all $t>0$. To prove that $K_p(\cdot,t)$ is decreasing on $(0,T)$ for each $t>0$, we follow [25] and

observe that the function $g(z) = e^{-z^{\alpha/2}}$ is completely monotone on the positive half-line $(0,\infty)$ for all $\alpha \in (0,2]$; that is, $(-1)^j \partial_z^j g(z) \geq 0$ for all $j \in \mathbb{N}$ and $z > 0$. Thus by Bernstein's theorem, $g$ is the Laplace transform of a non-negative finite measure $\nu_\alpha$ depending on $\alpha$, i.e. $e^{-z^{\alpha/2}} = \int_0^\infty e^{-\tau z} d\nu_\alpha(\tau)$. Setting $z = |x|^2$, the inverse Fourier transform of the Gaussian $e^{-\tau\xi^2}$ leads to the "subordination formula"[3]

$$K(x,t) = t^{-1/\alpha} \int_0^\infty \frac{1}{\sqrt{2\tau}} \exp\left(-\frac{t^{-2/\alpha}x^2}{4\tau}\right) d\nu_\alpha(\tau) \tag{2.28}$$

which is valid for all $x \in \mathbb{R}$ and $t > 0$. Periodizing (2.28) over $2T$-periodic cells as was done to derive (2.27), it follows that for all $\alpha \in (0,2)$ the $2T$-periodic kernel $K_p$ can be expressed as

$$\begin{aligned} K_p(x,t) &= t^{-1/\alpha} \int_0^\infty \frac{1}{\sqrt{2\tau}} \left[\sum_{n\in\mathbb{Z}} \exp\left(-\frac{(x+2nT)^2}{4t^{2/\alpha}\tau}\right)\right] d\nu_\alpha(\tau) \\ &= t^{-2/\alpha}\sqrt{2\pi} \int_0^\infty \left[\sum_{n\in\mathbb{Z}} \frac{1}{\sqrt{4\pi u}} \exp\left(-\frac{(x+2nT)^2}{4u}\right)\right] d\nu_\alpha(u), \end{aligned}$$

where the final equality follows from the variable substitution $u = t^{2/\alpha}\tau$. The integrand above may be recognized as the $2T$-periodized Gauss-Weierstrass kernel

$$\vartheta_u(x) := \sum_{n\in\mathbb{Z}} \frac{1}{\sqrt{4\pi u}} \exp\left(-\frac{(x+2nT)^2}{4u}\right), \tag{2.29}$$

hence we may express $K_p(x,t)$ concisely as

$$K_p(x,t) = t^{-2/\alpha}\sqrt{2\pi} \int_0^\infty \vartheta_u(x)\, d\nu_\alpha(u).$$

[3]This subordination formula is stated in [25] for the case $t = 1$ only. This more general formula follows from the scaling $K(x,t) = t^{-1/\alpha} K(t^{-1/\alpha}x, 1)$.

The monotonicity properties of the function $\vartheta_u(x)$ have been studied in [2, Theorem 4.2], where it was shown[4] to be strictly decreasing in $x$ on $(0,T)$ for all $u>0$. It now clearly follows that if $x,y\in(0,T)$ with $x<y$, then

$$K_p(y,t)-K_p(x,t)=t^{-2/\alpha}\sqrt{2\pi}\int_0^\infty(\vartheta_u(y)-\vartheta_u(x))\,d\nu_\alpha(u)<0,$$

i.e. $K_p(\cdot,t)$ is decreasing on $(0,T)$ for all $t>0$, as claimed. □

*Remark* 2.3.4. The subordination formula (2.28) conveniently encodes all spatial dependence on $\alpha$ into the non-negative measure $\nu_\alpha$, which facilitates studying the fractional heat kernel using familiar techniques of the classical heat kernel. Again, in order for this result to apply, we must restrict to $\alpha\in(0,2]$ as the function $g(z)=\exp(-z^{\alpha/2})$ fails to be completely monotone for $\alpha>2$.

To study the antiperiodic eigenvalues of $L$, we now further restrict the semigroup $e^{-\Lambda^\alpha t}$ to the subspace $L^2_{\mathrm{a}}(0,T)$ of $T$-antiperiodic functions. For such $f\in L^2_{\mathrm{a}}(0,T)$ we have the representation

$$e^{-\Lambda^\alpha t}f(x)=\int_0^T[K_p(x-y,t)-K_p(x-y-T,t)]\,f(y)\,dy=:\int_0^T K_a(x-y,t)f(y)\,dy$$

for the action of $e^{-\Lambda^\alpha t}$ on $T$-antiperiodic functions, where $K_a$ denotes the $T$-antiperiodic kernel

$$K_a(x,t):=K_p(x,t)-K_p(x-T,t). \tag{2.30}$$

See Figure 2.4. Next, we gather some important properties of $K_a$.

[4] While the results in [2] were stated only for the case $T=\pi$ they easily extend to this more general setting via scaling.

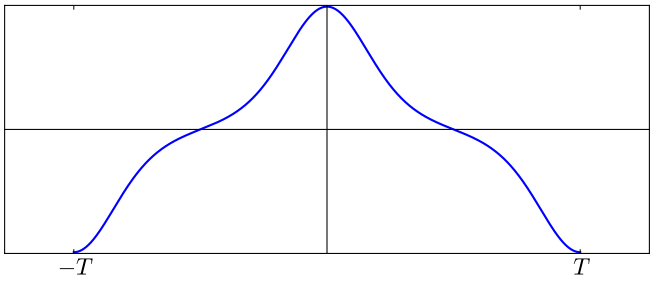


Figure 2.4: $K_a(x, t = 0.3)$, with $\alpha = 3/2$.

**Lemma 2.3.5** (Properties of $K_a$)**.** *For all $t > 0$ and $\alpha \in (0, 2]$, the function $K_a(\cdot, t)$ is even, $T$-antiperiodic and strictly positive for all $x \in (-T/2, T/2)$. Furthermore, $K_a(\cdot, t)$ is odd about $x = T/2$ and is strictly decreasing on $(0, T)$.*

*Proof.* The parity and antiperiodicity of $K_a$ follow directly from (2.30). Since all even, $T$-antiperiodic functions are odd[5] about $x = T/2$, it remains to show that $K_a(\cdot, t)$ is positive on $(-T/2, T/2)$ and strictly decreasing on $(0, T)$. To this end, fix $x \in (0, T/2)$ and observe that the evenness of $K_p(\cdot, t)$ implies that

$$K_a(x, t) = K_p(x, t) - K_p(T - x, t) > 0, \tag{2.31}$$

where the strict inequality follows since $K_p(\cdot, t)$ is strictly decreasing on $(0, T)$ by Lemma 2.3.3 and $0 < x < T - x < T$ for $x \in (0, T/2)$. Since $K_a(\cdot, t)$ is even for all $t > 0$, the positivity of $K_a(\cdot, t)$ on $(-T/2, T/2)$ follows. Similarly, differentiating (2.31) with respect to $x$, it follows that for $x \in (0, T)$ we have

$$\partial_x K_a(x, t) = \partial_x K_p(x, t) + \partial_x K_p(T - x, t) < 0$$

where we have used that $\partial_x K_p(x, t) < 0$ for all $x \in (0, T)$ by Lemma 2.3.3. □

[5] Indeed, if $f$ is even and $T$-antiperiodic then $f(x + T/2) = f(-x - T/2) = f(-x + T/2)$.

An important consequence of Lemma 2.3.5 which is visually evident from Figure 2.4 is that the semigroup $e^{-\Lambda^\alpha t}$ is not necessarily positivity improving (nor even positivity preserving) on $L^2_{\mathrm{a}}(0,T)$, since the convolution kernel $K_a$ is not positive, hence the antiperiodic ground states of the operator $L$ in (2.25) are not immediately characterized by standard Perron-Frobenius arguments. However, since the potential $V(x)$ in (2.25) is even, the operator $L$ maps even functions to even functions and odd functions to odd functions, respecting the orthogonal decomposition

$$L^2_{\mathrm{a}}(0,T) = L^2_{\mathrm{a,even}}(0,T) \oplus L^2_{\mathrm{a,odd}}(0,T),$$

where $L^2_{\mathrm{a,even}}(0,T)$, $L^2_{\mathrm{a,odd}}(0,T)$ denote the subspaces of even and odd functions in $L^2_{\mathrm{a}}(0,T)$, respectively. Precisely, the subspaces $L_{\mathrm{a,even}}(0,T)$ and $L_{\mathrm{a,odd}}(0,T)$ are invariant subspaces for $L$, and

$$\sigma_{L^2_{\mathrm{a}}(0,T)}(L) = \sigma_{L^2_{\mathrm{a,even}}(0,T)}(L) \cup \sigma_{L^2_{\mathrm{a,odd}}(0,T)}(L),$$

where we emphasize the above spectral decomposition need not be disjoint. Next, we consider the action of the semigroup $e^{-\Lambda^\alpha t}$ on the above invariant subspaces.

First, note that if $f \in L^2_{\mathrm{a,even}}(0,T)$ then

$$\begin{aligned} e^{-\Lambda^\alpha t} f(x) &= \frac{1}{2}\left[\int_0^T K_a(x-y,t) f(y)\,dy + \int_{-T}^0 K_a(x+y,t) f(y) dy\right] \\ &= \frac{1}{2}\left[\int_0^T K_a(x-y,t) f(y)\,dy + \int_0^T K_a(x+y-T,t) f(y-T)\,dy\right] \\ &= \frac{1}{2}\int_0^T \left[K_a(x-y,t) + K_a(x+y,t)\right] f(y)\,dy, \end{aligned}$$

where the final equality follows from the $T$-antiperiodicity of both $K_a(\cdot,t)$ and $f$. Observe that since $f(y)$ and $K_a(x-y,t)+K_a(x+y,t)$ are even and $T$-antiperiodic in $y$, they are

both odd functions in $y$ about $y = T/2$. Consequently, their product is even in $y$ about $y = T/2$, which yields the representation

$$e^{-\Lambda^\alpha t} f(x) = \int_0^{T/2} [K_a(x-y,t) + K_a(x+y,t)]\, f(y)\, dy \tag{2.32}$$

for the action of semigroup $e^{-\Lambda^\alpha t}$ on $L^2_{\text{a,even}}(0,T)$.

**Lemma 2.3.6.** *For all $x, y \in (-T/2, T/2)$ and $t > 0$, we have*

$$K_a(x-y,t) + K_a(x+y,t) > 0.$$

*In particular, the semigroup $e^{-\Lambda^\alpha t}$ restricted to $L^2_{\text{a,even}}(0,T)$ is positivity improving, i.e. if $f \in L^2_{\text{a,even}}(0,T)$ is non-trivial with $f(x) \geq 0$ for $x \in (-T/2, T/2)$, then $e^{-\Lambda^\alpha t} f(x) > 0$ for all $x \in (-T/2, T/2)$.*

*Proof.* We begin by proving the claim for $x, y \in (0, T/2)$. Fix $t > 0$ and define $G(x,y;t) := K_a(x-y,t) + K_a(x+y,t)$, and note that $G(x,y;t) = G(y,x;t)$ for all $x, y$. So, without loss of generality we need only prove that $G(x,y;t) > 0$ for all $(x,y) \in \mathcal{R} := \{(x,y) : 0 < x < T/2,\ 0 < y \leq x\}$. Observe that for all $(x,y) \in \mathcal{R}$, we have

$$0 \leq x - y < T/2 \quad \text{and} \quad 0 \leq x + y < T,$$

hence

$$\partial_x G(x,y;t) = \partial_x K_a(x+y,t) + \partial_x K_a(x-y,t) < 0$$

since $K_a(\cdot, t)$ is decreasing on $(0,T)$ by Lemma 2.3.5. Moreover, for all $y \in (0, T/2)$, we have

$$G(T/2, y; t) = K_a(T/2+y,t) + K_a(T/2-y,t) = 0$$

since $K_a(\cdot,t)$ is odd about $T/2$, again by Lemma 2.3.5. Thus for every $y_0 \in (0,T/2)$, the function $x \mapsto G(x,y_0;t)$ is decreasing on $y_0 < x < T/2$ toward the value $G(T/2,y_0;t) = 0$, hence it must be that $G(x,y;t) > 0$ for all $(x,y) \in \mathcal{R}$, and we conclude that $G(x,y;t) > 0$ for all $x,y \in (0,T/2)$. Finally, since $G(x,y;t) > 0$ for all $x,y \in (0,T/2)$, we also have that $G(x,y;t) > 0$ for all $x,y \in (-T/2,T/2)$ since $G$ is invariant under the maps $x \mapsto -x$ and $y \mapsto -y$. □

For the odd subspace, similar calculations to those above yield the representation

$$e^{-\Lambda^\alpha t} f(x) = \frac{1}{2} \int_0^T \left[ K_a(x-y,t) - K_a(x+y,t) \right] f(y)\, dy. \tag{2.33}$$

for the action of the semigroup $e^{-\Lambda^\alpha t}$ on $L^2_{\mathrm{a,odd}}(0,T)$.

**Lemma 2.3.7.** *For all $t > 0$ and $x,y \in (0,T)$, we have*

$$K_a(x-y,t) - K_a(x+y,t) > 0.$$

*In particular, the semigroup $e^{-\Lambda^\alpha t}$ restricted to $L^2_{\mathrm{a,odd}}(0,T)$ is positivity improving, i.e. if $f \in L^2_{\mathrm{a,odd}}(0,T)$ is nontrivial with $f(x) \geq 0$ for $x \in (0,T)$, then $e^{-\Lambda^\alpha t} f(x) > 0$ for all $x \in (0,T)$.*

*Proof.* Fix $t > 0$ and $x,y \in (0,T)$, and observe that the $T$-antiperiodicity of $K_a(\cdot,t)$ implies that

$$\begin{aligned}
&K_a(x-y,t) - K_a(x+y,t) \\
&= K_a(x-y,t) + K_a(x+y-T,t) \\
&= K_a\left(\left(x-\frac{T}{2}\right) - \left(y-\frac{T}{2}\right)\right) + K_a\left(\left(x-\frac{T}{2}\right) + \left(y-\frac{T}{2}\right)\right).
\end{aligned}$$

Since $x - T/2,\ y - T/2 \in (-T/2,T/2)$, the proof follows by Lemma 2.3.6. □

From Lemma 2.3.6 and Lemma 2.3.7, the ground state eigenfunctions of $e^{-\Lambda^\alpha t}$ acting on the invariant subspaces $L_{\text{a,even}}(0,T)$ and $L_{\text{a,odd}}(0,T)$ are positivity improving. Since the operator $L$ defined in (2.25) is a relatively compact perturbation of $-\Lambda^\alpha$, we can apply standard Perron-Frobenius arguments to deduce that the largest eigenvalues of $e^{-Lt}$ restricted to $H^{\alpha/2}_{\text{a,even}}(0,T)$ and $H^{\alpha/2}_{\text{a,odd}}(0,T)$ separately are simple with strictly positive eigenfunction on $(-T/2,T/2)$ and $(0,T)$, respectively; see [55, Theorem XIII.44], for instance.

**Theorem 2.3.8** (Antiperiodic Ground State Theory)**.** *Let $\alpha \in (1,2)$ and let $V : \mathbb{R} \to \mathbb{R}$ be an even, smooth, $T$-periodic potential and consider the linear operator $L = \Lambda^\alpha + V(x)$ acting on $L^2_{\text{a}}(0,T)$.*

*(a) The ground state eigenvalue of $L$ restricted to $L^2_{\text{a,even}}(0,T)$ is simple, and the corresponding $T$-antiperiodic, even eigenfunction is sign-definite on $(-T/2,T/2)$.*

*(b) The ground state eigenvalue of $L$ restricted to $L^2_{\text{a,odd}}(0,T)$ is simple, and the corresponding $T$-antiperiodic, odd eigenfunction is sign-definite on $(0,T)$.*

*Proof.* Parts (a) and (b) follow directly from Lemma 2.3.6, Lemma 2.3.7, and [55, Theorem XIII.44], as discussed above. □

While Theorem 2.3.8 establishes the simplicity of the even and odd antiperiodic ground state eigenvalues of $L$ on the respective subspace, it is natural to consider the *ordering* between these ground state eigenvalues. When the potential has sufficiently small amplitude, the ordering between odd and even $T$-antiperiodic ground state eigenvalues may be verified directly through the use of bifurcation theory: see, for example, Proposition 6.2 and Remark 6.3 in [53] where the analysis was carried out in a local context. In that case, the ground state eigenvalues agree at zero-amplitude and one tracks the splitting of these eigenvalues for very small amplitudes. For general amplitude potentials, however, in the local case $\alpha = 2$ it was shown in [19, Lemma 2.2] through the use ODE techniques and

increasing/decreasing rearrangement inequalities that the ordering of these ground states depends sensitively on the monotonicity properties of the periodic potential $V$ in (2.25). Using symmetric antiperiodic rearrangement inequalities, together with the above nonlocal ground state theory, we are able to extend the results of [19] to the nonlocal setting $\alpha \in (1,2)$; see Appendix B. Such information will be used heavily in the coming sections.

**Proposition 2.3.9** (Ground State Ordering)**.** *Let $\alpha \in (1,2)$ and let $V : \mathbb{R} \to \mathbb{R}$ be an even, smooth, $T$-periodic potential, and consider the linear operator $L = \Lambda^\alpha + V(x)$ acting on $L^2_{\mathrm{a}}(0,T)$.*

*(i) If the potential $V$ is nonincreasing on $(0,T/2)$, then the ground state $T$-antiperiodic eigenvalue of $L$ has at least one odd eigenfunction, i.e.*

$$\min \sigma \left( L\big|_{L^2_{\mathrm{a,odd}}(0,T)} \right) \leq \min \sigma \left( L\big|_{L^2_{\mathrm{a,even}}(0,T)} \right).$$

*(ii) If the potential $V$ is nondecreasing on $(0,T/2)$, then the ground state $T$-antiperiodic eigenvalue of $L$ has at least one even eigenfunction, i.e.*

$$\min \sigma \left( L\big|_{L^2_{\mathrm{a,even}}(0,T)} \right) \leq \min \sigma \left( L\big|_{L^2_{\mathrm{a,odd}}(0,T)} \right).$$

### 2.3.2 Antiperiodic Oscillation Theory

In addition to the above ground state theories, we require a Sturm-Liouville type oscillation theory to characterize the possible nodal patterns for the second antiperiodic eigenfunctions of the fractional Schrödinger operators $L_\pm$. To this end, first note that an $H^{\alpha/2}_{\mathrm{a}}(0,T)$-eigenfunction of $L_\pm$ is necessarily continuous, bounded, and can be chosen to be real-valued. Following the ideas in [25] and [39], we proceed by extending the eigenvalue

problem associated to $L_\pm$ on $L^2_{\rm a}(0,T)$ to an appropriate local problem in the upper half space.

Note that the operator $\Lambda^\alpha$ acting on $L^2_{\rm a}(0,T)$ can be viewed as the Dirichlet-to-Neumann operator for a suitable *local* problem in the antiperiodic half-strip $[0,T]\times(0,\infty)$. Indeed, following [10, 58], for a given $\alpha\in(0,2)$, there exists a constant $C(\alpha)$ such that for any $f\in H^\alpha_{\rm a}(0,T)$ we have

$$C(\alpha)\Lambda^\alpha f := \lim_{y\to 0^+} y^{1-\alpha} w_y(\cdot,y),$$

where $w =: E(f)\in C^\infty((0,\infty);H^{\alpha/2}_{\rm a}(0,T))\cap C([0,\infty);L^2_{\rm a}(0,T))$ is the unique solution to the elliptic boundary value problem

$$\begin{cases} \Delta w + \frac{1-\alpha}{y} w_y = 0, & \text{in} \quad [0,T]_{\rm antiper}\times(0,\infty) \\ w = f & \text{on} \quad [0,T]_{\rm antiper}\times\{0\} \end{cases}$$

As in [25, 39], it follows that the eigenvalue problems for $L_\pm$ on $L^2_{\rm a}(0,T)$ can be extended to an eigenvalue problem for a *local* elliptic problem in the antiperiodic upper-half space $[0,T]_{\rm antiper}\times(0,\infty)$. In this equivalent local setting, one can derive a variational characterization for the $T$-antiperiodic eigenvalues and eigenfunctions of $L_\pm$ as follows.

If $v\in L^2_{\rm a}(0,T)$ is an eigenfunction of $L_\pm$, then the extension $E(v)$ is in $C^0([0,T]_{\rm antiper}\times[0,\infty))$. Defining the zero set of $v$ to be

$$\mathcal{N} := \{(x,y)\in[0,T]_{\rm antiper}\times[0,\infty) : E(v)(x,y)=0\},$$

which is clearly closed in $[0,T]_{\rm antiper}\times[0,\infty)$, the *nodal domains* of $E(v)$ are the connected components of the open set $([0,T]_{\rm antiper}\times[0,\infty))\setminus\mathcal{N}$. Recalling the classical Courant nodal domain theorems yield an upper bound for the number of nodal domains of $E(v)$ in $[0,T]_{\rm antiper}\times(0,\infty)$, we find the following oscillation result.

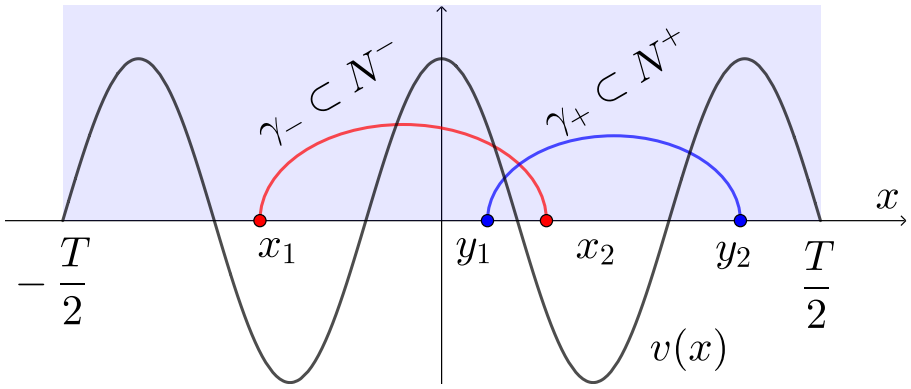


Figure 2.5: Curves $\gamma_\pm$ connecting points in nodal domains $N^\pm$ of the upper half space $[-T/2,T/2]_{\text{antiper}} \times [0,\infty)$.

**Lemma 2.3.10** (Antiperiodic Oscillation Theory)**.** *Under the hypothesis of Theorem 2.3.8, any even (resp. odd) $T$-antiperiodic eigenfunctions of $L$ associated with the second eigenvalue (not counting multiplicity[6]) has at most two sign changes over $(-T/2,T/2)$ (resp. $(0,T)$).*

*Proof.* The proof follows along the same lines as [39, Lemma 3.2] and [25, Theorem 3.1]; see also [40] for a combinatorial argument via non-crossing partitions. Consider the spectrum of $L$ acting on $L^2_{\text{a,even}}(0,T)$, and suppose that $v(x)$ is an even $T$-antiperiodic eigenfunction of $L$ associated with the its second eigenvalue $\lambda_2$, and suppose (to show a contradiction) that $v$ has at least three sign changes in $(-T/2,T/2)$. Since $v$ is even and $T$-antiperiodic, it must be that $v$ actually has at least four sign changes in $(-T/2,T/2)$, so there are points

$$-T/2 < x_1 < y_1 < x_2 < y_2 < x_3 < T/2$$

such that, up to switching signs, $v(x_j) < 0$ and $v(y_j) > 0$; see Figure 2.5. By a standard Courant nodal domain argument that the extension $E(v)$ can have at most two nodal domains in the strip $(-T/2,T/2) \times (0,\infty)$. Since the nodal domains are open and connected (thus pathwise connected) in $(-T/2,T/2) \times (0,\infty)$, we may find continuous curves

[6] That is, only the distinct elements of the $T$-antiperiodic spectrum of $L$ are listed.

$\gamma_\pm \subset C^0([0,1];[-T/2,T/2)\times[0,\infty))$ such that

$$\gamma_-(0)=x_1,\quad \gamma_-(1)=x_2,\quad \gamma_+(0)=y_1,\quad \gamma_+(1)=y_2$$

and

$$E(v)(\gamma_+(t))>0,\quad E(v)(\gamma_-(t))<0\quad \text{for all } \ t\in[0,1].$$

In particular, $\gamma_+(t)$ belongs to the same nodal domain for all $t\in(0,1)$, denoted $N^+$, while $\gamma_-(t)$ belongs to the same nodal domain $N^-$ for all $t\in(0,1)$. By the Jordan curve theorem, the curves $\gamma_\pm$ must cross at least once in $(-T/2,T/2)\times(0,\infty)$. Thus $N^+\cap N^-\neq\emptyset$, a contradiction of the fact that nodal domains are disjoint. A nearly identical argument shows that odd eigenfunctions corresponding to the second eigenvalue have at most two sign changes on $(0,T)$. □

### 2.3.3 Proof of Nondegeneracy

Now that we have information regarding the $T$-antiperiodic ground state eigenfunctions of $L_\pm$ and the nodal patterns for their second $T$-antiperiodic eigenfunctions, we aim to establish the nondegeneracy of the linearization $\delta^2\mathcal{E}(\phi)$. To this end, for each $\mu>0$ let $\phi(\cdot;\mu)\in H_{\mathrm{a}}^{\alpha/2}(0,T)$ be a real-valued local minimizer of $\mathcal{E}(\cdot;\mu):=\mathcal{E}(\cdot;0,\mu)$ over $H_{\mathrm{a}}^{\alpha/2}(0,T)$ subject to fixed $Q(u)=\mu$ and $N(u)=0$. Then by construction, the second derivative test for constrained extrema yields

$$\delta^2\mathcal{E}(\phi)|_{\{\delta Q(\phi),\delta N(\phi)\}^\perp}\geq 0,$$

where

$$\{\delta Q(\phi),\delta N(\phi)\}^\perp:=\Big\{h\in H_{\mathrm{a}}^{\alpha/2}([0,T];\mathbb{C}):\langle\phi,h\rangle=\big\langle i\phi',h\big\rangle=0\Big\}$$

denotes the tangent space at $\phi$ to the codimension two constrained subspace

$$\Sigma_\mu := \Big\{ \psi \in H^{\alpha/2}(0,T) : Q(\psi) = \mu, \;\; N(\psi) = 0 \Big\}$$

in $H^{\alpha/2}_{\rm a}(0,T)$. Recall that the inner product $\langle \cdot, \cdot \rangle$ is defined throughout as

$$\langle u, v \rangle = \mathrm{Re} \int_0^T u \bar{v} \, dx.$$

Thus $\delta^2 \mathcal{E}(\phi)$ has at most two negative $T$-antiperiodic eigenvalues. Specifically, since $\delta^2 \mathcal{E}(\phi)$ is diagonal and $\delta Q(\phi) = \phi$ and $\delta N(\phi) = i\phi'$ are real- and imaginary-valued, respectively, it follows that the linear operators $L_+$ and $L_-$ each have at most one negative $T$-antiperiodic eigenvalue, with

$$L_+\big|_{\{\delta Q(\phi)\}^\perp} \geq 0 \quad \text{and} \quad L_-\big|_{\{\mathrm{Im}(\delta N(\phi))\}^\perp} \geq 0. \tag{2.34}$$

**Lemma 2.3.11.** *Under the hypothesis of Proposition 2.3.1, the following are true:*

*(i) The operator $\delta^2 \mathcal{E}(\phi)$ acting on $L^2_{\rm a}(0,T)$ has at most one negative eigenvalue, with*

$$L_+ \geq 0 \quad \textit{and} \quad n_-(L_-) \leq 1.$$

*(ii) $\phi' \in \ker(L_+)$, and it corresponds to the ground state eigenfunction of $L_+$ restricted to the subspace of odd functions in $H^{\alpha/2}_{\rm a}(0,T)$.*

*(iii) $\phi \in \ker(L_-)$, and it corresponds to the ground state eigenfunction of $L_-$ restricted to the subspace of even functions in $H^{\alpha/2}_{\rm a}(0,T)$.*

*(iv) $\phi', \phi^{2\sigma}\phi' \in \mathrm{range}(L_-)$.*

*(v) $\phi^{2\sigma+1} \in \mathrm{range}(L_+)$.*

*Proof.* First, note that the profile equation (2.3) is equivalent to $L_-\phi = 0$, while differentiating the profile equation with respect to $x$ gives $L_+\phi' = 0$; see (2.24). Further, due to the monotonicity properties guaranteed by Lemma 2.2.6, we have $\phi$ is even and sign-definite on $(-T/2, T/2)$, hence $\phi$ is the ground state of $L_-$ acting on $L^2_{\text{a,even}}(0,T)$ by Theorem 2.3.8(a). Similarly, $\phi'$ is odd and is sign-definite on $(0,T)$, hence $\phi'$ is the ground state of $L_+$ acting on $L^2_{\text{a,odd}}(0,T)$ by Theorem 2.3.8(b). This establishes claims (ii) and (iii).

Moreover, the potentials

$$V_+(x) = (2\sigma+1)\phi^{2\sigma} + \omega, \quad V_-(x) = \phi^{2\sigma} + \omega \tag{2.35}$$

of $L_+$ and $L_-$ (respectively) are decreasing on $(0, T/2)$, so it follows from Proposition 2.3.9 that

$$0 = \min\sigma\left(L_+|_{L^2_{\text{a,odd}}}\right) \leq \min\sigma\left(L_+|_{L^2_{\text{a,even}}}\right),$$

hence $L_+$ has no negative eigenvalues, i.e. $L_+ \geq 0$. Further, $L_-$ can have at most one negative eigenvalue by by (2.34), hence $n_-(L_-) \leq 1$. This establishes claim (i).

To prove claims (iv) and (v), observe that $L_+ = L_- + 2\sigma\phi^{2\sigma}$. Hence

$$L_+\phi = L_-\phi + 2\sigma\phi^{2\sigma+1} = 2\sigma\phi^{2\sigma+1},$$

which establishes (v). Similarly,

$$\begin{aligned} 0 = L_+\phi' &= L_-\phi' + 2\sigma\phi^{2\sigma} \\ \implies L_-\phi' &= -2\sigma\phi^{2\sigma}, \end{aligned}$$

i.e. $\phi^{2\sigma} \in \mathrm{range}(L_-)$. Finally, differentiating the profile equation (2.3) with respect to $c$ gives

$$\Lambda^\alpha \frac{\partial \phi}{\partial c} + \omega \frac{\partial \phi}{\partial c} + \frac{\partial \omega}{\partial c}\phi + ic\frac{\partial \phi'}{\partial c} + i\phi' + |\phi|^{2\sigma}\frac{\partial \phi}{\partial c} + 2\sigma |\phi|^{2\sigma-2}\phi \mathrm{Re}\left(\phi \overline{\frac{\partial \phi}{\partial c}}\right) = 0,$$

where $\phi = \phi(\cdot; c, \mu)$ is a minimizer with corresponding Lagrange multiplier $\omega = \omega(c, \mu)$ as constructed in Proposition 2.2.2. Evaluating the above expression at $c = 0$ and taking imaginary parts yields, by reality of $\phi$ at $c = 0$,

$$\Lambda^\alpha \left(\frac{\partial \phi}{\partial c}\Big|_{c=0}\right) + \left(\omega \frac{\partial \phi}{\partial c}\right)\Big|_{c=0} + \phi^{2\sigma+1}\frac{\partial \phi}{\partial c}\Big|_{c=0} = -i\phi',$$

i.e. $L_-\left(\mathrm{Im}\,\dfrac{\partial \phi}{\partial c}\Big|_{c=0}\right) = -\phi'$. Thus $\phi' \in \mathrm{range}(L_-)$, completing (iv). □

*Remark* 2.3.12. In differentiating the profile equation at $c = 0$ to prove that $\phi' \in \mathrm{range}(L_-)$, we relied on the fact that the real-valued, $T$-antiperiodic standing profile $\phi(\cdot; \mu)$ is a member of a more general family of complex-valued $T$-antiperiodic traveling waves $\phi(\cdot; c, \mu)$ defined for $|c|$ sufficiently small; see Proposition 2.2.2 and Lemma 2.2.6. In the local case $\alpha = 2$, one may rely on the Galilean invariance of (2.1) to produce such a curve of traveling solutions near $c = 0$, and differentiating along this curve yields the same result. Since such an (exact) Galilean invariance does not exist for $\alpha \in (1, 2)$, for $\mu > 0$ the existence theory constructs a minimizer for each $c$, thus allowing one to vary $\phi$ smoothly as a function of $c$ near $c = 0$.

Finally, we are ready to establish the nondegeneracy of $L_\pm$.

*Proof of Proposition 2.3.1.* First, note that since $\phi^{2\sigma}$ is even and $T$-periodic by construction, the subspaces $L^2_{\mathrm{a,odd}}(0, T)$ and $L^2_{\mathrm{a,odd}}(0, T)$ of respectively even and odd $T$-antiperiodic functions are invariant subspaces of the operators $L_\pm$. In particular, the operators $L_\pm$ re-

spect the orthogonal decomposition

$$L^2_{\mathrm{a}}(0,T) = L^2_{\mathrm{a,odd}}(0,T) \oplus L^2_{\mathrm{a}}(0,T)_{\mathrm{even}}$$

so that

$$\sigma\left(L_{\pm}\big|_{L^2_{\mathrm{a}}(0,T)}\right) = \sigma\left(L_{\pm}\big|_{L^2_{\mathrm{a,odd}}(0,T)}\right) \cup \sigma\left(L_{\pm}\big|_{L^2_{\mathrm{a,even}}(0,T)}\right).$$

Since Lemma 2.3.11 implies that

$$\ker\left(L_{+}\big|_{L^2_{\mathrm{a,odd}}(0,T)}\right) = \mathrm{span}\left\{\phi'\right\} \quad \text{and} \quad \ker\left(L_{-}\big|_{L^2_{\mathrm{a,even}}(0,T)}\right) = \mathrm{span}\left\{\phi\right\},$$

it remains to verify that $\ker\left(L_{+}\big|_{L^2_{\mathrm{a,even}}(0,T)}\right)$ and $\ker\left(L_{-}\big|_{L^2_{\mathrm{a,odd}}(0,T)}\right)$ are trivial.

First, suppose there exists a non-trivial solution $v \in L^2_{\mathrm{a,even}}(0,T)$ of the equation $L_+ v = 0$. Since $L_+$ is self adjoint on $L^2_{\mathrm{a}}(0,T)$, the Fredholm alternative implies that $v$ must be orthogonal to the range of the operator $L_+$ acting on $L^2_{\mathrm{a}}(0,T)$. Since zero is the ground state eigenvalue of $L_+$ acting on $L^2_{\mathrm{a}}(0,T)$ by Lemma 2.3.11(i), it follows that $v$ is the even ground state eigenfunction for $L_+$ and hence, by Theorem 2.3.8, may be chosen to be strictly positive on $(-T/2, T/2)$. To reach the desired contradiction, observe that Lemma 2.3.11(v) implies the function $\phi^{2\sigma+1}$ is in the range of $L_+$ acting on $L^2_{\mathrm{a}}(0,T)$. Since $\phi^{2\sigma+1}$ is sign-definite on $(-T/2, T/2)$ we have that $\left\langle \phi^{2\sigma+1}, v\right\rangle \neq 0$, a contradiction of the Fredholm alternative. Consequently, $\ker(L_+|_{L^2_{\mathrm{a,even}}(0,T)}) = \{0\}$, hence

$$\ker\left(L_{+}\right) = \mathrm{span}\left\{\phi'\right\}. \tag{2.36}$$

That is, $L_+$ is nondegenerate on $L^2_{\mathrm{a}}(0,T)$.

Next, we turn our attention to $L_-$. First, we claim that $L_-$ has exactly one negative $T$-antiperiodic eigenvalue. To this end, suppose (to show a contradiction) that $L_-$ does

not have a negative eigenvalue. Since $L_-\phi = 0$ and $\phi$ is even, the ground state ordering (Proposition 2.3.9) implies that there exists $\psi \in L^2_{\text{a,odd}}(0,T)$ such that $L_-\psi = 0$ with $\psi$ being the ground state on $L_-|_{L^2_{\text{a,odd}}(0,T)}$. Then by Theorem 2.3.8(b), $\psi$ is sign-definite on $(0,T)$, hence $\langle \psi, \phi' \rangle \neq 0$, i.e. $\phi$ is not orthogonal to $\phi'$. But $\phi' \in \text{range}\left(L_-|_{L^2_{\text{a,odd}}(0,T)}\right) = \ker\left(L_-|_{L^2_{\text{a,odd}}(0,T)}\right)^\perp$, a contradiction of the Fredholm alternative. Thus it must be that $n_-(L_-) \geq 1$, which implies that $n_-(L_-) = 1$ by Lemma 2.3.11(i). Now, since $L_-\phi = 0$, it follows that $\lambda = 0$ is the second eigenvalue of $L_-$ acting on $L^2_{\text{a}}(0,T)$. As above, suppose there exists a nontrivial solution $v \in L^2_{\text{a,odd}}(0,T)$ to the equation $L_-v = 0$. By Lemma 2.3.10, $v$ may change signs at most twice on $(0,T)$. We will show that such a nontrivial $v$ cannot exist, again by using the Fredholm alternative. To this end, note that if $v$ is sign-definite on $(0,T)$, then the fact that $\phi' < 0$ on $(0,T)$ implies $\langle \phi', v \rangle \neq 0$, a contradiction of the Fredholm alternative since $\phi' \in \text{range}(L_-)$ by Lemma 2.3.11(iv). Thus, any nontrivial $v \in \ker(L_-)$ must change signs at least once in $(0,T)$ and, since odd $T$-antiperiodic functions are even about $x = T/2$, such a function must have exactly two sign changes in $(0,T)$; one at some $x = x_0 \in (0,T/2)$ and the other at $x = T - x_0 \in (T/2,T)$. Define

$$\eta(x) := \phi'(x)\left(\phi(x)^{2\sigma} - \phi(x_0)^{2\sigma}\right)$$

and note that $\eta \in \text{range}(L_-)$ by Lemma 2.3.11(iv). Further, $\eta$ changes signs at $x = x_0$ and $x = T - x_0$ by monotonicity of $\phi$ on $(0,T)$. Consequently, $\langle \eta, v \rangle \neq 0$, again contradicting the Fredholm alternative. Thus, it must be that $\ker\left(L_-|_{L^2_{\text{a,odd}}(0,T)}\right) = \{0\}$, and we conclude that

$$\ker(L_-) = \text{span}\{\phi\}, \tag{2.37}$$

verifying the nondegeneracy of $L_-$ on $L^2_{\text{a}}(0,T)$.

Finally, since $\mathcal{L} = \operatorname{diag}(L_+, L_-)$ is diagonal, we have by (2.36) and (2.37) that

$$\ker(\mathcal{L}) = \operatorname{span}\left\{ \begin{bmatrix} u \\ v \end{bmatrix} : u \in \ker(L_+), v \in \ker(L_-) \right\} = \operatorname{span}\left\{ \begin{bmatrix} \phi' \\ 0 \end{bmatrix}, \begin{bmatrix} 0 \\ \phi \end{bmatrix} \right\},$$

completing the proof of Proposition 2.3.1. □

We end this section by demonstrating that the generalized $L^2_{\mathrm{a}}(0,T)$-kernel of the linearized operator associated with (2.1) supports a Jordan structure if $\frac{\partial}{\partial c} N(\phi(\cdot;c,\mu))\Big|_{c=0} \neq 0$, which plays a central role in the forthcoming stability analysis. Note that linearizing (2.20) about $\phi(\cdot;\mu)$ produces the linear system

$$v_t = -i\delta^2 \mathcal{E}(\phi) v,$$

which, by separating variables $v(x,t) = e^{\lambda t} V(x)$ and decomposing into real and imaginary parts, leads to the spectral problem

$$\begin{bmatrix} 0 & 1 \\ -1 & 0 \end{bmatrix} \begin{bmatrix} L_+ & 0 \\ 0 & L_- \end{bmatrix} \begin{bmatrix} \operatorname{Re}(V) \\ \operatorname{Im}(V) \end{bmatrix} = \lambda \begin{bmatrix} \operatorname{Re}(V) \\ \operatorname{Im}(V) \end{bmatrix}.$$

**Proposition 2.3.13** (Jordan Block Structure)**.** *Under the hypotheses of Proposition 2.3.1, zero is a $T$-antiperiodic generalized eigenvalue of the linearized operator*

$$J\mathcal{L} := \begin{bmatrix} 0 & 1 \\ -1 & 0 \end{bmatrix} \begin{bmatrix} L_+ & 0 \\ 0 & L_- \end{bmatrix}$$

*associated to the profile $\phi_0 := \phi(\cdot; c = 0, \mu)$ with algebraic multiplicity four and geometric multiplicity two provided that $\dfrac{\partial}{\partial c} N(\phi(\cdot;c,\mu))\Big|_{c=0} \neq 0$.*

*Proof.* By Proposition 2.3.1, we have that $\dim\left(\ker\left(L_{\pm}\Big|_{L^2_{\mathrm{a}}(0,T)}\right)\right) = 1$, hence zero is a $T$-antiperiodic eigenvalue of $L_+$ and of $L_-$ with algebraic multiplicity at least one and geometric multiplicity precisely one, and

$$\ker(J\mathcal{L}) = \operatorname{span}\left\{\begin{bmatrix}\phi_0' \\ 0\end{bmatrix}, \begin{bmatrix}0 \\ \phi_0\end{bmatrix}\right\}.$$

To understand the generalized kernel of $J\mathcal{L}$, we try to solve

$$J\mathcal{L}\begin{bmatrix}\xi \\ \eta\end{bmatrix} = \begin{bmatrix}\phi_0' \\ \phi_0\end{bmatrix},$$

which leads to

$$L_+\xi = -\phi_0, \quad L_-\eta = \phi_0'.$$

From Lemma 2.3.11(iv), we have that $\eta = -\operatorname{Im}\left(\frac{\partial\phi}{\partial c}\Big|_{c=0}\right)$, and such a $T$-antiperiodic function $\xi$ exists by the Fredholm alternative since $\phi_0$ is orthogonal to $\ker(L_+)$. So, zero is is a generalized eigenvalue of $J\mathcal{L}$ with geometric multiplicity at least two and and algebraic multiplicity of at least four.

By the Fredholm alternative, the generalized kernel of $J\mathcal{L}$ terminates at height two provided that $\xi \perp \ker(L_-)$ and $\operatorname{Im}\left(\frac{\partial\phi}{\partial c}\Big|_{c=0}\right) \perp \ker(L_+)$, i.e. if $\langle\phi,\xi\rangle \neq 0$ and $\left\langle\phi_0', \operatorname{Im}\left(\frac{\partial\phi}{\partial c}\Big|_{c=0}\right)\right\rangle \neq 0$. Writing $\xi = \xi_{\text{even}} + \xi_{\text{odd}}$ as a sum of even and odd functions, we have by $T$-antiperiodicity of $\xi$ and the evenness and monotonicity of $\phi_0$ (see Lemma 2.2.6) that

$$\langle\phi_0,\xi\rangle = \underbrace{\langle\phi_0,\xi_{\text{even}}\rangle}_{\neq 0} + \underbrace{\langle\phi_0,\xi_{\text{odd}}\rangle}_{=0} \neq 0.$$

Further, by hypothesis we have

$$\begin{aligned} 0 \neq \frac{\partial}{\partial c} N(\phi(\cdot;c,\mu))\Big|_{c=0} &= \left\langle \delta N(\phi(\cdot;0,\mu)), \frac{\partial \phi}{\partial c}\Big|_{c=0} \right\rangle \\ &= \left\langle i\phi_0', \frac{\partial \phi}{\partial c}\Big|_{c=0} \right\rangle \\ &= \left\langle \phi_0', \mathrm{Im}\left( \frac{\partial \phi}{\partial c}\Big|_{c=0} \right) \right\rangle. \end{aligned}$$

So, the generalized kernel of $J\mathcal{L}$ has geometric multiplicity exactly two and algebraic multiplicity exactly four if $\frac{\partial}{\partial c} N(\phi(\cdot;c,\mu))\Big|_{c=0} \neq 0$, as claimed. □

## 2.4 Stability of Defocusing Constrained Energy Minimizers

Let $T > 0$ and $\mu_0 > 0$ be fixed and let $\phi_0 := \phi(\cdot;\mu_0)$ denote a real-valued, $T$-antiperiodic solution of the nonlocal profile equation (2.3) with $c = 0$ satisfying $Q(\phi_0) = \mu_0$, whose existence is guaranteed by Proposition 2.2.2 and Lemma 2.2.6. The profile $\phi_0$ is thus an equilibrium solution of the PDE

$$iu_t - \omega_0 u - \Lambda^\alpha u - |u|^{2\sigma} u = 0, \tag{2.38}$$

where $\omega_0 := \omega(0,\mu_0)$. In this section, we consider the stability of $\phi_0$ under the evolution of (2.38) to general complex-valued, $T$-antiperiodic perturbations or, equivalently, the stability of the standing wave solution $u(x,t;\mu_0) = e^{i\omega_0 t}\phi_0(x)$ under the evolution of (2.1) to such perturbations.

For $\alpha > 1$ and $\sigma > 0$, an iteration argument reveals that the Cauchy problem for (2.38) is locally in time well-posed in $H^{1/2+}_{\mathrm{a}}([0,T];\mathbb{C})$. Furthermore, using conservation laws

these local solutions can be extended to global ones in $H_{\mathrm{a}}^{\alpha/2}([0,T];\mathbb{C})$ provided the initial data is in $H_{\mathrm{a}}^{\alpha/2}(0,T)$. Throughout our analysis we work on an appropriate subspace $X \subseteq H_{\mathrm{a}}^{\alpha/2}([0,T];\mathbb{C})$ where the Cauchy problem associated with (2.20) is locally well-posed and where the functionals $\mathcal{H}, Q, N : X \to \mathbb{R}$ are smooth.

Observe that the evolution defined by (2.1), and hence of (2.38), is invariant under a two-parameter group of symmetries generated by spatial translations and unitary phase rotations. For each $w \in X$ this motivates us to define the group orbit

$$\mathcal{O}_w := \left\{ e^{i\beta} w(\cdot - x_0) : \beta, x_0 \in \mathbb{R} \right\} \subset X.$$

We say that the standing wave $\phi_0(\cdot;\mu_0)$ is *orbitally stable* if the group orbit $\mathcal{O}_{\phi_0}$ is stable under the evolution of (2.38), i.e. solutions of (2.38) remain close in the $X$-norm to $\mathcal{O}_{\phi_0}$ for all future times if their initial data is sufficiently close in the $X$-norm to $\mathcal{O}_{\phi_0}$. Setting

$$\mathcal{E}_0(u) := \mathcal{H}(u) + \omega_0 Q(u), \tag{2.39}$$

we recall from Lemma 2.2.6 that $\phi_0$ is a critical point of $\mathcal{E}_0$, i.e. that $\delta\mathcal{E}_0(\phi) = 0$, or, equivalently, that $\phi_0$ is a critical point of $\mathcal{H}$ subject to fixed $Q(u) = \mu_0$ and $N(u) = 0$. Furthermore, Proposition 2.3.1 shows that the kernel of the Hessian $\delta^2\mathcal{E}_0(\phi_0)$ is generated by the translation and phase rotation symmetries. Intuitively, as in finite dimensions, we expect the group orbit of $\phi_0$ to be stable provided the operator $\delta^2\mathcal{E}_0(\phi_0)$ is positive-definite at $\phi_0$. We will demonstrate this positive-definiteness and establish the orbital stability of the standing wave $\phi_0$ under the evolution of (2.38). The main orbital stability result is as follows:

**Theorem 2.4.1** (Orbital Stability)**.** *Suppose $\alpha \in (1,2]$, and let $\phi(\cdot;\mu_0) = \phi(\cdot;c=0,\mu_0) \in H_{\mathrm{a}}^{\alpha/2}(0,T)$ be a real-valued, $T$-antiperiodic local minimizer of $\mathcal{H}$ subject to $Q(u) = \mu_0$*

*and* $N(u) = 0$ *as constructed in Lemma 2.2.6. Suppose in addition that both* $\phi$ *and the associated Lagrange multiplier* $\omega$ *depend on* $\mu$ *and* $c$ *in a* $C^1$ *manner near* $(\mu, c) = (\mu_0, 0)$. *If*

$$\frac{\partial}{\partial c} N(\phi(\cdot; c, \mu_0))\Big|_{c=0} \neq 0, \tag{2.40}$$

*then for all* $\varepsilon > 0$ *sufficiently small there exists a constant* $C = C(\varepsilon)$ *such that if* $v \in X$ *with* $\|v\|_X \leq \varepsilon$ *and* $N(\phi(\cdot; \mu_0) + v) = 0$, *and if* $u(\cdot, t)$ *is a local in time solution of* (2.38) *with initial data* $u(\cdot, 0) = \phi(\cdot; \mu_0) + v$, *then* $u(\cdot, t)$ *can be continued to a solution for all* $t \geq 0$ *and*

$$\sup_{t \geq 0} \inf_{\beta, x_0 \in \mathbb{R}} \left\| u(\cdot, t) - e^{i\beta} \phi(\cdot - x_0; \mu_0) \right\|_X \leq C \|v\|_X.$$

*Remark* 2.4.2. As in the nondegeneracy theory in Section 2.3, the smooth dependence of $\phi$ and $\omega$ on the wave speed $c$ near $c = 0$ is crucial to our stability analysis. The requirement that these quantities *also* depend smoothly on the charge $\mu$ is needed to allow perturbations $v \in X$ for which $Q(\phi(\cdot; 0, \mu_0) + v) \neq \mu_0$, i.e. perturbations that slightly change the charge from that of the underlying wave. If restricting to a class of perturbations that preserve the charge, i.e. $v \in X$ such that $Q(\phi(\cdot; 0, \mu_0) + v) = \mu_0$, then $\phi$ and $\omega$ need not depend smoothly on $\mu$. See the proof of Theorem 2.4.1.

To begin the proof of Theorem 2.4.1, observe Proposition 2.3.1 and Lemma 2.3.11 imply that $\delta^2 \mathcal{E}_0(\phi_0)\Big|_{H_{\mathrm{a}}^{\alpha/2}(0,T)}$ has one negative direction and two neutral directions. To control these potentially unstable directions, we note that the evolution of (2.38) does not occur on the whole space $X$, but rather on the codimension two nonlinear manifold

$$\Sigma_0 := \{u \in X : Q(u) = \mu_0,\ N(u) = 0\}.$$

In particular, $\Sigma_0$ is an invariant set under the flow of (2.38), with $\mathcal{O}_{\phi_0} \subset \Sigma_0$. The key step in the proof of Theorem 2.4.1, we establish the coercivity of $\mathcal{E}_0$ on $\Sigma_0$ in a neighborhood

of $\mathcal{O}_{\phi_0}$ provided that condition (2.40) holds. To this end, we define

$$\mathcal{T}_0 := \operatorname{span}\{\delta Q(\phi_0), \delta N(\phi_0)\}^{\perp} = \operatorname{span}\{\phi_0, i\phi_0'\}^{\perp} \tag{2.41}$$

to be the tangent space in $X$ to $\Sigma_0$ at $\phi_0$, and establish the following technical result.

**Lemma 2.4.3** (Positive-Definiteness)**.** *Suppose that* $\dfrac{\partial}{\partial c} N(\phi(\cdot; c, \mu)\Big|_{c=0} \neq 0$. *Then*

$$\inf\left\{\left\langle \delta^2 \mathcal{E}_0(\phi) v, v\right\rangle : \|v\|_X = 1,\ v \in \operatorname{span}_{\mathbb{R}}\{\phi', i\phi, \phi, i\phi'\}^{\perp}\right\} > 0.$$

*Proof.* We will decompose $v \in X$ into real and imaginary parts $\vec{v} = \begin{bmatrix} \operatorname{Re}(v) & \operatorname{Im}(v) \end{bmatrix}^T$ and analyze the equivalent matrix formulation $\delta^2 \mathcal{E}_0(\phi) \sim \mathcal{L} := \operatorname{diag}(L_+, L_-)$ that acts on real and imaginary parts separately.

Define the projection $\widehat{\Pi} := \operatorname{diag}(\Pi, \Pi_0)$, where for real-valued $u \in X$,

$$\Pi u := u - \frac{\langle u, \phi\rangle}{\langle \phi, \phi\rangle}\phi, \quad \Pi_0 u := u - \frac{\langle u, \phi'\rangle}{\langle \phi', \phi'\rangle}\phi'.$$

Then for all $\vec{v} = \begin{bmatrix} v_1 \\ v_2 \end{bmatrix} \in \mathcal{T}_0 := \operatorname{span}\left\{\begin{bmatrix} \phi \\ 0 \end{bmatrix}, \begin{bmatrix} 0 \\ \phi' \end{bmatrix}\right\}^{\perp}$, we have $v_1 \perp \phi$ and $v_2 \perp \phi'$, hence

$$\widehat{\Pi}\vec{v} = \begin{bmatrix} \Pi v_1 \\ \Pi_0 v_2 \end{bmatrix} = \begin{bmatrix} v_1 \\ v_2 \end{bmatrix} = \vec{v}.$$

Moreover, it is easy to check that $\widehat{\Pi}$ is a symmetric operator, hence for all $\vec{v} \in \mathcal{T}_0$, we have

$$\langle \mathcal{L}\vec{v}, \vec{v}\rangle = \left\langle \mathcal{L}\vec{v}, \widehat{\Pi}\vec{v}\right\rangle = \left\langle \widehat{\Pi}\mathcal{L}\vec{v}, \vec{v}\right\rangle.$$

Due to the periodic boundary conditions, the spectrum of the symmetric operator $\Pi\delta^2\mathcal{E}_0(\phi_0)$ is real and purely discrete, consisting of isolated eigenvalues accumulating at $+\infty$. By the second derivative test for constrained extrema, we already have that $\left\langle \widehat{\Pi}\mathcal{L}\vec{v},\vec{v}\right\rangle = \langle \mathcal{L}\vec{v},\vec{v}\rangle \geq 0$ for all $\vec{v}\in\mathcal{T}_0$, so due to the spectral gap there exists $\lambda>0$ such that

$$\inf\left\{\left\langle \widehat{\Pi}\mathcal{L}\vec{v},\vec{v}\right\rangle : \|\vec{v}\|_{L^2(0,T)}=1,\ \vec{v}\in\mathcal{T}_0\cap\ker(\widehat{\Pi}\mathcal{L})^{\perp}\right\}\geq\lambda. \tag{2.42}$$

That is, $\left\langle \widehat{\Pi}\mathcal{L}\vec{v},\vec{v}\right\rangle \geq \lambda\|\vec{v}\|_{L^2(0,T)}$ for all $\vec{v}$ with $\|\vec{v}\|_{L^2(0,T)}=1$, which implies that

$$\left\langle \widehat{\Pi}\mathcal{L}\vec{v},\vec{v}\right\rangle \geq \lambda\|\vec{v}\|_X$$

for all $\|\vec{v}\|_X=1$ as well.

We claim that if $\vec{v}\in\mathcal{T}_0$, then $\vec{v}\in\ker(\widehat{\Pi}\mathcal{L})$ if and only if $\vec{v}\in\ker(\mathcal{L})$. It is clear that if $\vec{v}\in\ker(\mathcal{L})$, then $\vec{v}\in\ker(\widehat{\Pi}\mathcal{L})$. Conversely, suppose that $\vec{v}=\begin{bmatrix}v_1 & v_2\end{bmatrix}^T\in\mathcal{T}_0$ and $\vec{v}\in\ker(\widehat{\Pi}\mathcal{L})$. Then

$$\Pi L_+ v_1 = 0, \quad \Pi_0 L_- v_2 = 0,$$

hence

$$L_+ v_1 = a\phi, \quad L_- v_2 = b\phi'$$

for some $a,b\in\mathbb{R}$. Since $a\phi\perp\ker(L_+)$ and $b\phi'\perp\ker(L_-)$, by the Fredholm alternative there exist unique solutions in $X$ to the above equations:

$$\begin{aligned} v_1 &= aL_+^{-1}(\phi) =: a\xi \\ v_2 &= bL_-^{-1}(\phi') = -b\,\mathrm{Im}\left(\frac{\partial\phi}{\partial c}\Big|_{c=0}\right). \end{aligned}$$

However, we require $v_1 \perp \phi$, which occurs only if $a = 0$:

$$\begin{aligned} 0 &= \langle v_1, \phi \rangle \\ &= -a \langle \xi, \phi \rangle , \end{aligned}$$

which implies that $a = 0$ since $\langle \xi, \phi \rangle \neq 0$ as shown in Proposition 2.3.13. So, $v_1 \in \ker(L_+)$.

Moreover, we require $v_2 \perp \phi'$, which occurs only if $b = 0$:

$$\begin{aligned} 0 &= \left\langle v_2, \phi' \right\rangle \\ &= b \left\langle -\operatorname{Im}\left( \frac{\partial \phi}{\partial c}\Big|_{c=0} \right), \phi' \right\rangle \\ &= -b \, \frac{\partial}{\partial c} N(\phi(\cdot; c, \mu)\Big|_{c=0} \\ \implies b &= 0 \quad \text{since } \frac{\partial}{\partial c} N(\phi(\cdot; c, \mu)\Big|_{c=0} \neq 0 \text{ by hypothesis} \\ \implies v_2 &\in \ker(L_-). \end{aligned}$$

So, if $\vec{v} = \begin{bmatrix} v_1 & v_2 \end{bmatrix}^T \in \mathcal{T}_0$ and $\vec{v} \in \ker(\widehat{\Pi}\mathcal{L})$, then we have established that $\vec{v} \in \ker(\mathcal{L})$. It follows that

$$\mathcal{T}_0 \cap \ker(\widehat{\Pi}\mathcal{L})^\perp = \mathcal{T}_0 \cap \ker(\mathcal{L})^\perp,$$

hence by (2.42) we have

$$\begin{aligned} 0 &< \inf \left\{ \left\langle \widehat{\Pi}\mathcal{L}\vec{v}, \vec{v} \right\rangle : \|\vec{v}\|_X = 1, \ \vec{v} \in \mathcal{T}_0 \cap \ker(\mathcal{L})^\perp \right\} \\ &= \inf \left\{ \left\langle \delta^2 \mathcal{E}_0(\phi) v, v \right\rangle : \|v\|_X = 1, \ v \in \operatorname{span}_{\mathbb{R}} \left\{ \phi, i\phi', \phi', i\phi \right\}^\perp \right\}, \end{aligned}$$

as claimed. □

Next, we introduce the semidistance $\rho$ on $X$ defined via

$$\rho(u,v) := \inf_{(\beta,x_0)\in\mathbb{R}^2} \left\| u - e^{i\beta} v(\cdot - x_0) \right\|_X,$$

and observe that $\rho(u,v)$ simply measures the distance in $X$ from $u$ to the group orbit $\mathcal{O}_v$ or, equivalently, from $v$ to $\mathcal{O}_u$. Next, we show that the functional $\mathcal{E}_0$ is coercive on the nonlinear manifold $\Sigma_0$ with respect to the semidistance $\rho$.

**Proposition 2.4.4** (Coercivity)**.** *Under the hypothesis of Theorem 2.4.1, there exist constants $\varepsilon > 0$ and $C = C(\varepsilon) > 0$ such that if $u \in \Sigma_0$ with $\rho(u,\phi_0) < \varepsilon$, then*

$$\mathcal{E}_0(u) - \mathcal{E}_0(\phi_0) \geq C\rho(u,\phi_0)^2.$$

*Proof.* We claim that there exists a neighborhood $\mathcal{U}_\varepsilon \subset X$ of $\phi_0$ and continuously differentiable maps $\tau, \beta : \mathcal{U}_\varepsilon \to \mathbb{R}$ such that for all $u \in \mathcal{U}_\varepsilon$, we have $\rho(u,\phi_0) < \varepsilon$ and

$$\begin{cases} \tau(\phi_0) = 0 \\ \beta(\phi_0) = 0 \\ \left\langle e^{i\beta(u)} u(\cdot + \tau(u)), \phi_0' \right\rangle = 0 \\ \left\langle e^{i\beta(u)} u(\cdot + \tau(u)), i\phi_0 \right\rangle = 0. \end{cases} \tag{2.43}$$

To prove this, consider the $C^1$ functions $F_1, F_2 : \mathbb{R}\times\mathbb{R}\times X \to \mathbb{R}$ defined by

$$F_1(\tau,\beta,u) := \left\langle e^{i\beta} u(\cdot+\tau), \phi_0' \right\rangle, \quad F_2(\tau,\beta,u) := \left\langle e^{i\beta} u(\cdot+\tau), i\phi_0 \right\rangle$$

and note that $F_1(0,0,\phi_0) = \langle \phi_0, \phi_0' \rangle = 0$ and $F_2(0,0,\phi_0) = \langle \phi_0, i\phi_0 \rangle = 0$. Further,

$$\begin{aligned}
\left.\frac{\partial(F_1,F_2)}{\partial(\tau,\beta)}\right|_{(0,0,\phi_0)} &= \det \left.\begin{bmatrix} \langle e^{i\beta}u'(\cdot+\tau), \phi_0' \rangle & \langle ie^{i\beta}u(\cdot+\tau), \phi_0' \rangle \\ \langle e^{i\beta}u'(\cdot+\tau), i\phi_0 \rangle & \langle ie^{i\beta}u(\cdot+\tau), i\phi_0 \rangle \end{bmatrix}\right|_{(0,0,\phi_0)} \\
&= \langle \phi_0', \phi_0' \rangle \langle i\phi_0, i\phi_0 \rangle \\
&\neq 0.
\end{aligned}$$

Thus by the implicit function theorem there exists an open ball $\mathcal{U}_\varepsilon := \{u \in X : \|u - \phi_0\|_X < \varepsilon\}$ and $C^1$ maps $\tau, \beta : \mathcal{U}_\varepsilon \to \mathbb{R}$ with $\tau(\phi_0) = \beta(\phi_0) = 0$ such that

$$F_1(\tau(u), \beta(u), u) = F_2(\tau(u), \beta(u), u) = 0$$

for all $u \in \mathcal{U}_\varepsilon$, which completes the demonstration of (2.43). This neighborhood $\mathcal{U}_\varepsilon$ is also close to the group orbit $\mathcal{O}_{\phi_0}$ in the sense that, for all $u \in \mathcal{U}_\varepsilon$,

$$\begin{aligned}
\rho(u, \phi_0) &= \inf_{\tau,\beta\in\mathbb{R}} \left\| e^{i\beta}u(\cdot+\tau) - \phi_0 \right\|_X \\
&\leq \|u - \phi_0\|_X \\
&< \varepsilon,
\end{aligned}$$

as claimed.

Let $u \in \mathcal{U}_\varepsilon$. Since $\mathcal{E}_0$ is invariant under spatial translations, it will suffice to show that $\mathcal{E}_0(u(\cdot+\tau(u)) - \mathcal{E}(\phi_0) \geq C\rho(u(\cdot+\tau(u)), \phi_0)^2$. Fix $u \in \mathcal{U}_\varepsilon \cap \mathcal{T}_0$ and write

$$e^{i\beta(u)}u(\cdot+\tau(u)) = \phi_0 + C_1\phi_0 + iC_2\phi_0' + iC_3\phi_0 + C_4\phi_0' + y, \tag{2.44}$$

where $C_1, C_2, C_3, C_4 \in \mathbb{R}$ and $y \perp \operatorname{span}_{\mathbb{R}}\{\phi_0, i\phi_0, \phi_0', i\phi_0'\}$. Let

$$h := e^{i\beta(u)}u(\cdot + \tau(u)) - \phi_0 = C_1\phi_0 + iC_2\phi_0' + iC_3\phi_0 + C_4\phi_0' + y.$$

Taking inner products of (2.44) with $\phi_0'$ and with $i\phi_0$, then applying (2.43) yields $C_3 = C_4 = 0$, hence

$$h = C_1\phi_0 + iC_2\phi_0' + y.$$

Now,

$$\begin{aligned}
Q(u) &= Q(e^{i\beta(u)}u(\cdot + \tau(u))) \\
&= Q(\phi_0 + h) \\
&= Q(\phi_0) + \langle \delta Q(\phi_0), h\rangle + \mathcal{O}(\|h\|_X^2) \quad \text{by Taylor's theorem} \\
\implies 0 &= \langle \phi_0, h\rangle + \mathcal{O}(\|h\|_X^2) \quad \text{since } Q(u) = Q(\phi_0) \\
&= C_1 \|\phi_0\|_{L^2(0,T)}^2 + \mathcal{O}(\|h\|_X^2) \\
\implies C_1 &= \mathcal{O}(\|h\|_X^2).
\end{aligned}$$

Similarly,

$$\begin{aligned}
N(u) &= N(e^{i\beta(u)}u(\cdot + \tau(u))) \\
&= N(\phi_0 + h) \\
&= N(\phi_0) + \langle \delta N(\phi_0), h\rangle + \mathcal{O}(\|h\|_X^2) \\
\implies 0 &= \langle i\phi_0', h\rangle + \mathcal{O}(\|h\|_X^2) \\
\implies C_2 &= \mathcal{O}(\|h\|_X^2).
\end{aligned}$$

Again by Taylor's theorem,

$$\begin{aligned}
\mathcal{E}_0(u) &= \mathcal{E}_0(e^{i\beta(u)}u(\cdot+\tau(u))) \\
&= \mathcal{E}_0(\phi_0) + \langle \delta\mathcal{E}_0(\phi_0), h\rangle + \frac{1}{2}\left\langle \delta^2\mathcal{E}_0(\phi_0)h, h\right\rangle + o(\|h\|_X^2) \\
\implies \mathcal{E}_0(u) - \mathcal{E}_0(\phi_0) &= \frac{1}{2}\left\langle \delta^2\mathcal{E}_0(\phi_0)h, h\right\rangle + o(\|h\|_X^2) \\
&= \frac{1}{2}\left\langle \delta^2\mathcal{E}_0(\phi_0)y, y\right\rangle + \mathcal{O}(\|h\|_X^3) \\
&\geq C^*\|y\|_X^2 - \widetilde{C}\|h\|_X^3 \qquad \text{for some constants } C^* > \widetilde{C} \text{ by Lemma 2.4.3} \\
&\qquad\qquad\qquad\qquad\qquad\qquad\qquad\qquad\qquad\qquad \text{upon possibly taking } \varepsilon \text{ smaller } (\|h\|_X < \varepsilon) \\
&= C^*\left\|h - C_1\phi_0 - iC_2\phi_0'\right\|_X^2 - \widetilde{C}\|h\|_X^3 \\
&\geq C\|h\|_X^2 \qquad \text{for some constant } C > 0 \text{ since } C_1, C_2 = \mathcal{O}(\|h\|_X^2) \\
&= C\left\|e^{i\beta(u)}u(\cdot+\tau(u)) - \phi_0\right\|_X^2 \\
&\geq \rho(u,\phi_0)^2.
\end{aligned}$$

So, there exist constants $\varepsilon, C > 0$ such that $\mathcal{E}_0(u) - \mathcal{E}_0(\phi_0) \geq C\rho(u,\phi_0)^2$ whenever $\rho(u,\phi_0) < \varepsilon$, as claimed. □

Equipped with the coercivity estimate in Proposition 2.4.4 above, we now establish orbital stability of $\phi_0$ with respect to complex-valued, $T$-antiperiodic perturbations.

*Proof of Theorem 2.4.1.* This proof follows the approach of [26, Proposition 3.1], [39, Theorem 4.1]. For the minimizer $\phi_0$, let $\delta > 0$ be such that Proposition 2.4.4 holds, i.e. that there exists constant $C_1 > 0$ such that $C_1\rho(\psi,\phi_0) \leq \mathcal{E}_0(\psi) - \mathcal{E}_0(\phi_0)$ for all $\psi \in \Sigma_0$ with $\rho(\psi,\phi_0) < \delta$, and let $v \in X$ satisfy $\|v\|_X \leq \varepsilon$ for some $\varepsilon > 0$ small. Since $\phi_0$ is a critical point of $\mathcal{E}_0$, Taylor's theorem implies that $\mathcal{E}_0(\phi_0 + v) - \mathcal{E}_0(\phi_0) \leq C_2\varepsilon^2$ for some constant $C_2 > 0$. Furthermore, notice that if $\phi_0 + v \in \Sigma_0$, then the unique solution $u(\cdot,t)$ of (2.38) with $u(\cdot,0) = \phi_0 + v$ remains in $\Sigma_0$ so long as it exists since $Q$ and $N$ are conserved under

the flow of fNLS. Since $\mathcal{E}_0(u(\cdot,t)) = \mathcal{E}_0(u(\cdot,0)) = \mathcal{E}_0(\phi_0+v)$ independently of $t$, we have

$$C_1\rho(u(\cdot,t),\phi_0)^2 \leq \mathcal{E}_0(\phi_0+v) - \mathcal{E}_0(\phi_0) \leq C_2\varepsilon^2$$

for all $t \geq 0$, provided $\varepsilon$ is taken small enough so that $C_2\varepsilon^2 < C_1\delta^2$. This establishes the orbital stability of $\phi_0$ to such perturbations.

Now consider the case that $\phi_0 + v \notin \Sigma_0$ but $\|v\|_X \leq \varepsilon$ and $N(\phi_0+v) = 0$. First, we claim that the mapping

$$(c,\mu) \mapsto (N(\phi(\cdot;c,\mu)), Q(\phi(\cdot;c,\mu)))$$

is a period-preserving diffeomorphism from a neighborhood of $(c,\mu) = (0,\mu_0)$ onto a neighborhood of $(N,Q) = (0,\mu_0)$. Indeed, consider the Jacobian

$$\left.\frac{\partial(N,Q)}{\partial(c,\mu)}\right|_{\substack{c=0\\ \mu=\mu_0}} = \det \begin{bmatrix} \left.\frac{\partial}{\partial c}N(\phi(\cdot;c,\mu_0))\right|_{c=0} & \left.\frac{\partial}{\partial c}Q(\phi(\cdot;c,\mu_0))\right|_{c=0} \\ \left.\frac{\partial}{\partial \mu}N(\phi(\cdot;0,\mu))\right|_{\mu=\mu_0} & \left.\frac{\partial}{\partial \mu}Q(\phi(\cdot;0,\mu))\right|_{\mu=\mu_0} \end{bmatrix}$$

and note that

$$\begin{aligned} \left.\frac{\partial}{\partial\mu}N(\phi(\cdot;0,\mu))\right|_{\mu=\mu_0} &= \left\langle \delta N(\phi_0), \frac{\partial\phi}{\partial\mu}(\cdot;0,\mu_0)\right\rangle_X \\ &= \left\langle i\phi_0', \frac{\partial\phi}{\partial\mu}(\cdot;0,\mu_0)\right\rangle_X \\ &= 0 \end{aligned}$$

since $\phi_0'$ and $\frac{\partial\phi}{\partial\mu}(\cdot;0,\mu_0)$ are real-valued functions, and

$$\left.\frac{\partial}{\partial\mu}Q(\phi(\cdot;0,\mu))\right|_{\mu=\mu_0} = \left.\frac{\partial}{\partial\mu}\mu\right|_{\mu=\mu_0} = 1.$$

Thus

$$\frac{\partial(N,Q)}{\partial(c,\mu)}\bigg|_{\substack{c=0\\ \mu=\mu_0}} = \frac{\partial}{\partial c} N(\phi(\cdot;c,\mu_0))\Big|_{c=0} \neq 0$$

by hypothesis, so there exists $\widetilde{\mu} \in \mathbb{R}$ with $\widetilde{\mu} = \mathcal{O}(\varepsilon)$ such that $\widetilde{\phi} := \phi(\cdot;0,\mu_0+\widetilde{\mu})$ is a real-valued, $T$-antiperiodic standing wave of fNLS (2.38) satisfying $Q(\widetilde{\phi}) = Q(\phi_0+v)$ and $\rho(\phi_0,\widetilde{\phi}) = \mathcal{O}(\varepsilon)$. Defining

$$\widetilde{\mathcal{E}}(u) := \mathcal{E}(u) + \omega(0,\mu_0+\widetilde{\mu})Q(u),$$

we have that $\widetilde{\phi}$ minimizes $\widetilde{\mathcal{E}}$ subject to the constraints $Q \equiv Q(\phi_0+v)$ and $N \equiv 0$. By Proposition 2.4.4, there exist constants $\delta, C_1 > 0$ such that

$$C_1\rho(\psi,\widetilde{\phi}) \leq \widetilde{\mathcal{E}}_0(\psi) - \widetilde{\mathcal{E}}_0(\widetilde{\phi})$$

for all $\psi \in \widetilde{\Sigma}_0 := \{u \in X : Q(u) = \mu_0+\widetilde{\mu},\ N(u) = 0\}$ such that $\rho(\psi,\widetilde{\phi}) < \delta$. By conservation of $Q$ and $N$, we have that $u(\cdot,t) \in \widetilde{\Sigma}_0$ for all $t$, hence the above coercivity estimate gives

$$C_1\rho(u(\cdot,t),\widetilde{\phi}) \leq \widetilde{\mathcal{E}}_0(\psi) - \widetilde{\mathcal{E}}_0(\widetilde{\phi})$$

whenever $\rho(u(\cdot,t),\widetilde{\phi}) < \delta$.

Since $\widetilde{\phi}$ is a critical point of $\widetilde{\mathcal{E}}$, we also have that

$$\begin{aligned}
\widetilde{\mathcal{E}}(u(\cdot,t)) - \widetilde{\mathcal{E}}(\widetilde{\phi}) &= \widetilde{\mathcal{E}}(\phi_0+v) - \widetilde{\mathcal{E}}(\widetilde{\phi}) \\
&= \widetilde{\mathcal{E}}(\widetilde{\phi} + (\phi_0 - \widetilde{\phi} + v)) - \widetilde{\mathcal{E}}(\widetilde{\phi}) \\
&= \mathcal{O}(\|\phi_0 - \widetilde{\phi} + v\|_X^2) \\
&= \mathcal{O}(\varepsilon^2),
\end{aligned}$$

hence there exists $C_2 > 0$ such that $\widetilde{\mathcal{E}}(u(\cdot,t)) - \widetilde{\mathcal{E}}(\widetilde{\phi}) \leq C_2\varepsilon^2$ for all $t \geq 0$. So,

$$C_1\rho(u(\cdot,t),\widetilde{\phi})^2 \leq C_2\varepsilon^2$$

for all $t \geq 0$, provided $\varepsilon$ is taken to be small enough so that $C_2\varepsilon^2 < C_1\delta^2$.

Finally, by the triangle inequality, we have for $\varepsilon$ sufficiently small that

$$\rho(u(\cdot,t),\phi_0)^2 = \Big(\rho(u(\cdot,t),\widetilde{\phi}) + \rho(\widetilde{\phi},\phi_0)\Big)^2 = \mathcal{O}(\varepsilon^2)$$

for all $t \geq 0$. Thus $\phi_0$ is orbitally stable to small perturbations that "slightly" change $Q$ yet preserve $N$, establishing Theorem 2.4.1. □

*Remark* 2.4.5. From the above proof, the assumption in Theorem 2.4.1 that $\phi$, $\omega$ depend smoothly on $\mu$ is only needed when considering perturbations $v$ such that $\phi_0 + v \notin \Sigma_0$ and $N(\phi_0 + v) = 0$. So, these assumptions can be removed if one is willing to restrict to perturbations $v$ that preserve the charge and angular momentum of the underlying wave.

# Chapter 3

# Numerical Bifurcation and Spectral Stability of Wavetrains in Bidirectional Whitham Models

## 3.1 Introduction

While the Euler equations form the de facto model for water waves, analysis of this very general model remains difficult, and simpler models have been proposed. Using KdV as a starting point, which is known to be a good model for waves of large wavelength in shallow water, Whitham [66] proposed the model

$$u_t + \mathcal{M}u_x + uu_x = 0,$$

where the operator $\mathcal{M}$ is a Fourier multiplier with symbol $m(\xi) = \sqrt{\tanh(\xi)/\xi}$, that incorporates the full unidirectional dispersion relation for the Euler equations in an effort to better capture mid- and high-frequency phenomena found in the Euler equations, such as wave steepening/peaking. His equation, now referred to as the *Whitham equation*, has received considerable attention in recent years, having been investigated analytically ([24], [21], [20], [37]) as well as numerically ([60], [24], [57]). These studies have found that the unidirectional Whitham equation not only captures wave steepening and derivative blow-up

[36], but also exhibits a highest cusped traveling wavetrain [23], existence of smooth solitary traveling waves [23], as well as the famous Benjamin-Feir, or modulational, instability for small amplitude wavetrains [37]. Furthermore, generalizations of Whitham's equation accounting for constant vorticity and surface tension have been studied [38]. However, the Whitham equation fails to capture particular high-frequency (spectral) instabilities of small periodic wavetrains due to the unidirectionality of wave propagation; see [18, 17].

Recently there has been interest in bidirectional Whitham models [52, 20, 35, 54, 22, 12] in an effort to discover models that capture more of the important qualitative properties of the full Euler equations, e.g. existence of smooth solitary waves and peaked traveling waves, and both high-frequency and modulational instabilities of small periodic wavetrains. These are often built as full-dispersion generalizations of the nonlinear shallow water equations

$$\begin{cases} u_t = -\eta_x - uu_x \\ \eta_t = -u_x - (\eta u)_x. \end{cases} \tag{3.1}$$

However, there does not seem to be a unique way to generalize (3.1) to incorporate the full dispersion relation for the Euler equations. Indeed, several different models can be found in the literature, all of which claim to be bidirectional Whitham equations. One of the main goals of this chapter is to numerically investigate the existence and stability of periodic wavetrains of both small and large amplitude, including the existence of highest peaked / cusped traveling waves, providing numerical confirmation of known analytical results as well as offering new conjectures for large amplitude waves in hopes of spurring further analytical study.

In this chapter, we will study three fully-dispersive shallow water wave models that have been presented in the literature. In [52], the bidirectional Whitham equation (written

here in non-dimensional form) is derived from the Euler equations:

$$\begin{cases} u_t &= -\eta_x - uu_x \\ \eta_t &= -\mathcal{K}u_x - (\eta u)_x \end{cases} \tag{3.2}$$

where the operator $\mathcal{K}$ incorporates the full-Euler dispersion and is defined via its symbol

$$\widehat{\mathcal{K}f}(n) := \frac{\tanh(n)}{n}\,\widehat{f}(n), \quad n \in \mathbb{Z}. \tag{3.3}$$

Here, $\eta$ represents the fluid height and $u = \phi_x$ with $\phi(x,t) = \phi(x,\eta(x,t),t)$ denoting the trace of the velocity potential at the free surface. A quick calculation shows that the dispersion relation of (3.2) agrees *exactly* with that of the full Euler equations: taking the linear part of (3.2) and differentiating the first equation with respect to $t$ and the second equation with respect to $x$ yields

$$u_{tt} = \mathcal{K}u_{xx}.$$

With $u(x,t) = Ae^{i(kx-\omega t)}$ for $A \in \mathbb{R}$, we have

$$A(-i\omega)^2 e^{i(kx-\omega t)} = A(ik)^2\,\frac{\tanh(k)}{k}e^{i(kx-\omega t)} \implies \omega^2 = k\tanh(k),$$

the exact dispersion relation of the full Euler equations.

While the well-posedness of this system is not fully understood, a recent result [22, Theorem 1] establishes that (3.2) is locally well-posed for all initial data $\eta(x,0) = \psi(x)$, $u(x,0) = \phi(x)$ with $\inf\psi > 0$. Though this result does not prove that the system is ill-posed for initial data having negative infimum, numerical evidence suggests that this is indeed the case: see Section 3.3.1 for further details. Furthermore, in [20] a class of $2\pi$-periodic traveling wave solutions of (3.2) was constructed, and it was proven that there exists a highest wave with a logarithimically-cusped singularity. Concerning the stability

of wavetrains, it has recently been shown that there exists a critical wavenumber $\kappa_c \approx 1.008$ such that all $2\pi/\kappa$-periodic wavetrains of (3.2) of sufficiently small amplitude are modulationally unstable provided $\kappa > \kappa_c$: see [54]. Our studies numerically confirm this rigorous modulational instability result, and we investigate the presence of such instabilities for large amplitude wavetrains as well.

Alternatively, [35] proposes the non-dimensional, full dispersion shallow water model

$$\begin{cases} u_t &= -\mathcal{K}\eta_x - uu_x \\ \eta_t &= -u_x - (\eta u)_x, \end{cases} \tag{3.4}$$

where $\mathcal{K}$, $u$, and $\eta$ are as in (3.2). Moreover, [35], establishes the local well-posedness of (3.4), the existence of even, small-amplitude, $2\pi/\kappa$-periodic wavetrains for all $\kappa > 0$, and that this system possesses a critical wavenumber $\kappa_c \approx 1.610$ such that all periodic waves of sufficiently small amplitude are modulationally unstable for $\kappa > \kappa_c$. In Section 3.3.2 below, we numerically study the existence and stability of wavetrain solutions of (3.4), including those of large amplitudes. We note that, in contrast with (3.2), it appears branches of smooth periodic traveling waves in (3.4) bifurcating from a zero-amplitude state do not appear to peak/cusp; rather, we posit that such waves of arbitrarily large amplitude are smooth.

Lastly, in [18, Section 5], a bidirectional *Boussinesq-Whitham* model is proposed:

$$u_{tt} = \partial_x^2(u^2 + \mathcal{K}u), \tag{3.5}$$

which we write as a first order system:

$$\begin{cases} u_t &= \eta \\ \eta_t &= \partial_x^2(u^2 + \mathcal{K}u). \end{cases} \tag{3.6}$$

This model is based on the so-called "bad Boussinesq" equation

$$u_{tt} = \partial_x^2 \left(u^2 + u + u_{xx}\right)$$

from shallow water theory. Although (3.6) is known to be ill-posed, see [35, Appendix C], it has nevertheless been shown to exhibit high-frequency instabilities of small amplitude periodic wavetrains, which are known to exist in the full Euler equations; see [50, 17]. In Section 3.3.3 below, we numerically study the existence and stability of large-amplitude periodic wavetrains of (3.6) and provide numerical evidence that the bifurcation branch of such such solutions terminates with a peaked or cusped wave.

To streamline our discussion and to set up a framework amenable to "black-box" computations, we will view each of the systems (3.2), (3.4), and (3.6) in a very general framework of the form

$$\begin{cases} u_t &= F(\vec{u}, \vec{\eta}) \\ \eta_t &= G(\vec{u}, \vec{\eta}), \end{cases} \tag{3.7}$$

where

$$\vec{u} := (u, \partial_x u, \partial_x^2 u, \ldots, \partial_x^n u), \quad \vec{\eta} := (\eta, \partial_x \eta, \partial_x^2 \eta, \ldots, \partial_x^n \eta).$$

For the models being considered, one of $F$ or $G$ will incorporate the Euler dispersion operator $\mathcal{K}$. Upon transforming $x \mapsto x - ct$ in (3.7), traveling wave solutions with wave speed $c$ satisfy (with a slight abuse of notation)

$$\begin{cases} u_t &= cu_x + F(\vec{u}, \vec{\eta}) =: F(\vec{u}, \vec{\eta}; c) \\ \eta_t &= c\eta_x + G(\vec{u}, \vec{\eta}) =: G(\vec{u}, \vec{\eta}; c), \end{cases} \tag{3.8}$$

and equilibrium solutions $(u(x,t),\eta(x,t)) = (\phi(x),\psi(x))$ of the above traveling wave system satisfy the profile equations

$$\begin{cases} F(\vec{\phi},\vec{\psi};c) &= 0 \\ G(\vec{\phi},\vec{\psi};c) &= 0. \end{cases} \tag{3.9}$$

Assuming that one can resolve either $\psi(x)$ in terms of $\phi(x)$ or $\phi(x)$ in terms of $\psi(x)$ in (3.9), which will fortunately be the case for our intended applications, we can conveniently express a single profile equation for, say, $\phi$ in the form

$$\mathcal{K}\phi = g(c,\phi), \tag{3.10}$$

where $\mathcal{K}$ is as in (3.3) and $g$ implicitly relates the wave speed $c$ and its corresponding profile $\phi$. Using this framework, we implement numerical methods for each model to compute a global bifurcation of periodic solutions from a constant amplitude state, as well as the spectrum of the linearization for a sampling of waves of various heights. See Section 3.2 and Appendix C for detailed discussions of these methods.

Through numerical experiments, we find that, from the perspective of bifurcation and stability of periodic wavetrains, the three models discussed above have many similar qualitative features. We find that periodic traveling waves in each of these models indeed exhibit both high-frequency and modulational instabilities for waves of sufficiently large amplitude. However, high-frequency instabilities for small amplitude waves as predicted by the full Euler equations are numerically imperceptible for the models considered here, suggesting that these models fail to capture high-frequency instabilities in arbitrarily small amplitude waves. Furthermore, we find that while the global bifurcation branches of smooth periodic wavetrains for the models (3.2) and (3.5) seem to terminate in a highest singular (peaked/cusped) wave, our numerical experiments lead us to conjecture that the cor-

responding branches for the model (3.4) extend to arbitrarily high amplitude smooth solutions. Furthermore, while the model (3.4) is known to be locally well-posed [35], the model (3.2) is only known to be *conditionally* locally well-posed [22], requiring that the height profile $\eta$ of the initial data be uniformly positive. In Section 3.3.1 below we provide strong numerical evidence that the local evolution of (3.2) is in fact *ill-posed* if the positivity condition on $\eta$ is removed. This leads us to construct new branches of periodic wavetrains of (3.2) with uniformly positive $\eta$, which had previously been unstudied: see Section 3.3.1 below.

The outline of this chapter is as follows. In Section 3.2 we discuss the numerical bifurcation techniques used to construct the global bifurcation curves of periodic wavetrain solutions with fixed period. In Section 3.3 we present our main results for each of the models (3.2), (3.4), and (3.5): see Sections 3.3.1, 3.3.2, and 3.3.3, respectively. Further, in Section 3.3.1 describes in detail the numerical methods used to approximate the stability spectrum associated to periodic wavetrains of (3.2). Section 3.4 provides a concluding summary of the main observations of this chapter. In Appendix C we detail how these numerical stability methods extend to more general models, including (3.4) and (3.5). Throughout, the parameters of the numerical methods (e.g. number of Fourier modes used) are chosen by experiment to ensure that the behavior of the computed waves and their corresponding spectra are qualitatively correct. See Appendix D for further details.

## 3.2 Numerical Bifurcation Methods

In this section we discuss the methods used to numerically approximate the even, $2\pi$-periodic solutions of the bidirectional Whitham models. In summary, the approximations will be obtained by truncating an expansion of the profile $\phi$ in an appropriate Fourier basis and discretizing the integrals that yield the Fourier coefficients. The resulting expression

will then be used to form a discretized version of the profile equation (3.10), which will be enforced at a fixed number of *collocation points* in order to yield a nonlinear system of equations which may be solved, for example, via Newton's method. Using the local bifurcation theory for the model to generate an "initial guess" for the nonlinear system solver, an algorithm known as the *pseudo-arclength method* will be employed as a robust method for simultaneously continuing the values of the wave speed and its corresponding approximate profiles along a global bifurcation branch.

### 3.2.1 Cosine Collocation Method

Note that even, $2\pi/\kappa$-periodic functions $\phi = \phi(x)$ are naturally represented in a cosine series

$$\phi(x) = \sum_{n=0}^{\infty} \widehat{\phi}(n)\cos(n\kappa x), \tag{3.11}$$

where

$$\widehat{\phi}(n) = \begin{cases} \dfrac{\kappa}{\pi}\displaystyle\int_0^{\pi/\kappa} \phi(x)\,dx & \text{if } n = 0 \\ \dfrac{2\kappa}{\pi}\displaystyle\int_0^{\pi/\kappa} \phi(x)\cos(n\kappa x)\,dx & \text{if } n \geq 1. \end{cases} \tag{3.12}$$

Partitioning the interval $[0, \pi/\kappa]$ into $N$ subintervals, for each $n \in \mathbb{N}_0$ we discretize the integrals in (3.12) by the midpoint method as

$$\int_0^{\pi/\kappa} \phi(x)\cos(n\kappa x)\,dx \approx \sum_{i=1}^{N} \phi(x_i)\cos(n\kappa x_i)\frac{\pi}{\kappa N}, \tag{3.13}$$

where the $x_i = \dfrac{(2i-1)\pi}{2\kappa N}$ for $i = 1, 2, \ldots, N$ are the so-called *collocation* points on $[0, \pi/\kappa]$. Using this approximation in (3.12), we obtain the following approximations of the series coefficients:

$$\widehat{\phi}(n) \approx \widehat{\phi}_N(n) := w(n)\sum_{i=1}^{N} \phi(x_i)\cos(n\kappa x_i), \tag{3.14}$$

where

$$w(n) := \begin{cases} 1/N & \text{if } n = 0 \\ 2/N & \text{if } n \geq 1. \end{cases}$$

Using this approximation for the series coefficients in (3.11), and truncating the series to $N$ terms, we obtain

$$\begin{aligned} \phi(x) \approx \phi_N(x) &:= \sum_{n=0}^{N-1} \left[ w(n) \sum_{i=1}^{N} \phi(x_i) \cos(n\kappa x_i) \right] \cos(n\kappa x) \\ &= \sum_{i=1}^{N} \left[ w(n) \sum_{n=0}^{N-1} w(n) \cos(n\kappa x_i) \cos(n\kappa x) \right] \phi(x_i). \end{aligned} \tag{3.15}$$

Moreover, note that since $\phi$ is even, so is $\mathcal{K}\phi$, where again $\mathcal{K}$ is defined as in (3.3) . It follows we can approximate $\mathcal{K}\phi(x)$ similarly by truncating cosine series expansion and again approximating coefficients with (3.14):

$$\begin{aligned} \mathcal{K}\phi(x) &= \sum_{n=0}^{\infty} \widehat{\mathcal{K}\phi}(n) \cos(n\kappa x) \\ &\approx \sum_{n=0}^{N-1} \widehat{\mathcal{K}\phi_N}(n) \cos(n\kappa x) \\ &= \sum_{n=0}^{N-1} \widehat{\mathcal{K}}(n) \widehat{\phi}_N(n) \cos(n\kappa x) \\ &= \sum_{i=1}^{N} \left[ \sum_{n=0}^{N-1} w(n) \frac{\tanh(\kappa n)}{\kappa n} \cos(n\kappa x_i) \cos(n\kappa x) \right] \phi(x_i) =: (\mathcal{K}\phi)_N(x). \end{aligned} \tag{3.16}$$

Thus we arrive at an approximate profile equation:

$$(\mathcal{K}\phi)_N(x) = g(c, \phi_N(x)). \tag{3.17}$$

For notational convenience, going forward we denote evaluation of $\phi_N$ and $(\mathcal{K}\phi)_N$ at each collocation point $x_i$ via a superscript:

$$\phi_N^i := \phi_N(x_i), \quad \text{and} \quad (\mathcal{K}\phi)_N^i := (\mathcal{K}\phi)_N(x_i).$$

Enforcing (3.17) at each $x_i$ yields a nonlinear system

$$f_i(c, \phi_N^1, \phi_N^2, \ldots, \phi_N^N) := g(c, \phi_N^i) - (\mathcal{K}\phi)_N^i = 0, \quad i = 1, \ldots, N, \tag{3.18}$$

which we will endeavor to solve for wave speed $c$ and approximate points $\phi_N^1, \ldots, \phi_N^N$ on the corresponding profile.

*Remark* 3.2.1. Note that the system defined by (3.18) is actually underdetermined, as it contains $N+1$ unknowns but only $N$ equations. However, as discussed below, the numerical continuation algorithm will impose an additional condition as these solutions are computed along the global bifurcation branch, at each step yielding a well-defined, full-rank system.

### 3.2.2 Numerical Continuation by the Pseudo-Arclength Method

To solve the discretized profile system (3.18), we use the *pseudo-arclength* method, a numerical continuation algorithm which is well-known to the numerical bifurcation community. Nevertheless, we provide a summary of the method here.

For further notational convenience, let $y := (c, \phi_N^1, \ldots, \phi_N^N) \in \mathbb{R}^{N+1}$ and define $f : \mathbb{R}^{N+1} \to \mathbb{R}^N$ by $f(y) := (f_1(y), \ldots, f_N(y))$. Then to solve (3.18), we seek $y$ such that

$$f(y) = 0. \tag{3.19}$$

The pseudo-arclength method is a *predictor-corrector* method; given a point on the solution curve $f(y) = 0$, another solution is found by first applying an extrapolation (*predictor*) from the known solution, followed by a *corrector* process that projects the extrapolation back onto the solution curve. More specifically, the pseudo-arclength method follows the following program:

1. Given a point $y_0 \in \mathbb{R}^{N+1}$ with $f(y_0) = 0$, a unit tangent direction $z_0$ to the solution curve at $y_0$, and a step size $h$, form the predictor $y_1^p$ by extrapolating $h$ units along $z_0$, i.e. $y_1^p := y_0 + hz_0$.

2. Project $y_0^p$ back onto the solution curve $f(y) = 0$ along the direction orthogonal to $z_0$. That is, solve for $y_1$ in the augmented nonlinear system

$$\begin{cases} f(y_1) &= 0 \\ z_0 \cdot (y_1 - y_1^p) &= 0. \end{cases}$$

3. For the next step of the method, a suitable tangent vector $z_1$ to the solution curve at the point $y_1$ can be found by solving for $z_1$ in the following system of $N+1$ equations and $N+1$ unknowns:

$$\begin{cases} Df(y_1)z_1 &= 0 \\ z_0 \cdot z_1 &= 1. \end{cases} \tag{3.20}$$

Note that the $z_1$ solved for in (3.20) will not necessarily be of unit length and should therefore be normalized before further iteration. Steps (1)-(3) above can be iterated to continue from a solution $y_k$ to another point $y_{k+1}$ such that $f(y_{k+1}) = 0$. See Figure 3.1 for a graphical illustration of the method.

*Remark* 3.2.2. The first equation in (3.20) is the *tangency condition* ensuring that $z_1$ is tangent to the solution curve at $y_1$. The second equation is an *orientation condition* guar-

anteeing that the angle between $z_0$ and $z_1$ is acute. Hence the tangent vectors will be consistently oriented from one iteration to the next so that the method always makes "forward progress", not backtracking toward the previous solution point. Together, these conditions form a full-rank system that can also be solved using a nonlinear equation solver. In theory, any positive number could be used on the right-hand side of the orientation condition of (3.20). The only difference would be the magnitude of the solution $z_1$, which is inconsequential as this initial solution is scaled to unit length before further iteration.

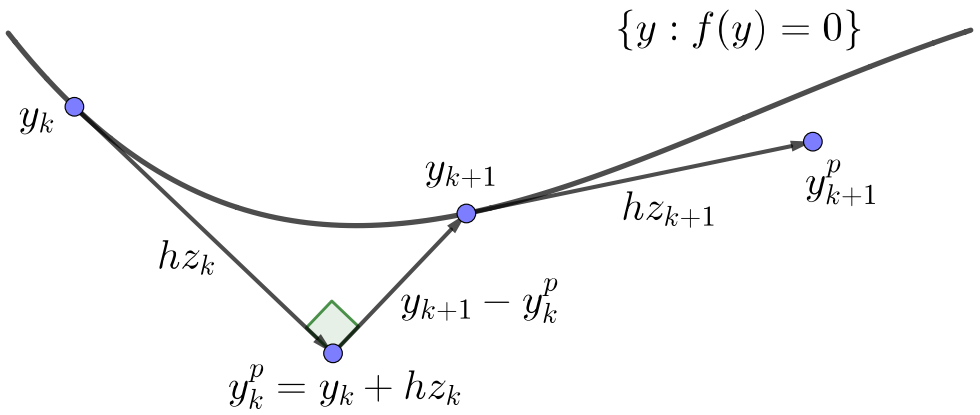


Figure 3.1: Illustration of the pseudo-arclength method: via a predictor-corrector scheme, for a given point $y_k$ such that $f(y_k) = 0$ the method computes $y_{k+1}$ such that $f(y_{k+1}) = 0$ and a consistently-oriented tangent direction $z_{k+1}$ at $y_{k+1}$.

As is evident from Step (1) of the pseudo-arclength algorithm given above, it is necessary to start the method with an initial point $y_0$ such that $f(y_0) = 0$. We can find such a point near the start of the bifurcation branch via the local bifurcation theory for the model, which yields curves $c = c(\varepsilon)$ and $\phi = \phi(x;\varepsilon)$ that trace the bifurcation branch for $\varepsilon > 0$ small. Indeed, for small $\varepsilon_0 > 0$ fixed, consider

$$y_0 := (c(\varepsilon_0), \phi(x_1;\varepsilon_0), \phi(x_2;\varepsilon_0), \ldots, \phi(x_N;\varepsilon_0)). \tag{3.21}$$

This $y_0$ does not necessarily solve $f(y_0) = 0$ exactly, but by virtue of $\varepsilon_0$ being small, $y_0$ should be *very close* to the solution curve. Thus we may use this $y_0$ as a good "initial guess" to seed the pseudo-arclength method. Moreover, since the local bifurcation curve is parameterized by $\varepsilon$ for $\varepsilon > 0$ small, we compute the tangent direction to the local bifurcation curve at $y_0^*$ by differentiating with respect to $\varepsilon$ at $\varepsilon_0$ and normalizing to unit length:

$$z_0^* := \left( c'(\varepsilon_0), \frac{\partial \phi}{\partial \varepsilon}(x_1; \varepsilon_0), \frac{\partial \phi}{\partial \varepsilon}(x_2; \varepsilon_0), \ldots, \frac{\partial \phi}{\partial \varepsilon}(x_N; \varepsilon_0) \right), \quad z_0 := \frac{z_0^*}{|z_0^*|},$$

Now, $z_0^*$ is not necessarily tangent to the solution curve, but since $\varepsilon_0 > 0$ is small, $z_0^*$ is very nearly tangent to the solution curve at $y_0$ as found above, and we take $z_0 := z_0^*/|z_0^*|$ as the initial tangent direction.

*Remark* 3.2.3. In practice it does not matter that $z_0$ is not exactly tangent to the solution curve at $y_0$. The accuracy of the $y_0$ and $z_0$ obtained from the local bifurcation formulas affects the quality of the first predictor $y_1^p$, but for small $\varepsilon_0$ these initial inaccuracies are mitigated by the Newton solver in steps (2) and (3) of the method to obtain $y_1$ and $z_1$. Then, fortunately, all future iterations will have highly accurate starting points and tangent directions from which to form their predictors.

## 3.3 Numerical Results

In this section, we present our main numerical results for each of the bidirectional Whitham models (3.2), (3.4), and (3.6). Precisely, we implement the program outlined by the numerical bifurcation methods described in Section 3.2 to compute small and large amplitude traveling periodic profiles, and we produce the global bifurcation diagrams of periodic traveling waves with fixed period. Moreover, we study the stability of these waves to localized (i.e. integrable on $\mathbb{R}$) perturbations by using a Fourier-Floquet-Hill method [16] to numer-

ically compute the spectrum of the associated linearized operators. We begin our analysis by demonstrating the relevant details of the computations for the model (3.2). Since the details for the models (3.4) and (3.6) are highly similar, only a summary of their relevant formulas will be provided.

### 3.3.1 Analysis of System (3.2)

We begin our analysis by considering the existence of periodic traveling waves for the bidirectional Whitham model (3.2):

$$\begin{cases} u_t &= -\eta_x - uu_x \\ \eta_t &= -\mathcal{K}u_x - (\eta u)_x. \end{cases}$$

Recall that in the modeling of shallow water waves, $\eta$ represents the fluid height and $u$ is the trace of the velocity potential at the free surface. Transforming to traveling wave coordinates $x \mapsto x - ct$, such solutions are seen to be stationary, spatially periodic solutions $(u(x,t),\eta(x,t)) = (\phi(x),\psi(x))$ of the evolutionary equation

$$\begin{cases} u_t &= -\eta_x - uu_x + cu_x =: F(u,u_x,\eta,\eta_x;c) \\ \eta_t &= -\mathcal{K}u_x - (\eta u)_x + c\eta_x =: G(u,u_x,\eta,\eta_x;c), \end{cases} \tag{3.22}$$

hence the profiles $\phi,\psi$ satisfy the system

$$\begin{cases} 0 &= -\psi' - \phi\phi' + c\phi' \\ 0 &= -\mathcal{K}\phi' - (\psi\phi)' + c\psi'. \end{cases} \tag{3.23}$$

Upon integrating (3.23) and setting constants of integration to zero[1], we can resolve $\psi$ in terms of $\phi$ in (3.23) to obtain

$$\begin{aligned}\psi &= c\phi - \frac{1}{2}\phi^2 \\ \mathcal{K}\phi &= \frac{1}{2}\phi^3 - \frac{3}{2}c\phi^2 + c^2\phi =: g(c,\phi).\end{aligned} \tag{3.24}$$

As explained in [20], one should not expect (3.24) to admit smooth solutions of arbitrary amplitude. Indeed, notice that if $\phi$ is an $H^1$ solution of (3.24) then differentiating (3.24) yields

$$\mathcal{K}\phi' = \left(\frac{3}{2}\phi^2 - 3c\phi + c^2\right)\phi' \implies \phi' = \frac{\mathcal{K}\phi'}{\frac{3}{2}\phi^2 - 3c\phi + c^2}. \tag{3.25}$$

The operator $\mathcal{K}$ improves the smoothness of its operand by exactly one order, hence by (3.25) we have that $\phi'$ is as smooth as $\phi$ so long as $\frac{3}{2}\phi^2 - 3c\phi + c^2 \neq 0$, in which case a bootstrap argument demonstrates that $\phi$ is in fact $C^\infty$. When continuing from constant solutions, i.e. solutions with height zero, the breakdown of smoothness occurs when $\frac{3}{2}\phi^2 - 3c\phi + c^2 = 0$ or, more precisely, when the bifurcation branch intersects the curve $\phi = \left(1 - \frac{1}{\sqrt{3}}\right)c$. Thus we expect (as is shown in [20]) that periodic solutions of (3.24) along the bifurcation branch with fixed period will have a maximum amplitude of

$$\max\phi(x) = \gamma := c\left(1 - \frac{1}{\sqrt{3}}\right).$$

See [20] for details of the above arguments.

[1]Note by Galilean invariance, one of the two integration constants can always be set to zero. For our analysis, we set the other integration constant to zero for simplicity. See [20] for details.

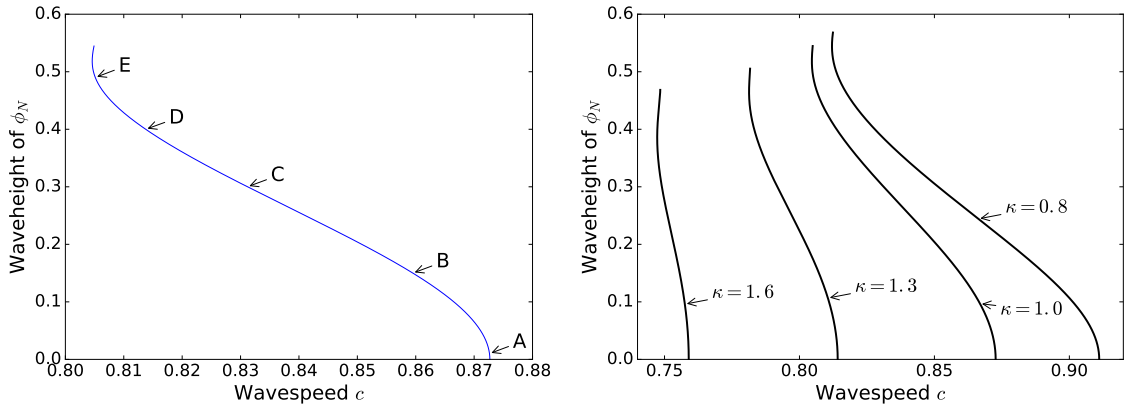


(a) (b)

Figure 3.2: (a) A numerical approximation of the global bifurcation branch of $2\pi$-periodic ($\kappa = 1$), even traveling solutions of (3.24) is displayed, with specific points A-E labeled for forthcoming computations: Point A at $c \approx 0.8726$, height $\approx 0.01$; Point B at $c \approx 0.8595$, height $\approx 0.15$; Point C at $c \approx 0.8312$, height $\approx 0.30$; Point D at $c \approx 0.8138$, height $\approx 0.40$; Point E at $c \approx 0.8051$, height $\approx 0.49$. (b) Bifurcation branches of $2\pi/\kappa$-periodic solutions of (3.24) for varying values of $\kappa$. Notice all these curves experience a turning point near the top of the branch.

### Analysis of Waves Bifurcating from Zero

To study the $2\pi/\kappa$-periodic traveling wave solutions of (3.24) bifurcating from the trivial state $\phi \equiv 0$, we use the profile equation (3.24) in combination with the following local bifurcation formulas (see [20, Proposition 5.1])

$$\phi(x;\varepsilon) := \varepsilon\cos(\kappa x) + \frac{3c_\kappa\varepsilon^2}{4}\left(\frac{1}{c_\kappa^2 - 1} + \frac{\cos(2\kappa x)}{c_\kappa^2 - c_{2\kappa}^2}\right) + \mathcal{O}(\varepsilon^3) \tag{3.26}$$

$$c(\varepsilon) := c_\kappa + \frac{3\varepsilon^2}{8}\left[-\frac{1}{2c_\kappa} + 3c_\kappa\left(\frac{1}{c_\kappa^2 - 1} + \frac{1}{2(c_\kappa^2 - c_{2\kappa}^2)}\right)\right], \quad c_\ell := \sqrt{\frac{\tanh(\ell)}{\ell}}, \tag{3.27}$$

and apply the pseudo-arclength method as discussed in Section 3.2.2 to compute approximations $\phi_N(x_i)$ of the profile $\phi(x_i)$ at the collocation points $x_i = \dfrac{(2i-1)\pi}{\kappa N}$ for $i = 1, \ldots, N$, continuing while $\phi(0) \approx \phi_N(x_1) < \gamma$. A global bifurcation plot of waveheight vs. wave

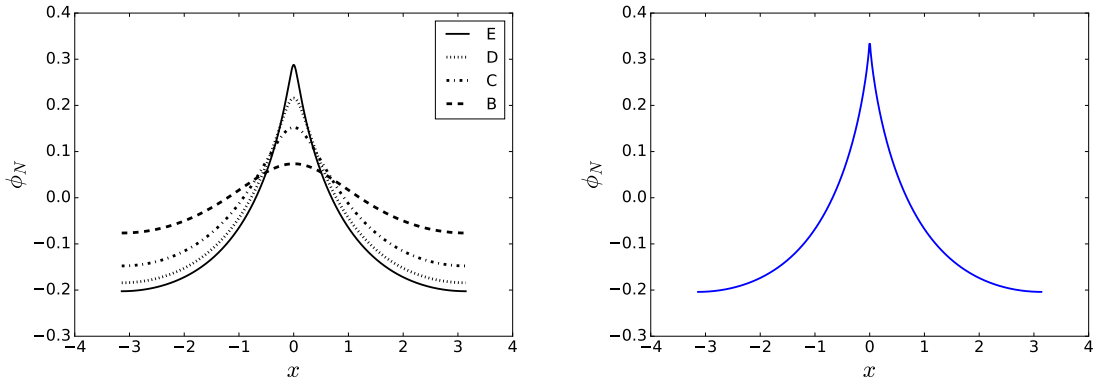


(a) (b)

Figure 3.3: (a) Profiles corresponding to the sampled points on the branch of $2\pi$-periodic solutions of in Figure 3.2(a): Point B at $c \approx 0.8595$, height $\approx 0.15$; Point C at $c \approx 0.8312$, height $\approx 0.30$; Point D at $c \approx 0.8138$, height $\approx 0.40$; Point E at $c \approx 0.8051$, height $\approx 0.49$. (b) A nearly "highest" wave high up the bifurcation branch in Figure 3.2(a).

speed for various wavenumbers $\kappa$ is shown in Figure 3.2(b), where we define

$$\text{waveheight} := \max_{x\in[0,\pi/\kappa]} \phi(x) - \min_{x\in[0,\pi/\kappa]} \phi(x) = \phi(0) - \phi(\pi/\kappa),$$

which is well-defined due to the monotonicity properties of even solutions along the global bifurcation branch as demonstrated in [20].

To illustrate the our numerical results for this model, we sample a selection of points along the global bifurcation diagram as described in Figure 3.2(a). As shown in Figure 3.3(a), the crest at the maximum of the smooth profiles along the global bifurcation branch becomes sharper as the waveheight increases, appearing to converge to a non-trivial profile with a singularity at the origin. The existence and qualitative properties of this highest singular wave has been studied analytically in [20], where it was shown the highest wave has a logarithmic cusp of order $|x \ln |x||$ near the top of the bifurcation curve: see Figure 3.3(b). We refer the interested reader to [20] for details.

In addition to the existence of a highest singular wave, we also wish to understand the dynamical stability of the smooth periodic solutions constructed above. To this end, we wish to determine the spectrum of the linearization of (3.22) about such a smooth periodic traveling wave $\phi$. To linearize the traveling wave system (3.22) about the velocity profile $\phi$ described above and the corresponding height profile $\psi = c\phi - \frac{1}{2}\phi^2$, we write

$$\begin{aligned} u(x,t) &= \phi(x) + \varepsilon v(x,t) + \mathcal{O}(\varepsilon^2) \\ \eta(x,t) &= \psi(x) + \varepsilon w(x,t) + \mathcal{O}(\varepsilon^2) \end{aligned} \tag{3.28}$$

where, since we are interested in the stability to *localized* perturbations, we require that $v(\cdot,t), w(\cdot,t) \in L^2(\mathbb{R})$ at each time $t > 0$ for which they are defined. Substituting these expansions into the first equation of (3.22) yields

$$\begin{aligned} \varepsilon v_t &= (-\psi' - \phi\phi' + c\phi') + \varepsilon\left[-\phi' v + (c-\phi)v_x - w_x\right] + \mathcal{O}(\varepsilon^2) \\ \varepsilon w_t &= (-\mathcal{K}\phi' - (\psi\phi)' + c\psi') + \varepsilon\left[-\psi' v - \psi v_x - \mathcal{K}v_x - \psi' w + (c-\phi)w\right] + \mathcal{O}(\varepsilon^2) \end{aligned} \tag{3.29}$$

as $\varepsilon \to 0$, where the $\mathcal{O}(1)$ terms vanish per the equilibrium system (3.23). Taking $\varepsilon \to 0$ above and applying separation of variables to decompose the perturbations as

$$(v(x,t), w(x,t)) = e^{\lambda t}(v(x), w(x))$$

yields the spectral problem on $L^2(\mathbb{R}) \times L^2(\mathbb{R})$:

$$\begin{cases} \lambda v = -\phi' v + (c-\phi)v_x - w_x \\ \lambda w = -\psi' v - \psi v_x - \mathcal{K}v_x - \psi' w + (c-\phi)w \\ \qquad\quad =: \mathcal{L}\begin{bmatrix} v \\ w \end{bmatrix}. \end{cases} \tag{3.30}$$

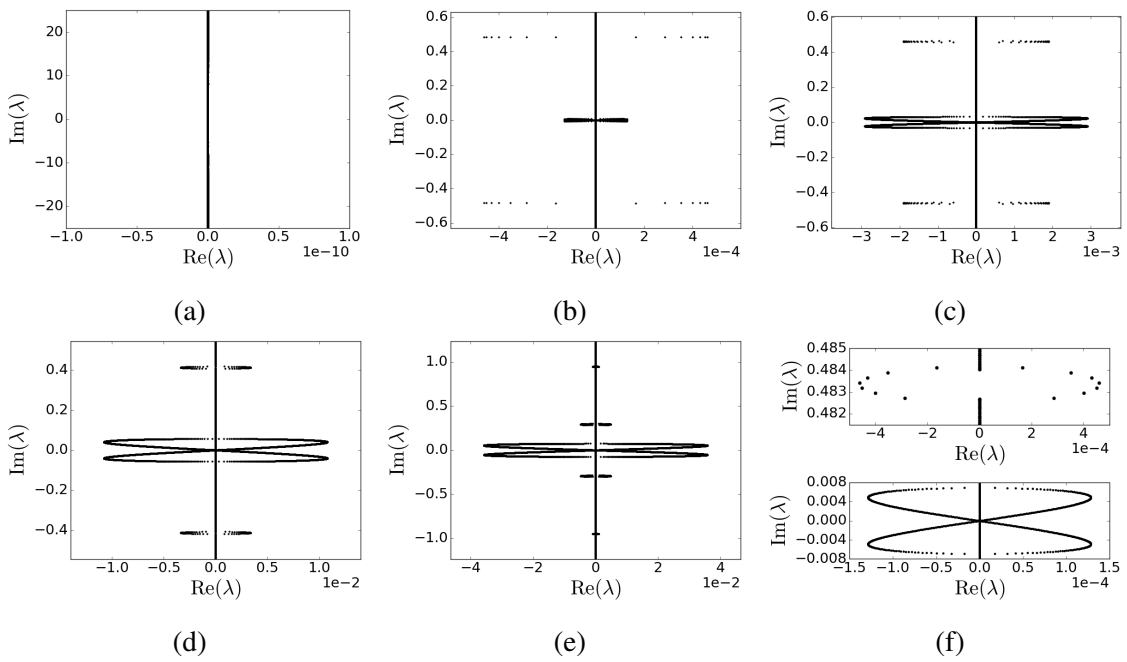


Figure 3.4: (a)-(e) Numerical approximations of the spectrum of $\mathcal{L}$ corresponding to the linearization of (3.2) about the profiles corresponding to the points A-E, respectively, along the bifurcation branch for $2\pi$-periodic solutions in Figure 3.2(a). (f) Zoom-in on the high-frequency instability (top) and the modulational instability (bottom) in the spectral plot (b).

By Floquet theory, we know the spectrum associated to $\mathcal{L}$ is purely essential, containing no isolated eigenvalues of finite multiplicity: see [56, 8]. Indeed, one can show that $\lambda$ belongs to the $L^2(\mathbb{R})$-spectrum of $\mathcal{L}$ if and only if there exists a so-called "Bloch parameter" $\mu \in [0,1)$ such that (3.30) has a bounded solution satisfying

$$(v,w)(x+2\pi/\kappa) = e^{i\kappa\mu}(v,w)(x)$$

for all $x \in \mathbb{R}$. It follows that the perturbations $(v,w)$ in (3.30) can be expanded in "Bloch" form as

$$v(x) = \sum_{l\in\mathbb{Z}} \widehat{V}(l)e^{i\kappa(\mu+l)x}, \quad w(x) = \sum_{l\in\mathbb{Z}} \widehat{W}(l)e^{i\kappa(\mu+l)x}. \tag{3.31}$$

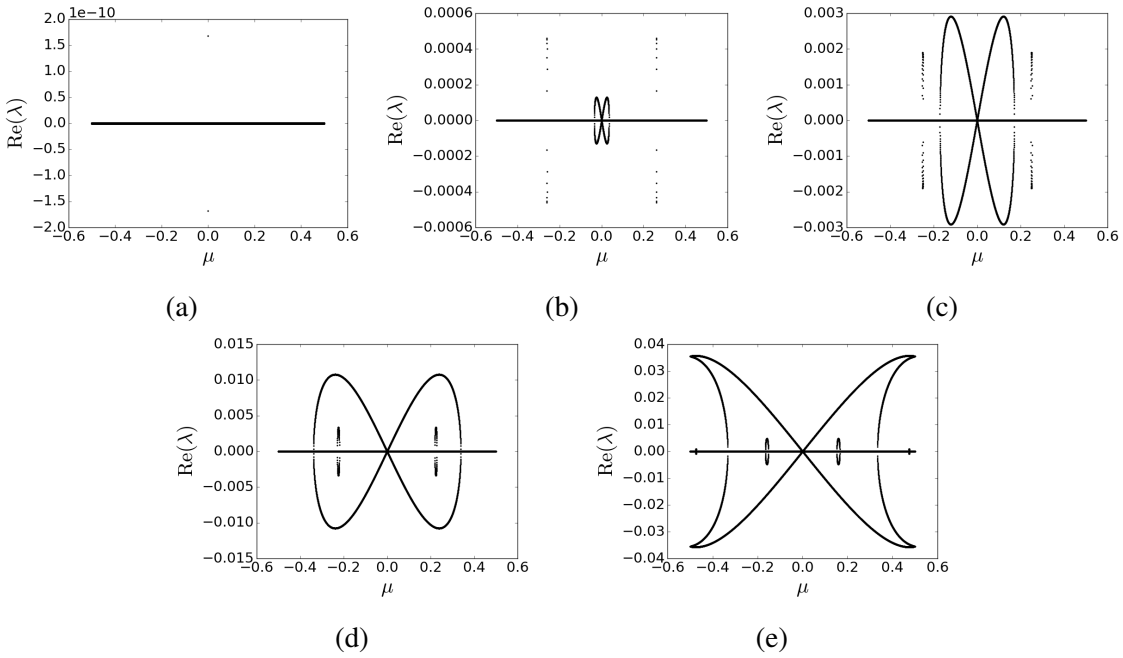


Figure 3.5: (a)-(e) Plots of the growth rates $\mathrm{Re}(\lambda)$ vs. $\mu$ for each of the spectral plots (a)-(e), respectively, in Figure 3.4.

Substituting the expansions (3.31) for $v$ and $w$ into the first equation of (3.30), we obtain

$$\lambda \sum_{m\in\mathbb{Z}} \widehat{V}(m) e^{i\kappa m x} = \sum_{m\in\mathbb{Z}} \sum_{l\in\mathbb{Z}} \Big[ \Big( ic\kappa(\mu+l)\delta_{m,l} - i\kappa(\mu+m)\widehat{\phi}(m-l) \Big) \widehat{V}(l) - i\kappa(\mu+l)\widehat{W}(l) \Big] e^{i\kappa m x},$$

where $\widehat{\phi}(n)$ denotes the $n$th Fourier coefficient associated to the periodic profile $\phi$. It follows that each $m \in \mathbb{Z}$ we must have

$$\lambda \widehat{V}(m) = \sum_{l\in\mathbb{Z}} \Big[ \widehat{A}^{\mu}(m,l)\widehat{V}(l) + \widehat{B}^{\mu}(m,l)\widehat{W}(l) \Big], \tag{3.32}$$

where

$$\widehat{A}^{\mu}(m,l) = ic\kappa(\mu+l)\delta_{m,l} - i\kappa(\mu+m)\widehat{\phi}(m-l)$$

$$\widehat{B}^{\mu}(m,l) = -i\kappa(\mu+l)\delta_{m,l}$$

with $\delta_{m,n}$ denoting the Kronecker delta. Similarly, substituting the expansions (3.31) into the second equation of (3.30) yields, for each $m \in \mathbb{Z}$,

$$\lambda\widehat{W}(m) = \sum_{l\in\mathbb{Z}} \left[\widehat{C}^{\mu}(m,l)\widehat{V}(l) + \widehat{D}^{\mu}(m,l)\widehat{W}(l)\right], \tag{3.33}$$

where

$$\widehat{C}^{\mu}(m,l) = -i\kappa(\mu+m)\widehat{\psi}(m-l) - i\kappa(\mu+l)\widehat{\mathcal{K}}(\kappa(\mu+l))\delta_{m,l}$$
$$\widehat{D}^{\mu}(m,l) = ic\kappa(\mu+l)\delta_{m,l} - i\kappa(\mu+m)\widehat{\phi}(m-l).$$

Defining the bi-infinite matrices

$$\widehat{A}^{\mu} := [\widehat{A}^{\mu}(m,l)]_{m,l\in\mathbb{Z}}, \quad \widehat{B}^{\mu} := [\widehat{B}^{\mu}(m,l)]_{m,l\in\mathbb{Z}},$$
$$\widehat{C}^{\mu} := [\widehat{C}^{\mu}(m,l)]_{m,l\in\mathbb{Z}}, \quad \widehat{D}^{\mu} := [\widehat{D}^{\mu}(m,l)]_{m,l\in\mathbb{Z}}$$

entry-wise for row-$m$ and column-$l$ with $m,l \in \mathbb{Z}$, the system (3.32)-(3.33) can be written in block bi-infinite matrix form as

$$\lambda \left[\begin{array}{c} \widetilde{V} \\ \hline \widetilde{W} \end{array}\right] = \left[\begin{array}{c|c} \widehat{A}^{\mu} & \widehat{B}^{\mu} \\ \hline \widehat{C}^{\mu} & \widehat{D}^{\mu} \end{array}\right] \left[\begin{array}{c} \widetilde{V} \\ \hline \widetilde{W} \end{array}\right] =: \widehat{\mathcal{L}}^{\mu} \left[\begin{array}{c} \widetilde{V} \\ \hline \widetilde{W} \end{array}\right], \tag{3.34}$$

where $\widetilde{V}, \widetilde{W}$ denote the bi-infinite arrays

$$\begin{cases} \widetilde{V} := \left[\ldots \quad \widetilde{V}(-2) \quad \widetilde{V}(-1) \quad \widetilde{V}(0) \quad \widetilde{V}(1) \quad \widetilde{V}(2) \quad \ldots\right]^T \\ \widetilde{W} := \left[\ldots \quad \widetilde{W}(-2) \quad \widetilde{W}(-1) \quad \widetilde{W}(0) \quad \widetilde{W}(1) \quad \widetilde{W}(2) \quad \ldots\right]^T. \end{cases}$$

For each $\mu$, the spectrum of $\widehat{\mathcal{L}}^{\mu}$ consists of countably many discrete eigenvalues with finite multiplicity and, furthermore, by the above considerations we have the spectral decomposition

$$\sigma_{L^2(\mathbb{R})}(\mathcal{L}) = \bigcup_{\mu\in[0,1)} \sigma(\widehat{\mathcal{L}}^{\mu}).$$

We numerically approximate the spectrum of the bi-infinite matrix $\widehat{\mathcal{L}}^{\mu}$ by taking a sequence of $\mu$ in a finite discretization of $[0,1)$, truncating each block of $\widehat{\mathcal{L}}^{\mu}$ in (3.34) to finite dimension, and computing the eigenvalues of the truncated matrix using a standard matrix eigenvalue solver. See Appendix C for further discussion. See Figure 3.4 for plots of the spectrum at the sampled points on the bifurcation diagram of $2\pi$-periodic solutions in Figure 3.2(a), as well as Figure 3.5 for plots of the growth rate $\mathrm{Re}(\lambda)$ vs. the Bloch parameter $\mu$. It is known that the full Euler equations exhibit high-frequency instabilities (visually characterized by "bubbles" of spectrum emanating from the imaginary axis from points away from the origin) in small-amplitude periodic traveling waves; however, we discover that while this model demonstrates both high-frequency and modulational instabilities for waves of sufficiently high amplitude, a high-frequency instability is numerically undetectable for small amplitude waves: see Figure 3.4(a) and Figure 3.5(a) below. Whether such instabilities are actually nonexistent or simply not detected for small amplitude waves in our numerics is unclear.

Solutions of different wavelength can be generated by varying the value of $\kappa$, as shown in the plot of the bifurcation diagrams for various $\kappa$ in Figure 3.2(b). In [35], an analysis of asymptotically small amplitude waves shows that there exists a critical value $\kappa_c$ such that all waves are modulationally unstable for all $\kappa > \kappa_c$ where $\kappa_c \approx 1.008$. Inspired by this analysis, we performed numerical experiments varying the value of $\kappa$ for small, but fixed, waveheights, finding very good agreement with the results in [35]. Figure 3.6(a) demonstrates that waves with waveheight $0.01766$ and corresponding to $\kappa = 1.005$ are mod-

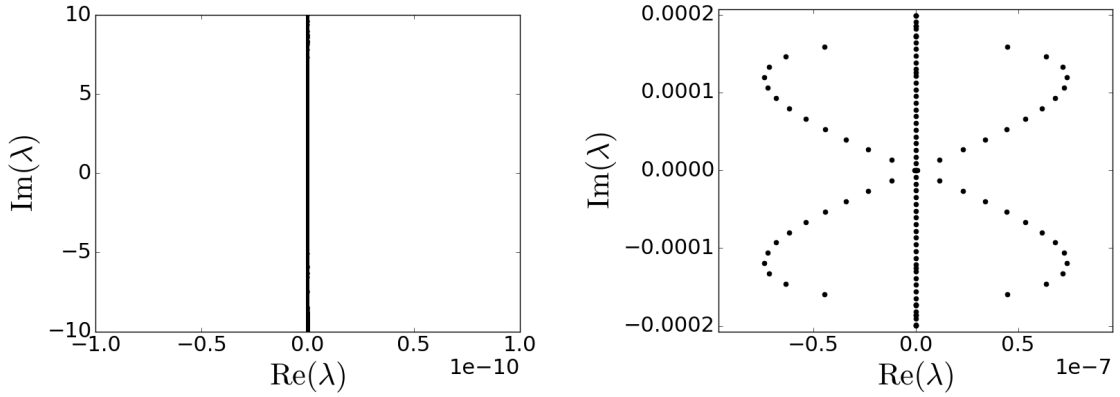


(a) (b)

Figure 3.6: Evidence of the Benjamin-Feir instability in (3.2) for waveheight $0.01766$. In(a) we have $\kappa = 1.005$ while in (b) we have $\kappa = 1.008$.

ulationally stable, while for $\kappa = 1.008$ a modulational instability appears for waves of the same height: see Figure 3.6(b).

**Time Evolution and Ill-Posedness**

The numerical findings in the previous section are restricted to waves bifurcating from the zero constant state in the bidirectional Whitham model (3.2). This is largely motivated by the fact that the structure of the global bifurcation branch was recently studied analytically in [20]. In an effort to understand the *nonlinear* dynamics about the numerically computed profiles in Figure 3.2(a), we use a sixth-order pseudospectral operator splitting method [67] to evolve (3.22) with the numerical solutions as initial data, with the expectation that the initial profile translates as a traveling wave with corresponding wave speed $c$, mapping onto itself after an integral number of temporal periods $T = \frac{2\pi}{\kappa c}$. Interestingly, however, such time evolution attempts failed, resulting in wild oscillations after a short amount of time, e.g. 35.4% of a temporal period for a $2\pi$-periodic wave of small waveheight $\max \psi - \min \psi \approx 0.00109$ and wave speed $c \approx 0.872693$. See Figure 3.7. This seems to suggest that

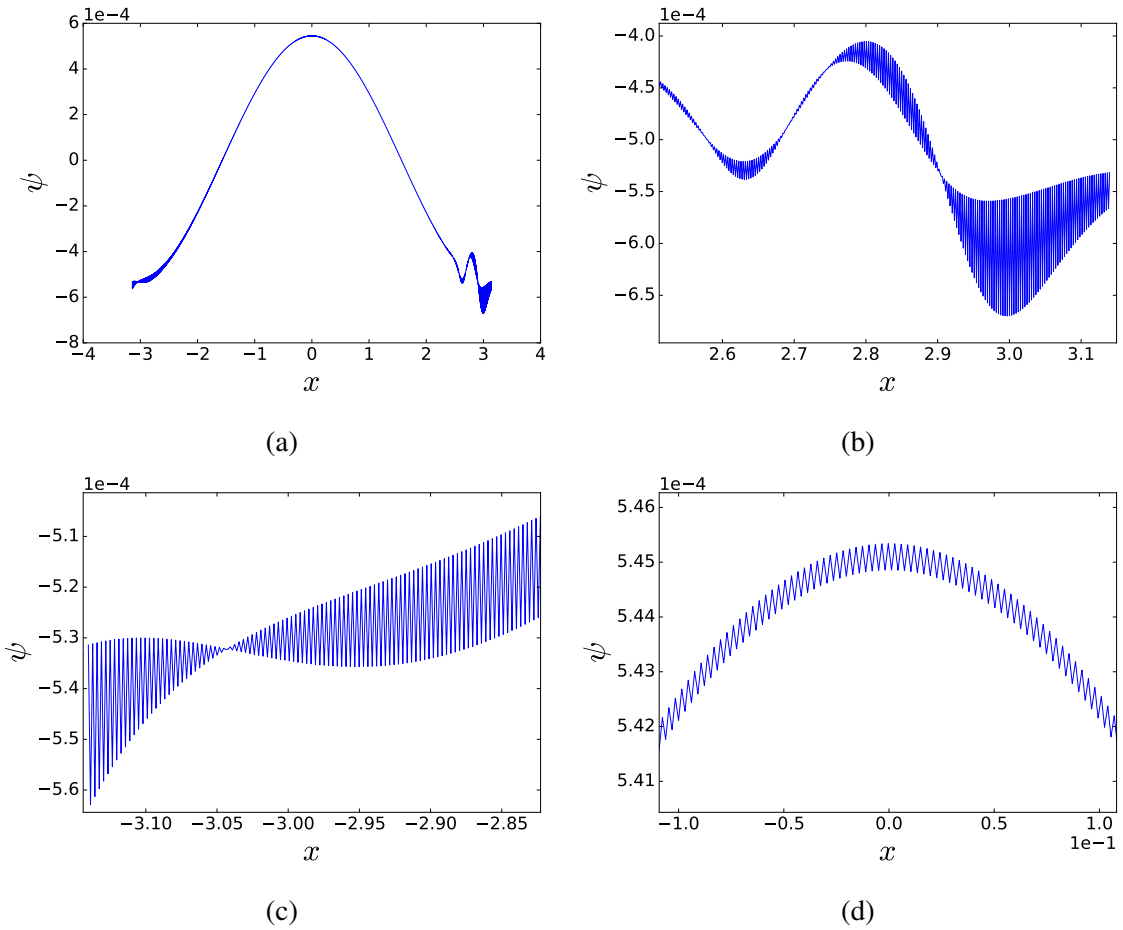


Figure 3.7: Numerical evidence of ill-posedness of (3.2) for initial data $\eta(x,0) = \psi(x)$ having negative infimum. (a) The result of a short time evolution of a $2\pi$-periodic wave ($\kappa = 1$) with small waveheight $\max\psi - \min\psi \approx 0.00109$, $c \approx 0.872693$. We zoom in near the rightmost and leftmost of the waves in (b) an (c), respectively. In (d) we observe that oscillations also are forming near the positive maxima, although the oscillations there are not as pronounced as near the minima.

either the solutions computed in Figure 3.2(a) are in fact *not* traveling wave solutions of (3.2), or that the local evolution in the PDE (3.2) about such waves is ill-posed.

In this direction, we note that it has recently been reported in [22, Theorem 1] that (3.2) is locally well-posed for all initial data $\eta(x,0) = \psi(x)$, $u(x,0) = \phi(x)$ with $\inf_{x\in[0,2\pi)} \psi(x) > 0$. As the height profiles about the waves along the bifurcation curves constructed above all have a *strictly negative infimum*, it follows that the local well-posedness result in [22] does not apply to the waves constructed in the previous section and, extension, also not to the waves constructed in [20]. The time evolution results reported in Figure 3.7 strongly indicate that the positivity assumption on the height profile $\eta$ in [22] is *sharp* and cannot be removed in general.

In contrast, waves of (3.2) having strictly positive profile that are constructed by bifurcating from a positive constant state exhibit local well-posedness in time. See Figure 3.10 and the surrounding discussion. See Appendix D.2 for further details about the time evolution.

**Analysis of Waves with Positive Height Profile**

Given the well-posedness result [22] and the apparent failure of the waves considered in Section 3.3.1 to have well-posed local dynamics, we attempt to construct wavetrain solutions of (3.2) for which the local evolution is well-posed, i.e. solutions of (3.22) that have *strictly positive height profiles* $\eta(x)$, by bifurcating from a *positive* constant state. As discussed in [20], the curves of trivial solutions for (3.22) are given by

$$c \mapsto 0, \quad c \mapsto \Gamma_{\pm}(c) := \frac{3c \pm \sqrt{8+c^2}}{2},$$

and the waves studied in Section 3.3.1 above bifurcate from the zero-amplitude state, where the height profiles $\eta(x)$ all have strictly negative infima. Since $\Gamma_{-}(c) > 0$ for all $c > 1$, this

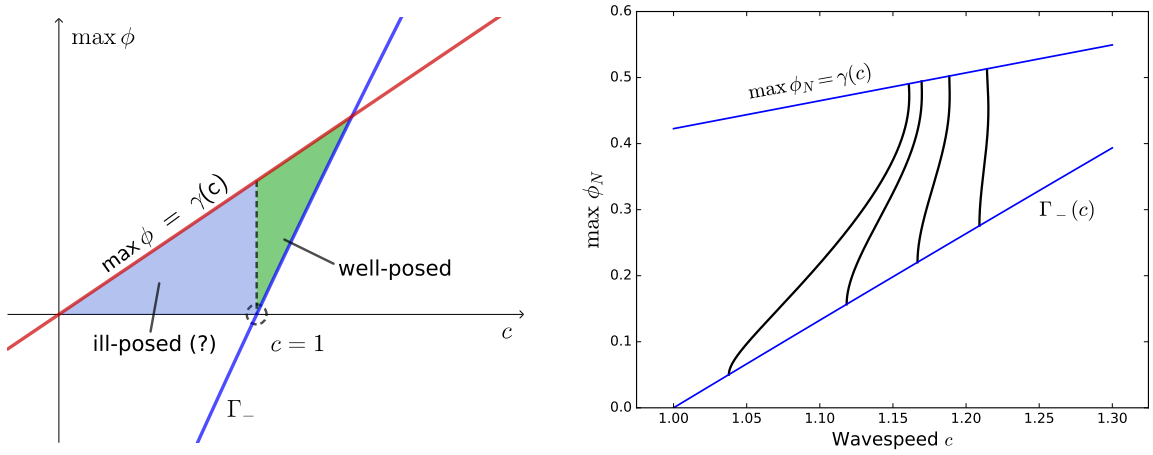


(a) (b)

Figure 3.8: (a) Bifurcation diagram of (3.24). Waves bifurcating from the zero state are likely ill-posed, while waves bifurcating from a non-zero constant state (curve $\Gamma_-$) are well-posed. (b) Numerical approximations of the bifurcation branches of even, one-sided monotone, $2\pi/\kappa$ periodic solutions of (3.24). From left to right, $\kappa = 0.5, 1.0, 1.3, 1.6$.

motivates an attempt to construct waves that bifurcate from the $\Gamma_-$ curve, which (at least for small waveheight) are guaranteed to fall into the regime of well-posedness: see Figure 3.8 below.

To this end, observe that non-zero constant profiles $\phi$ of (3.24) satisfy

$$Q(\phi; c) := c^2 - 1 - \frac{3}{2}c\phi + \frac{1}{2}\phi^2 = 0. \tag{3.35}$$

Let $(\phi_*, c_*)$ be a solution of (3.35) for $c_* > 1$. In order for non-trivial, real-valued, even, periodic solutions to branch from the constant state at $c_*$, the kernel of the Fréchet derivative $\delta_\phi Q(\phi_*; c_*)$ must be non-trivial. If $v \in \ker(\delta_\phi Q(\phi_*; c_*))$ with $v(x) = \sum_{n=0}^{\infty} \widehat{v}(n)\cos(n\kappa x)$, then

$$0 = \delta_\phi Q(\phi_*; c_*)v = \left(\mathcal{K} - c_*^2 + 3c_*\phi_* - \frac{3}{2}\phi_*^2\right)v.$$

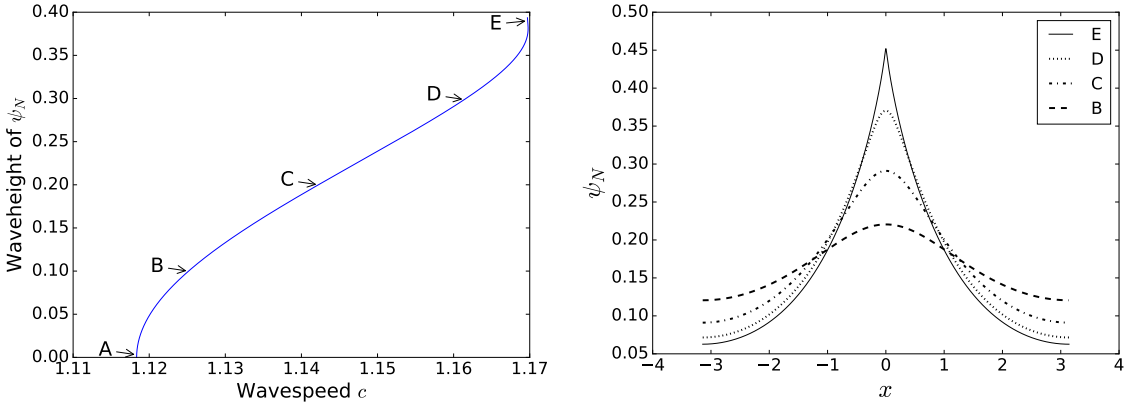


(a) (b)

Figure 3.9: Positive $2\pi$-periodic equilibrium profiles $\eta(x,t) = \psi(x)$ bifurcating from constant positive state. In (a), we show the global bifurcation branch with points A-E labeled for forthcoming computations: Point A at $c \approx 1.1184$, height $\approx 0.003$; Point B at $c \approx 1.1252$, height $\approx 0.15$; Point C at $c \approx 0.8312$, height $\approx 0.30$; Point D at $c \approx 0.8138$, height $\approx 0.40$; point E at $c \approx 0.8051$, height $\approx 0.49$. In (b), we show the height profiles $\psi$ associated to the waves A-E of increasing waveheight along the branch in (a).

Taking the Fourier transform yields

$$0 = \left(\widehat{\mathcal{K}}(\kappa n) - c_*^2 + 3c_*\phi_* - \frac{3}{2}\phi_*^2\right)\widehat{v}(n), \quad n \in \mathbb{N}_0,$$

and we see that if

$$\widehat{\mathcal{K}}(\kappa n_0) - c_*^2 + 3c_*\phi_* - \frac{3}{2}\phi_*^2 = 0 \tag{3.36}$$

for fixed $n_0 \in \mathbb{N}_0$, then

$$\operatorname{span}\{\cos(\kappa n_0 x)\} = \ker(\delta_\phi Q(\phi_*, c_*)).$$

Combining (3.35) and (3.36) yields a system of necessary conditions for a non-trivial branch of $2\pi/(\kappa n_0)$-periodic traveling wave solutions of (3.2) to appear:

$$\begin{cases} c_*^2 - 1 - \frac{3}{2}c_*\phi_* + \frac{1}{2}\phi_*^2 &= 0 \\ \widehat{\mathcal{K}}(\kappa n_0) - c_*^2 + 3c_*\phi_* - \frac{3}{2}\phi_*^2 &= 0. \end{cases} \tag{3.37}$$

For positive wave speed, this system has a unique solution $(c_*(n_0), \phi_*(n_0))$ for each $n_0 \in \mathbb{N}_0$. In the case of $n_0 = \kappa = 1$, corresponding to $2\pi$-periodic solutions of (3.24), we find

$$c_* \approx 1.11834, \quad \phi_* \approx 0.15677.$$

By standard Lyapunov-Schmidt arguments, it can be shown that a local bifurcation of $2\pi$-periodic wavetrains of asymptotically small waveheight occurs at $(\phi_*, c_*)$. In particular, one finds the following local bifurcation formulas:

$$\begin{aligned} \phi(x;a) &:= \phi_* + a\cos(\kappa n_0 x) + \mathcal{O}(a^2) \\ c(a) &:= c_* + \frac{3-4q}{24\phi_* - 16c_*}a^2 + \mathcal{O}(a^3), \quad q := \frac{3}{4}\left[\frac{\phi_* - c_*}{\widehat{\mathcal{K}}(2\kappa n_0) - c_*^2 + 3c_*\phi_* - \frac{3}{2}\phi_*^2}\right]. \end{aligned}$$

Using the methods of Section 3.2 to approximate the wave profiles, we obtain a branch of solutions, depicted in Figure 3.9 as waveheight vs. wave speed, with all the height profiles $\psi$ possessing a strictly positive infimum and an increasingly sharp crest for large wave-heights. In particular, we note that the time evolution about these waves indeed appears to be *well-posed*. In fact, a time evolution of a $2\pi$-periodic solution of (3.2) with wave speed $c \approx 1.1698$ and $\max\psi - \min\psi \approx 0.387$ over 15 temporal periods $15T = 15 \cdot 2\pi/c$ closely

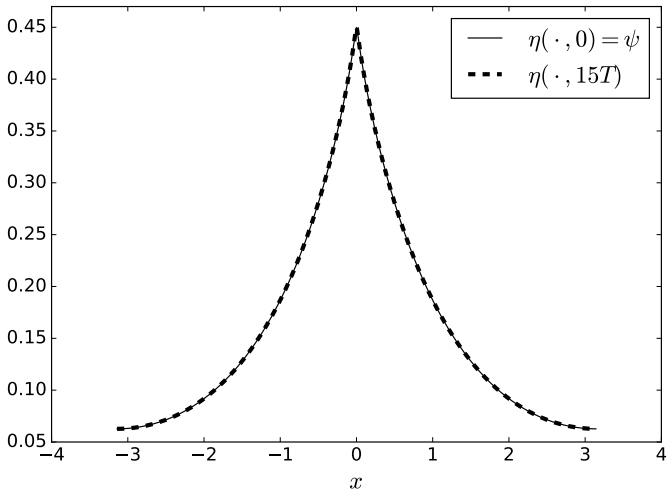


Figure 3.10: A time evolution of (3.2) using a positive equilibrium profile as initial data appears stationary after 15 temporal periods, mapping closely onto itself.

mapped the initial data onto itself, with residual

$$\|\eta(\cdot, 15T) - \psi\|_{L^2} \approx 3.5 \times 10^{-6}.$$

See Figure 3.10. This demonstrates that these computed profiles with positive minimum indeed form traveling wave solutions of (3.2) that exhibit locally well-posed time evolution.

Concerning the stability of these $2\pi$-periodic positive height waves, we find that they behave similarly to ill-posed waves discussed in the previous section, with waves of sufficiently large height demonstrating modulational and high-frequency instabilities: see Figure 3.11. In fact, Figure 3.11(a) suggests that $2\pi$-periodic waves of small amplitude exhibit modulational instability.

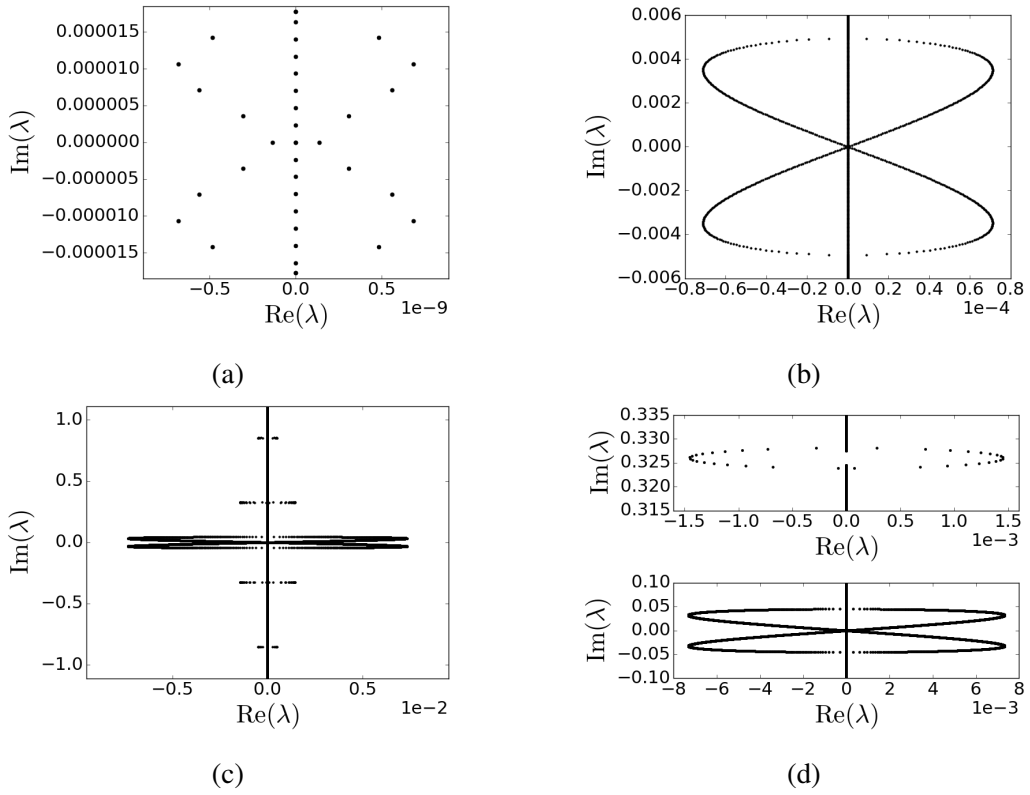


Figure 3.11: Spectral plots for $2\pi$-periodic positive waves for (3.2) at points A (a), B (b), and D (c) along the bifurcation branch of $2\pi$-periodic solutions in Figure 3.9. (d) Zoom-in on the high-frequency instability (top) and the modulational instability (bottom) in the spectral plot (c).

### 3.3.2 Analysis of System (3.4)

We now turn our attention to the bidirectional Whitham model (3.4):

$$\begin{cases} u_t &= -\mathcal{K}\eta_x - uu_x \\ \eta_t &= -u_x - (\eta u)_x. \end{cases}$$

In particular, we are interested in performing an analogous study for (3.4) that was performed for the model (3.2) in Section 3.3.1 above. Below, we compute global bifurcation diagrams, including large amplitude solutions, and analyze the spectrum of the linearization of (3.4) about these solutions.

As mentioned in the introduction, this model was proposed and analyzed in [35], which examines the local bifurcation and spectral stability of asymptotically small amplitude periodic traveling waves, finding that this model exhibits the Benjamin-Feir instability. Precisely, they prove the existence of a critical wavenumber $\kappa_c \approx 1.610$ such that asymptotically small-amplitude wavetrains of period $2\pi/\kappa$ are modulationally unstable when $\kappa > \kappa_c$ ("super-critical"), while they are spectrally stable for $0 < \kappa < \kappa_c$ ("subcritical"). Below, we numerically confirm this result for small amplitude waves, and also demonstrate that large amplitude waves are spectrally unstable in both the sub-critical and super-critical regimes. See Figure 3.14 for spectrum plots in the super-critical case and Figure 3.15 for spectrum plots the sub-critical case. Furthermore, from our experiments we make a conjecture regarding the nonexistence of a singular wave of greatest height.

To generate profiles, we follow the program of the numerical methods described in Section 3.2. First, we transform (3.4) to traveling wave coordinates:

$$\begin{cases} u_t &= cu_x - \mathcal{K}\eta_x - uu_x =: F(u, u_x, \eta, \eta_x; c) \\ \eta_t &= c\eta_x - u_x - (\eta u)_x =: G(u, u_x, \eta, \eta_x; c). \end{cases}$$

An equilibrium solution $(u, \eta)(x, t) = (\phi, \psi)(x)$ of the above traveling wave system satisfies

$$\begin{cases} -c\phi' + \mathcal{K}\psi' + \phi\phi' &= 0 \\ -c\psi' + \phi' + (\psi\phi)' &= 0 \end{cases}$$

which, upon integrating and setting integration constants to zero, yields

$$\begin{cases} -c\phi + \mathcal{K}\psi + \frac{1}{2}\phi^2 &= 0 \\ -c\psi + \phi + \psi\phi &= 0. \end{cases}$$

Then resolving $\phi$ in terms of $\psi$ yields the scalar profile equation

$$\mathcal{K}\psi = \frac{c^2\psi}{1+\psi} - \frac{c^2\psi^2}{2(1+\psi)^2} =: g(c,\psi). \tag{3.38}$$

Using the methods in Section 3.2.1, we numerically compute the bifurcation branch and periodic profiles with various waveheights with super-critical $\kappa = 1.611$: see Figure 3.12(a)-(c). Further, in Figure 3.12(d) we compute bifurcation branches of $2\pi/\kappa$-periodic profiles for various $\kappa$.

In contrast to the model (3.2) analyzed in Section 3.3.1 above, we conjecture that the bifurcation branches associated with (3.4) will *not possess peaked/cusped waves of maximum height*. In fact, we believe the profiles along the global bifurcation branches will be smooth for arbitrarily large waveheight. To see this, observe that differentiating the profile equation (3.38) and rearranging yields

$$\psi' = \frac{c^2}{(1+\psi)^3}\mathcal{K}\psi'.$$

Since $\mathcal{K}\psi'$ has the same regularity as $\psi$, we have that $\psi'$ is smooth so long as the wave speed $c$ remains bounded away from zero and the profiles $\psi$ remain bounded away from $\psi = -1$ along the bifurcation branch. From Figure 3.12, it seems plausible that *both* of these conditions hold uniformly along the bifurcation branch, indicating that the bifurcation branch does not terminate in a highest wave. See Figure 3.12(d) for a periodic profile of large waveheight having a visibly smooth crest. We leave the analytical verification of this conjecture as an interesting open problem.

*Remark* 3.3.1. Since this model is conjectured to not possess peaked/cusped waves of maximum height, the waveheight vs. wave speed plots in Figures 3.12(a), (d) were stopped at height 3. As seen in Figure 3.12(a), a turning point occurs near waveheight 3, after which

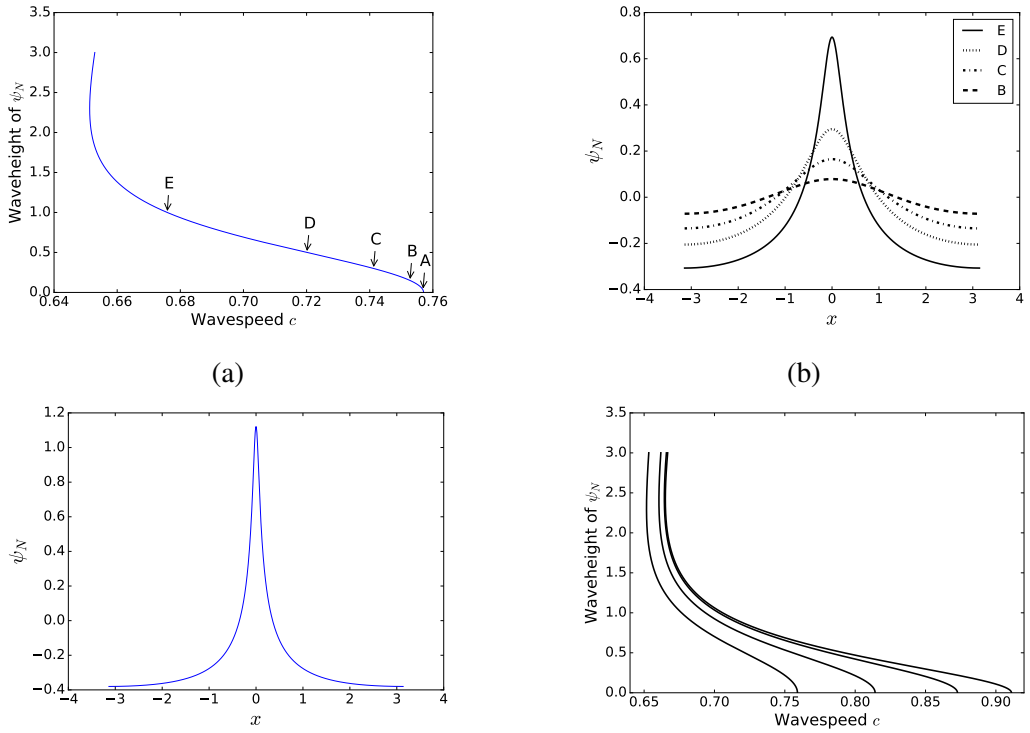


(a) (b)

(c) (d)

Figure 3.12: Bifurcation branches of (3.38) for super-critical $\kappa = 1.611 > \kappa_c$. (a) Locations on the bifurcation branch of periodic solutions corresponding to super-critical $\kappa = 1.611$ of (3.38) that are sampled for profile and spectral plots: Point A at $c \approx 0.7569$, height $\approx 0.03$; Point B at $c \approx 7528$, height $\approx 0.15$; Point C at $c \approx 0.7412$, height $\approx 0.30$; Point D at $c \approx 0.7201$, height $\approx 0.50$; Point E at $c \approx 0.6759$, height $\approx 1.00$. (b) Profiles corresponding to the points along the bifurcation branch labeled in (a). (c) A super-critical wave ($\kappa = 1.611$) of large waveheight; $c \approx 0.6745$, waveheight $\approx 1.500$. The crest of the wave is still smooth despite the large waveheight. (d) Numerical approximations of the $2\pi/\kappa$ periodic solutions of (3.38) with wave speed $c$. From left to right, $\kappa = 1.6, 1.3, 1, 0.8$.

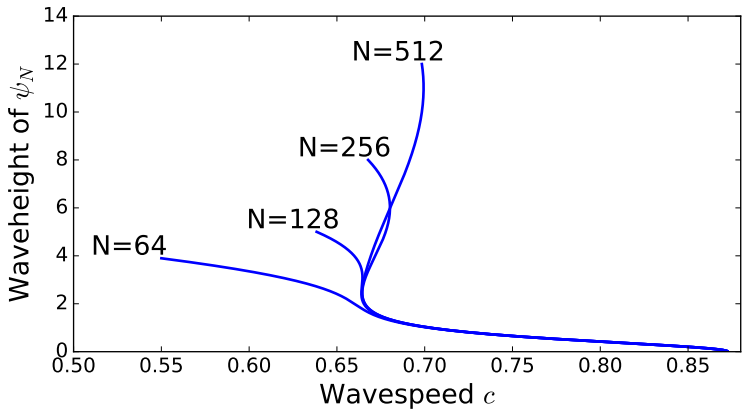


Figure 3.13: Secondary turning points in the bifurcation diagrams for system (3.4) are present at large waveheight, but this is believed to be purely due to truncation since its location increases as the number of Fourier modes $N \in \{64, 128, 256, 512\}$ increases.

the wave speed increases as the waveheight increases. Numerically, a second turning point is also observed for waves of larger height, but we believe that this second turning point is only due to truncation, at its location varies considerably as larger numbers of Fourier modes $N$ are used. See Figure 3.13.

To study the dynamical stability of the periodic wavetrains computed in Figure 3.12, we use the general methods of Appendix C. In particular, we build truncated bi-infinite matrices whose eigenvalues approximate the spectrum of the linearization:

$$\begin{aligned}
\widehat{A}^{\mu}(m,l) &= ic\kappa(\mu+l)\delta_{m,l} - i\kappa(\mu+m)\widehat{\phi}(m-l) \\
\widehat{B}^{\mu}(m,l) &= -i\kappa(\mu+l)\widehat{\mathcal{K}}(\kappa(\mu+l))\delta_{m,l} \\
\widehat{C}^{\mu}(m,l) &= -i\kappa(\mu+l)\delta_{m,l} - i\kappa(\mu+m)\widehat{\psi}(m-l) \\
\widehat{D}^{\mu}(m,l) &= ic\kappa(\mu+l)\delta_{m,l} - i\kappa(\mu+m)\widehat{\phi}(m-l).
\end{aligned}$$

Plots of the spectrum at the sampled points along the bifurcation branch in Figure 3.12(a) are shown in Figure 3.14. In particular, Figure 3.14(a) demonstrates a modulational instability for a small waveheight, while the other plots for larger waveheights show both a

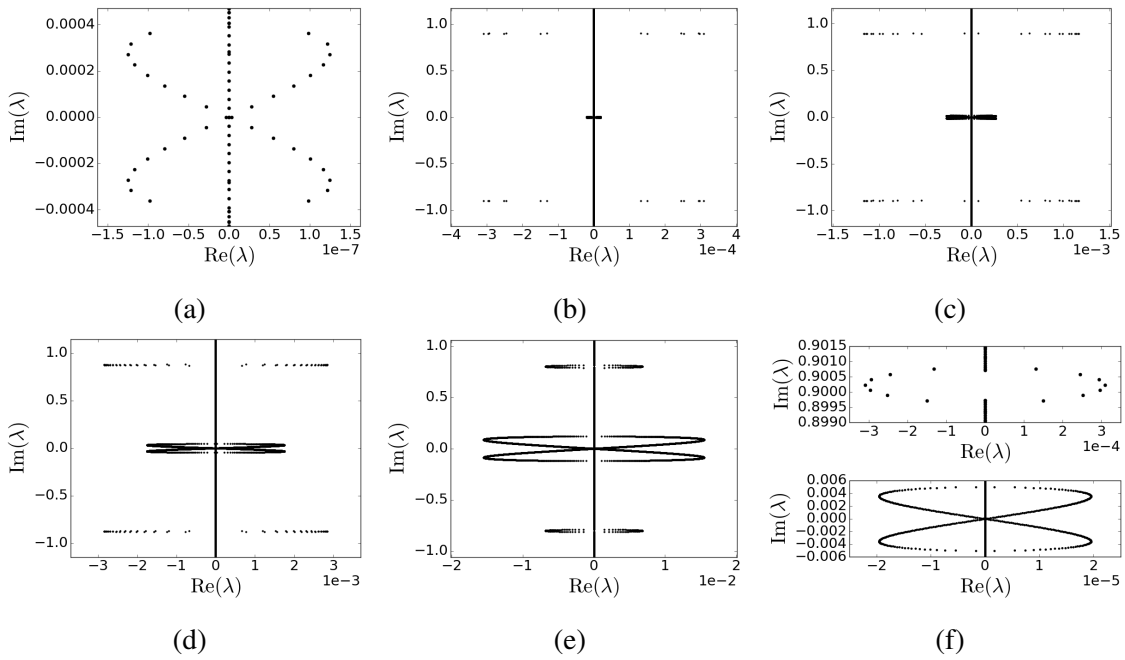


Figure 3.14: (a)-(e) Spectral plots for $2\pi/\kappa$-periodic waves A-E selected along the bifurcation branch in Figure 3.12(a) with super-critical $\kappa = 1.611$. (f) Zoom-in on the high-frequency instability (top) and modulational instability (bottom) for the spectrum in (b).

modulational instability and a high-frequency instability. Moreover, plots of the growth rate $\mathrm{Re}(\lambda)$ vs. $\mu$ for these spectra are shown in Figure 3.16. Moreover, the spectral stability of small-amplitude sub-critical solutions is shown in Figure 3.15(a), as predicted by analytical theory in [35]. However, even for $\kappa$ in the sub-critical regime, waves of sufficiently large waveheight develop both modulational and high-frequency instabilities (see Figure 3.15(b)) while small amplitude waves are spectrally stable. Moreover, waves are stable with respect to co-periodic perturbations.

### 3.3.3 Boussinesq-Whitham

Finally, we now turn our attention to the scalar *Boussinesq-Whitham* model (3.5) proposed in [18, Section 5]:

$$u_{tt} = \partial_x^2(u^2 + \mathcal{K}u).$$

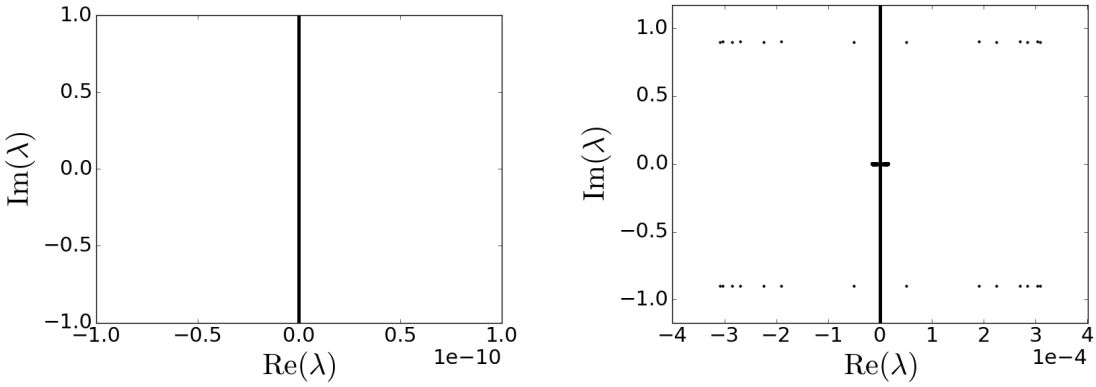


(a) (b)

Figure 3.15: Spectral plots for small $2\pi/\kappa$-periodic solutions of (3.38) with sub-critical $\kappa = 1.609 < \kappa_c$). In (a), the waveheight of the underlying wave $\psi$ is $0.03$, while in (b) it is $0.15$.

Since [18] does not provide details for the local bifurcation theory of this model, we sketch the Lyapunov-Schmidt reduction here. Writing the second order equation (3.5) as a first order system, we have

$$\begin{cases} u_t &= \eta \\ \eta_t &= \partial_x^2(u^2 + \mathcal{K}u), \end{cases}$$

and changing to traveling wave coordinates yields

$$\begin{cases} u_t &= \eta + cu_x =: F(u, u_x, \eta, \eta_x; c) \\ \eta_t &= c\eta_x + \partial_x^2(u^2 + \mathcal{K}u) := G(u, u_x, \eta, \eta_x; c). \end{cases}$$

Equilibrium solutions $(u, \eta) = (\phi, \psi)$ of this system satisfy

$$\begin{cases} -c\phi' &= \psi \\ -c\psi' &= (\phi^2 + \mathcal{K}\phi)'', \end{cases} \tag{3.39}$$

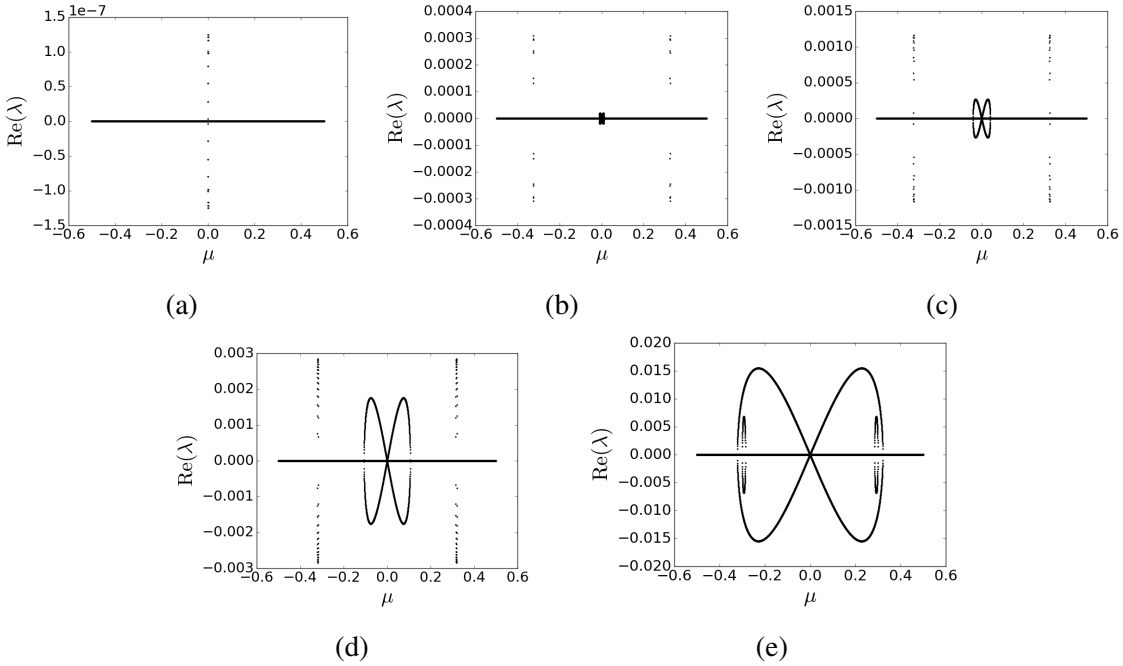


Figure 3.16: (a)-(e) $\mathrm{Re}(\lambda)$ vs. $\mu$ for each of the spectral plots (a)-(e), respectively, for the super-critical $\kappa$ in Figure 3.14.

in which we can resolve $\psi$ in terms of $\phi$ by integrating the second equation, setting the resulting constant of integration to zero. This yields the relation

$$-c\psi = (\phi^2 + \mathcal{K}\phi)'.$$

Using this relationship in the first equation of (3.39) and integrating, again setting the constant of integration to zero, yields the scalar profile equation

$$\mathcal{K}\phi = c^2\phi - \phi^2 =: g(c,\phi). \tag{3.40}$$

for the velocity profile $\phi$.

Concerning the smoothness of solutions of (3.40), note that differentiating (3.40) implies that

$$\mathcal{K}\phi' = (c^2 - 2\phi)\phi' \implies \phi' = \frac{\mathcal{K}\phi'}{c^2 - 2\phi}. \tag{3.41}$$

As before, since $\mathcal{K}\phi'$ has the same regularity as $\phi$, we have by (3.41) that $\phi'$ is as smooth as $\phi$ so long as $c^2 - 2\phi \neq 0$. Precisely, we see that smoothness should be expected to break down if the bifurcation branch of periodic solutions of (3.40) intersects the curve $\phi = c^2/2$ non-trivially. So, in our numerical bifurcation calculations we stop the continuation algorithm when the maximum value of the approximated wave exceeds $c^2/2$.

In order to use (3.40) to perform a numerical continuation, we first obtain local bifurcation curves from zero amplitude in order to accurately seed the continuation algorithm. Recasting (3.40) as a solution of

$$Q(\phi; c) := \mathcal{K}\phi + \phi^2 - c^2\phi = 0,$$

the variational derivative of $Q$ with respect to $\phi$ evaluated at $\phi = 0$ is

$$\delta_\phi Q(0; c) = \mathcal{K} - c^2 \mathrm{Id}. \tag{3.42}$$

By the implicit function theorem, no bifurcation can occur unless $\ker(\mathcal{K} - c^2\mathrm{Id})$ is nontrivial. Restricting to even, real-valued, $2\pi/\kappa$-periodic functions, we find that for wave speed $c_\kappa := \sqrt{\widehat{\mathcal{K}}(\kappa)} = \sqrt{\tanh(\kappa)/\kappa}$, the kernel of (3.42) is indeed non-trivial, with

$$\ker(\mathcal{K} - c_\kappa^2 \mathrm{Id}) = \mathrm{span}\{\cos(\kappa x)\}.$$

Per a standard Lyapunov-Schmidt reduction argument, to bifurcate from the zero state at $c = c_0$, write

$$c(\varepsilon) = c_0 + \varepsilon c_1 + \varepsilon^2 c_2 + \varepsilon^3 c_3 + \mathcal{O}(\varepsilon^4),$$
$$\phi(x;\varepsilon) = 0 + \varepsilon\cos(\kappa x) + \varepsilon^2 v_2 + \varepsilon^3 v_3 + \mathcal{O}(\varepsilon^4).$$

Then for $\phi$ to be a profile of (3.40), we must have

$$0 = Q(0 + \varepsilon\cos(x) + \varepsilon^2 v_2 + \varepsilon^3 v_3 + \cdots; c_0 + \varepsilon c_1 + \varepsilon^2 c_2 + \varepsilon^3 c_3 + \cdots).$$

Expanding the above expression in a Taylor series about $(\phi, c) = (0, c_0)$ and collecting terms, we obtain a local bifurcation curve $\{(c(\varepsilon), \phi(x;\varepsilon))\}_{|\varepsilon|\ll 1}$ of non-trivial $2\pi/\kappa$-periodic traveling wave solutions $\phi(x;\varepsilon)$ of (3.40) with wave speed $c(\varepsilon)$. In fact, we obtain the following asymptotic formulas describing the local bifurcation curve for $|\varepsilon| \ll 1$:

$$c(\varepsilon) = c_\kappa + \frac{\varepsilon^2}{4c_\kappa}\left[\frac{1}{c_\kappa^2 - 1} + \frac{1}{c_\kappa^2 - c_{2\kappa}^2}\right] + \mathcal{O}(\varepsilon^3)$$
$$\phi(x;\varepsilon) = \varepsilon\cos(\kappa x) + \frac{\varepsilon^2}{2}\left[\frac{1}{c_\kappa^2 - 1} + \frac{1}{c_\kappa^2 - c_{2\kappa}^2}\right]\cos(2\kappa x) + \mathcal{O}(\varepsilon^3),$$

where $c_\kappa = \sqrt{\widehat{\mathcal{K}}(\kappa)} = \sqrt{\tanh(\kappa)/\kappa}$.

Using the above bifurcation formulas, along with the methods of Sections 3.2.1 and 3.2.2, we can generate numerical bifurcation diagrams of $2\pi/\kappa$-periodic even solutions for this model: see Figures 3.17(a), (d). Numerical approximations of the profiles at the sampled locations on the bifurcation branch of $2\pi$-periodic solutions are displayed in Figure 3.17(a) are presented in Figure 3.17(b). Near the top of the bifurcation branch of $2\pi$-periodic solutions, the profiles begin to display a cusp singularity, similar to what was observed in the model (3.2) in Section 3.3.1 above. See Figure 3.17(c).

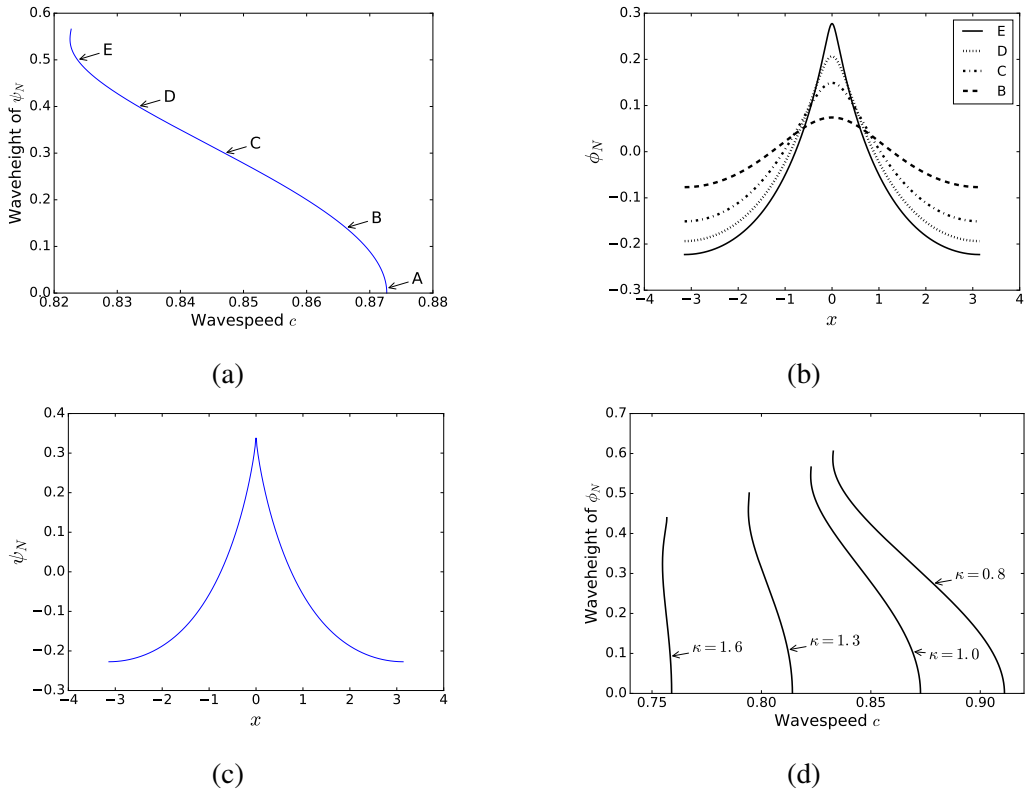


Figure 3.17: (a) Numerical approximation of the bifurcation branch of even, $2\pi$-periodic solutions of (3.40), with with specific points A-E labeled for forthcoming computations: Point A at $c \approx 0.8727$, height $\approx 0.01$; Point B at $c \approx 0.8662$, height $\approx 0.14$; Point C at $c \approx 0.8470$, height $\approx 0.30$; Point D at $c \approx 0.8333$, height $\approx 0.4$; Point E at $c \approx 0.8237$, height $\approx 0.50$. (b) the profiles associated to the sampled points A-E in (a). (c) A (nearly peaked) $2\pi$-periodic profile near the top of the bifurcation branch of $2\pi$-periodic solutions, corresponding to $c \approx 0.8227$, waveheight $\approx 0.5650$. (d) The bifurcation branches of $2\pi/\kappa$-periodic solutions of (3.40) for varying $\kappa$.

To study the stability of these periodic traveling wave solutions, we again follow the method of Appendix C and define the following bi-infinite matrices whose eigenvalues, after finite-dimensional truncation, approximate the spectrum of the corresponding linearization:

$$\widehat{A}^{\mu}(m,l) = ic\kappa(\mu+l)\delta_{m,l}$$

$$\widehat{B}^{\mu}(m,l) = \delta_{m,l}$$

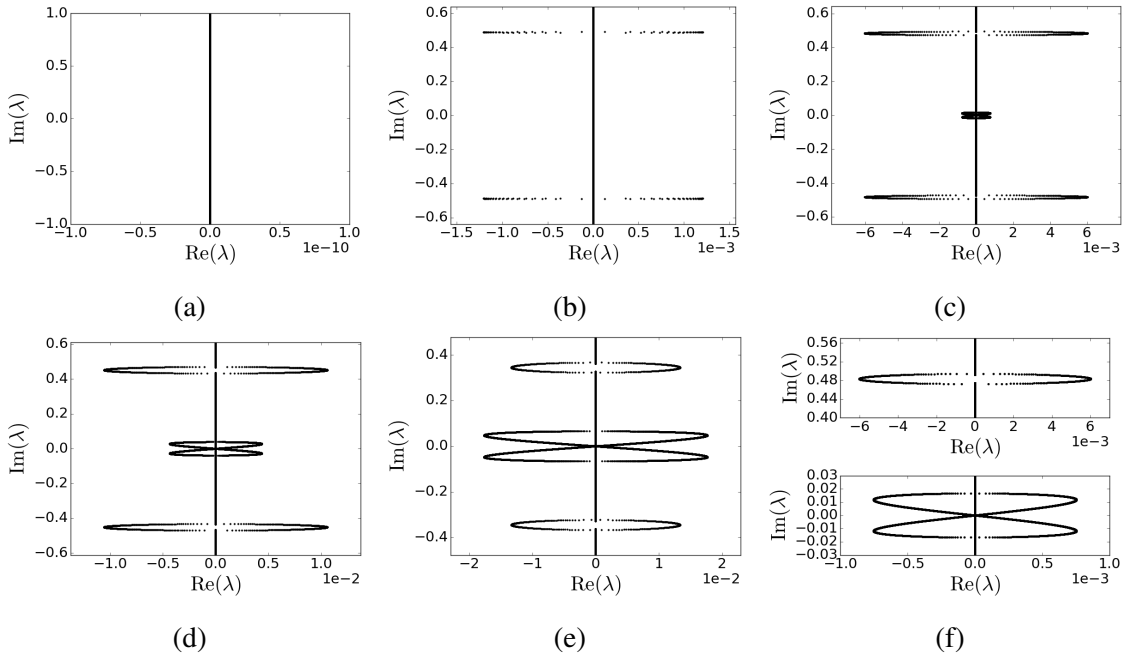


Figure 3.18: (a)-(e) Spectral plots for Boussinesq-Whitham at the points A-E, respectively, sampled along the bifurcation branch for $2\pi$-periodic solutions in Figure 3.17(a). (f) A zoom-in on the high-frequency instability (top) and modulational instability (bottom) for the spectral plot (c).

$$\widehat{C}^{\mu}(m,l) = -2\kappa^2(\mu+m)^2\widehat{\phi}(m-l) - \kappa^2(\mu+l)^2\widehat{\mathcal{K}}(\kappa(\mu+l))\delta_{m,l}$$
$$\widehat{D}^{\mu}(m,l) = ic\kappa(\mu+l)\delta_{m,l}.$$

Plots of the spectrum, along with the growth rates $\mathrm{Re}(\lambda)$ with respect to the Bloch parameter $\mu$, are shown in Figures 3.18 and 3.19, respectively. Based on these numerics, we see that, similar to the other models considered here, all waves of sufficiently large wave-height appear to exhibit both modulational and high-frequency instabilities, while high-frequency instabilities for asymptotically small waves are unobserved in our experiments. Furthermore, all computed waves appear to be spectrally stable with respect to co-periodic perturbations.

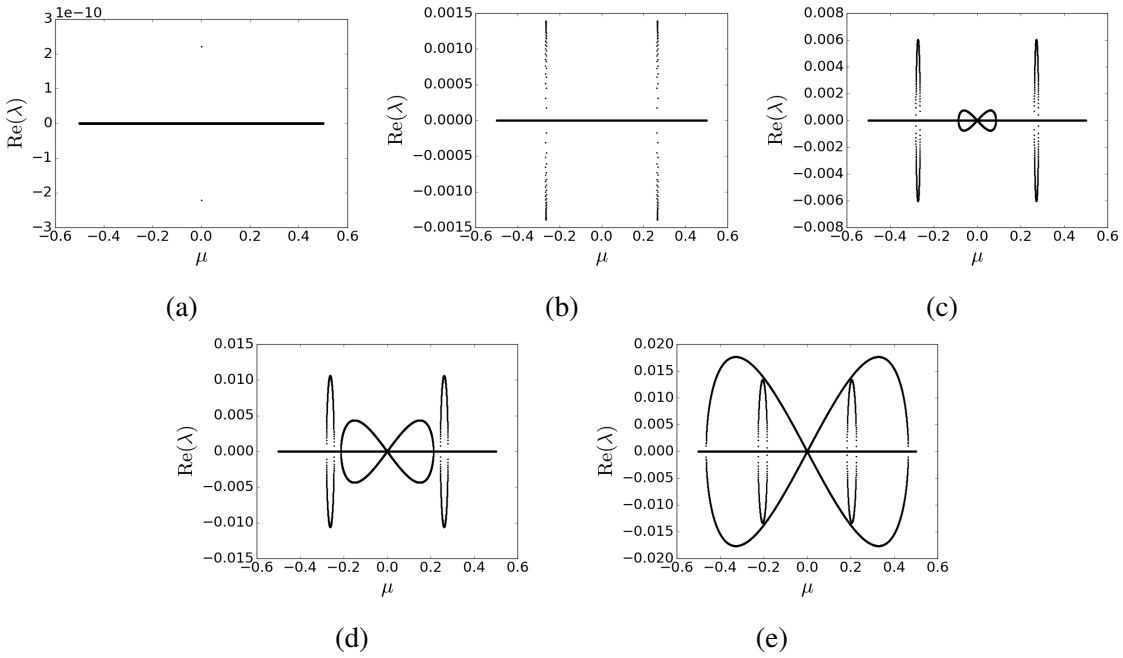


Figure 3.19: (a)-(e) $\mathrm{Re}(\lambda)$ vs. $\mu$ for each of the spectral plots (a)-(e), respectively, of Boussinesq-Whitham shown in Figure 3.18.

## 3.4 Summary

Using robust numerical methods, we have presented numerically-computed waveheight vs. wave speed global bifurcation diagrams for three fully-dispersive bidirectional Whitham models and studied the spectral stability of such waves by numerically approximating the spectrum of their associated linearized operators in both small and large amplitude regimes. Our results confirm a number of analytical results concerning the stability of asymptotically small waves in these models and provide new insight into the existence and stability of large amplitude waves, including highest singular waves. We note that while these models compare similarly with regard to existence and stability, we find evidence that the model (3.4) does not have a highest singular wave. Furthermore, we provide numerical evidence that the conditional well-posedness result in [22] is in fact *sharp*, in the sense that local evolution of initial data with height profiles with negative minima appears to be ill-posed.

This has led us to construct and analyze new wavetrain solutions of (3.2) with strictly positive height profile, ensuring the local dynamics about such waves is indeed well-posed.

# Appendix A

# Variational Derivatives

Here we briefly demonstrate the computation of first and second variational derivatives of a functional as applied to the fNLS conserved quantities (2.7), (2.8), and (2.9). Recall that these functionals are defined as

$$\mathcal{H}(u) := K(u) + P(u) = \frac{1}{2}\int_0^T \left( \left| \Lambda^{\alpha/2} u \right|^2 - \frac{\gamma}{\sigma+1} |u|^{2\sigma+2} \right) dx, \tag{A.1}$$

$$Q(u) := \frac{1}{2}\int_0^T |u|^2 \, dx, \tag{A.2}$$

$$N(u) := \frac{i}{2}\int_0^T \overline{\Lambda^{1/2} u} \, H \Lambda^{1/2} u \, dx \tag{A.3}$$

and act on $H^{\alpha/2}(0,T)$ for $\alpha \in (1,2]$. Then their *variational derivatives* $\mathcal{H}'$, $Q'$ , and $N'$ are maps from $H^{\alpha/2}(0,T)$ to the dual space $H^{\alpha/2}(0,T)^*$, which is isometrically isomorphic to $H^{-\alpha/2}(0,T)$ over $\mathbb{R}$ by the Riesz representation theorem; in particular, for each $u \in H^{\alpha/2}(0,T)$ there exists a unique $\delta\mathcal{H}(u) \in H^{-\alpha/2}(0,T)$ such that

$$\mathcal{H}'(u)(v) = \langle \delta\mathcal{H}(u), v \rangle := \mathrm{Re} \int_0^T \delta\mathcal{H}(u) \bar{v} \, dx$$

for all $v \in H^{\alpha/2}(0,T)$. This pairing *identifies* the map $\mathcal{H}'(u)$ with its corresponding functional $\delta\mathcal{H}(u)$, hence we will abuse notation and simply say $\mathcal{H}'(u) = \delta\mathcal{H}(u)$.

## A.1 Hamiltonian

In computing the first variation of (A.1), we will make use of the following identity for $u, v \in \mathbb{C}$ and $\varepsilon \in \mathbb{R}$, $k > 0$:

$$\begin{aligned} |u+\varepsilon v|^{2k} &= [(u+\varepsilon v)(\bar{u}+\varepsilon \bar{v})]^k \\ &= \left[|u|^2 + 2\varepsilon \operatorname{Re}(u\bar{v}) + \mathcal{O}(\varepsilon^2)\right]^k \\ &= |u|^{2k} + 2\varepsilon k \operatorname{Re}(u\bar{v})\,|u|^{2k-2} + \mathcal{O}(\varepsilon^2). \end{aligned} \tag{A.4}$$

Let $u, v \in X$ and $\varepsilon \in \mathbb{R}$. Then compute

$$\begin{aligned} \mathcal{H}(u+\varepsilon v) &= \frac{1}{2}\int_0^T \left[\left|\Lambda^{\alpha/2}(u+\varepsilon v)\right|^2 + \frac{\gamma}{\sigma+1}\,|u+\varepsilon v|^{2(\sigma+1)}\right] dx \\ &= \frac{1}{2}\int_0^T \Big[\left|\Lambda^{\alpha/2}u\right|^2 + 2\varepsilon \operatorname{Re}(\Lambda^{\alpha/2}u\,\overline{\Lambda^{\alpha/2}v}) \\ &\qquad - \frac{\gamma}{\sigma+1}\left(|u|^{2\sigma+2} + 2\varepsilon(\sigma+1)\operatorname{Re}(u\bar{v})\,|u|^{2\sigma}\right)\Big] dx + \mathcal{O}(\varepsilon^2) \end{aligned}$$

by using expansion (A.4)

$$\begin{aligned} \implies \mathcal{H}(u+\varepsilon v) - \mathcal{H}(u) &= \varepsilon \int_0^T \left[\operatorname{Re}(\Lambda^{\alpha/2}u\,\overline{\Lambda^{\alpha/2}v}) - \gamma \operatorname{Re}(u\bar{v})\,|u|^{2\sigma}\right] dx + \mathcal{O}(\varepsilon^2) \\ &= \varepsilon\left[\left\langle \Lambda^{\alpha/2}u, \Lambda^{\alpha/2}v\right\rangle - \left\langle \gamma\,|u|^{2\sigma}u, v\right\rangle\right] + \mathcal{O}(\varepsilon^2) \\ &= \varepsilon\left[\langle \Lambda^{\alpha}u, v\rangle - \left\langle \gamma\,|u|^{2\sigma}u, v\right\rangle\right] + \mathcal{O}(\varepsilon^2) \quad \text{since } \Lambda^{\alpha/2} \text{ is symmetric} \\ &= \varepsilon\left\langle \Lambda^{\alpha}u - \gamma\,|u|^{2\sigma}u, v\right\rangle + \mathcal{O}(\varepsilon^2). \end{aligned}$$

Then

$$\frac{\mathcal{H}(u+\varepsilon v) - \mathcal{H}(u)}{\varepsilon} = \left\langle \Lambda^{\alpha}u - \gamma\,|u|^{2\sigma}u, v\right\rangle + \mathcal{O}(\varepsilon),$$

and taking $\varepsilon \to 0$ we conclude that

$$\delta\mathcal{H}(u) = \Lambda^\alpha u - \gamma |u|^{2\sigma} u.$$

The second variation is found similarly: for $u, v, w \in X$, compute

$$\begin{aligned}
\langle \delta\mathcal{H}(u+\varepsilon v), w\rangle &= \left\langle \Lambda^\alpha(u+\varepsilon v) - \gamma |u+\varepsilon v|^{2\sigma}(u+\varepsilon v), w \right\rangle \\
&= \left\langle \Lambda^\alpha u + \varepsilon\Lambda^\alpha v - \gamma\left(|u|^{2\sigma} + 2\varepsilon\sigma \operatorname{Re}(\bar{u}v)|u|^{2\sigma-2} + \mathcal{O}(\varepsilon^2)\right)(u+\varepsilon v), w \right\rangle \\
&= \left\langle \Lambda^\alpha u - \gamma|u|^{2\sigma}u, w\right\rangle + \varepsilon\left\langle \Lambda^\alpha v - \gamma|u|^{2\sigma}v - 2\gamma\sigma\operatorname{Re}(\bar{u}v)|u|^{2\sigma-2}u, w\right\rangle \\
&\qquad + \mathcal{O}(\varepsilon^2) \\
&= \langle \delta\mathcal{H}(u), w\rangle + \varepsilon\left\langle \Lambda^\alpha v - \gamma|u|^{2\sigma}v - 2\gamma\sigma u\operatorname{Re}(\bar{u}v)|u|^{2\sigma-2}, w\right\rangle + \mathcal{O}(\varepsilon^2).
\end{aligned}$$

So, we have the bilinear form

$$\delta^2\mathcal{H}(u)(v) = \Lambda^\alpha v - \gamma|u|^{2\sigma}v - 2\gamma\sigma\operatorname{Re}(\bar{u}v)|u|^{2\sigma-2}u.$$

As an operator, $\delta^2\mathcal{H}(u) = \Lambda^\alpha - \gamma|u|^{2\sigma} - 2\gamma\sigma\operatorname{Re}(\bar{u}\,\cdot)|u|^{2\sigma-2}u$.

## A.2 Charge

For $u, v \in X$, compute

$$\begin{aligned}
Q(u+\varepsilon v) &= \frac{1}{2}\int_0^T |u+\varepsilon v|^2\, dx \\
&= \frac{1}{2}\int_0^T \left[|u|^2 + 2\varepsilon\operatorname{Re}(u\bar{v}) + \mathcal{O}(\varepsilon^2)\right] dx \\
\implies Q(u+\varepsilon v) - Q(u) &= \varepsilon\operatorname{Re}\int_0^T u\bar{v}\, dx + \mathcal{O}(\varepsilon^2)
\end{aligned}$$

$$= \varepsilon \langle u, v \rangle + \mathcal{O}(\varepsilon^2).$$

So, $\delta Q(u) = u$.

To compute the second variation, let $u, v, w \in X$ and compute

$$\begin{aligned} \langle \delta Q(u + \varepsilon v), w \rangle &= \langle u + \varepsilon v, w \rangle \\ &= \langle u, w \rangle + \varepsilon \langle v, w \rangle \\ &= \langle \delta Q(u), w \rangle + \varepsilon \langle v, w \rangle . \end{aligned}$$

So,

$$\delta^2 Q(u)(v) = v.$$

As an operator, $\delta^2 Q(u) = 1$.

## A.3 Angular Momentum

For $u, v \in X$, compute

$$\begin{aligned} N(u + \varepsilon v) &= \frac{i}{2} \int_0^T (\overline{u + \varepsilon v}) (u + \varepsilon v)_x \, dx \\ &= \frac{i}{2} \int_0^T (\bar{u} u_x + \varepsilon [\bar{u} v_x + \bar{v} u_x]) \, dx + \mathcal{O}(\varepsilon^2) \\ \implies N(u + \varepsilon v) - N(u) &= \frac{\varepsilon i}{2} \int_0^T [\bar{u} v_x + \bar{v} u_x] \, dx \\ &= \frac{\varepsilon i}{2} \int_0^T [-\bar{u}_x v + \bar{v} u_x] \, dx \quad \text{by integration by parts} \\ &= \frac{\varepsilon}{2} \int_0^T \left[ \overline{i u_x \bar{v}} + i u_x \bar{v} \right] dx \\ &= \frac{\varepsilon}{2} \int_0^T 2 \operatorname{Re}(i u_x \bar{v}) \, dx \end{aligned}$$

$$= \varepsilon \langle iu_x, v \rangle .$$

So, $\delta N(u) = iu_x$.

To compute the second variation, let $u, v, w \in X$ and compute

$$\begin{aligned} \langle \delta N(u + \varepsilon v), w \rangle &= \langle iu_x + \varepsilon iv_x, w \rangle \\ &= \langle \delta N(u), w \rangle + \varepsilon \langle iv_x, w \rangle . \end{aligned}$$

So,

$$\delta^2 N(u)(v) = iv_x.$$

As an operator, $\delta^2 N(u) = i\partial_x$.

# Appendix B

# Antiperiodic Rearrangement Inequalities

In this section, we establish results pertaining to symmetric decreasing rearrangements of $T$-antiperiodic functions and their consequences. A nice introduction to rearrangements can be found in [47, Chapter 3], and [44] provides a much more in-depth treatment of the subject.

Given a function $f \in L^2_{\text{per}}([0,2T];\mathbb{R}) \cup C^0(\mathbb{R})$ we will end up using *four separate equimeasurable rearrangements* of $f$, which we will describe below. Throughout, we denote the Lebesgue measure on $\mathbb{R}/2T\mathbb{Z}$ by $m$. Given a continuous $2T$-periodic function $f : \mathbb{R} \to \mathbb{R}$, we define the $2T$-periodic symmetric decreasing rearrangement $f^{*_{2T}}$ of $f$ on $(-T,T)$ by

$$f^{*_{2T}}(x) = \inf\{t : m(\{z \in (-T,T) : f(z) > t\}) \leq 2|x|\} \quad \text{for } x \in [-T,T]$$

and note that $f^{*_{2T}}$ is even, nonincreasing on $(0,T)$, and satisfies $f^{*_{2T}}(0) = \max_{x\in\mathbb{R}} f(x)$ and $f^{*_{2T}}(T) = \min_{x\in\mathbb{R}} f(x)$. Similarly, we define the $2T$-periodic rearrangement $f^{\#_{2T}}(x)$ by

$$f^{\#_{2T}}(x) = f^{*_{2T}}(x - T/2)$$

and note that $f^{\#}$ is even about $x = T/2$, nondecreasing on $(-T/2, T/2)$ and satisfies $f^{\#_{2T}}(T/2) = \max_{x\in\mathbb{R}} f(x)$ and $f^{\#_{2T}}(-T/2) = \min_{x\in\mathbb{R}} f(x)$. Both $f^{*_{2T}}$ and $f^{\#_{2T}}$ have the same distribution functions as $f$ on $(-T, T)$ so that, in particular,

$$\|f\|_{L^p(-T,T)} = \|f^{*_{2T}}\|_{L^p(-T,T)} = \|f^{\#_{2T}}\|_{L^p(-T,T)}$$

for all $f \in L^p_{\mathrm{per}}(0,T)$ and $1 \le p \le \infty$. Of special interest here is that if $f$ is $T$-antiperiodic, then $f^{*_{2T}}$ is an even, $T$-antiperiodic function on $\mathbb{R}$ while $f^{\#_{2T}}$ is an odd, $T$-antiperiodic function on $\mathbb{R}$.

Our first result is an analogue of the classical Pólya-Szegö inequality, which states that the kinetic energy is nonincreasing under symmetric decreasing rearrangement.

**Lemma B.0.1** (Pólya-Szegö)**.** *For all $\alpha \in (1,2)$ and $f \in H^{\alpha/2}_{\mathrm{per}}([0,2T];\mathbb{R})$, we have*

$$\int_{-T}^{T} \left|\Lambda^{\alpha/2} f^{*_{2T}}\right|^2 dx = \int_{-T}^{T} \left|\Lambda^{\alpha/2} f^{\#_{2T}}\right|^2 dx \le \int_{-T}^{T} \left|\Lambda^{\alpha/2} f\right|^2 dx.$$

*In particular, if such an $f$ is $T$-antiperiodic, then*

$$\int_{-T/2}^{T/2} \left|\Lambda^{\alpha/2} f^{*_{2T}}\right|^2 dx = \int_{-T/2}^{T/2} \left|\Lambda^{\alpha/2} f^{\#_{2T}}\right|^2 \le \int_{-T/2}^{T/2} \left|\Lambda^{\alpha/2} f\right|^2 dx.$$

*Proof.* Given $f \in H^{\alpha/2}_{\mathrm{a}}([0,T];\mathbb{R})$, observe that for all $t > 0$ we have

$$\left\langle f, e^{-\Lambda^\alpha t} f \right\rangle = \int_{-T}^{T}\int_{-T}^{T} f(x) K_p(x-y,t) f(y)\, dxdy, \tag{B.1}$$

where $K_p(x,t)$ is the $2T$-periodic integral kernel associated to the semigroup $e^{-\Lambda^\alpha t}$ defined in (2.27). By Lemma 2.3.3, $K_p(\cdot,t) = K_p^{*_{2T}}(\cdot,t)$ for all $t > 0$ and hence the Bernstein-

Taylor Theorem [4, Theorem 2] we have

$$\int_{-T}^{T}\int_{-T}^{T} f(x)K_p(x-y,t)f(y)\,dxdy \le \int_{-T}^{T}\int_{-T}^{T} f^{*2T}(x)K_p(x-y,t)f^{*2T}(y)\,dxdy$$

so that

$$\left\langle f, e^{-\Lambda^\alpha t} f \right\rangle \le \left\langle f^{*2T}, e^{-\Lambda^\alpha t} f^{*2T} \right\rangle$$

for all $f \in H_{\mathrm{a}}^{\alpha/2}([0,T];\mathbb{R})$ and $t > 0$. Since $f$ and $f^{*2T}$ are equimeasurable, it follows that

$$\frac{\left\langle f, e^{-\Lambda^\alpha t} f \right\rangle - \|f\|^2_{L^2(-T,T)}}{t} \le \frac{\left\langle f^{*2T}, e^{-\Lambda^\alpha t} f^{*2T} \right\rangle - \|f^{*2T}\|^2_{L^2(-T,T)}}{t}$$

for all $t > 0$. Taking $t \to 0^+$ yields the desired result for the rearrangement $f^{*2T}$. The corresponding result for $f^{\#_{2T}}$ and the restriction to $T$-antiperiodic functions now follows trivially. □

Next, we complement the above result by considering the effect of the above rearrangements on linear potentials.

**Lemma B.0.2.** *Let $V : \mathbb{R} \to \mathbb{R}$ be an even, smooth and $T$-periodic potential.*

*(i) If $V(x)$ is nonincreasing on $(0, T/2)$, then*

$$\int_{-T/2}^{T/2} V(x) f^2(x) dx \ge \int_{-T/2}^{T/2} V(x) \left(f^{\#_{2T}}\right)^2 (x) dx$$

*for all continuous $f \in L^2_{\mathrm{a}}([0,T];\mathbb{R})$.*

*(ii) If $V(x)$ is nondecreasing on $(0, T/2)$, then*

$$\int_{-T/2}^{T/2} V(x) f^2(x) dx \ge \int_{-T/2}^{T/2} V(x) \left(f^{*2T}\right)^2 (x) dx$$

*for all continuous* $f \in L^2_{\mathrm{a}}([0,T];\mathbb{R})$.

*Proof.* We begin by proving (i). Notice by the hypothesis on $V$, the function $(-V(x))$ is even about $x = T/2$ and is nonincreasing on $(T/2, T)$. By the Riesz inequality [47, Section 3.4] we thus have

$$\int_0^T (-V(x)) f^2(x) dx \leq \int_0^T (-V(x)) \left(f^2\right)^{\#_T}(x) dx,$$

where here $(f^2)^{\#_T}$ denotes the $T$-periodic rearrangement of the $T$-periodic function $f^2$ taken to be even about $x = T/2$ and nonincreasing on $(T/2, T)$. Since antiperiodicity of $f$ implies

$$\left(f^2\right)^{\#_T}(x) = \left(f^{\#_{2T}}\right)^2(x) \quad \forall x \in (0,T),$$

the estimate in (i) follows.

Similarly, if $V$ satisfies the hypotheses of (ii), then the Riesz inequality again gives

$$\int_0^T (-V(x)) f^2(x) dx \leq \int_0^T (-V(x)) \left(f^2\right)^{*_T}(x) dx,$$

where here $(f^2)^{*_T}$ denotes the $T$-periodic rearrangement of the $T$-periodic function $f^2$ taken to be even about $x = 0$ and nonincreasing on $(0, T/2)$. Antiperiodicity of $f$ again implies that

$$\left(f^2\right)^{*_T}(x) = \left(f^{*_{2T}}\right)^2(x) \quad \forall x \in (0,T/2),$$

the estimate in (ii) follows. □

We now come to the main result of this appendix, providing an ordering between the even and odd ground state antiperiodic eigenvalues of a periodic Schrödinger operator $L = -\Lambda^\alpha + V$ in terms of the monotonicity properties of the potential $V$.

*Proof.* Proof of Proposition 2.3.9 First, assume that $V(x)$ satisfies the hypothesis of (i) and suppose that $\psi$ is an eigenfunction associated to the ground state eigenvalue of $L$ acting on $L^2_{\mathrm{a,even}}(0,T)$, normalized to be real-valued and $\|\psi\|_{L^2(0,T)} = 1$. Then by Lemma B.0.1 and Lemma B.0.2

$$\begin{aligned}
\min\sigma\left(L\big|_{L^2_{\mathrm{a,even}}(0,T)}\right) &= \int_0^T \left|\Lambda^{\alpha/2}\psi\right|^2 dx + \int_0^T V(x)\psi(x)^2 dx \\
&\geq \int_0^T \left|\Lambda^{\alpha/2}\psi^{\#_{2T}}\right|^2 dx + \int_0^T V(x)\left(\psi^{\#_{2T}}\right)^2(x)dx \\
&\geq \min\sigma\left(L\big|_{L^2_{\mathrm{a,odd}}(0,T)}\right),
\end{aligned}$$

where the last inequality is justified since $\|\psi^{\#_{2T}}\|_{L^2(0,T)} = 1$. This verifies (i). A similar proof establishes the ordering in (ii). □

As a final useful inequality, we establish that $K$ does not increase under taking complex modulus.

**Lemma B.0.3** (Diamagnetic Inequality)**.** *Suppose* $\alpha \in (1,2]$ *and* $u \in H_a^{\alpha/2}([0,T];\mathbb{C})$. *Then*

$$K(|u|) \leq K(u).$$

*Proof.* Observe that

$$\begin{aligned}
\int_{-T}^T \left|\Lambda^{\alpha/2}u\right|^2 dx &= \left\langle \Lambda^{\alpha/2}u, \Lambda^{\alpha/2}u\right\rangle_{L^2(-T,T)} \\
&= \langle \Lambda^\alpha u, u\rangle_{L^2(-T,T)} \\
&= -\frac{d}{dt}\Big|_{t=0^+}\left\langle e^{-\Lambda^\alpha t}u, u\right\rangle_{L^2(-T,T)}. \qquad \text{(B.2)}
\end{aligned}$$

Further, by (B.1),

$$\begin{aligned}\left\langle e^{-\Lambda^\alpha t}u,u\right\rangle_{L^2(-T,T)} &= \int_{-T}^{T}\int_{-T}^{T}\overline{u(x)}K_p(x-y,t)u(y)\,dy\,dx\\ &\le \int_{-T}^{T}\int_{-T}^{T}|u(x)|\,K_p(x-y)\,|u(y)|\,dy\,dx \quad \text{since } K_p(\cdot,t) \text{ is positive}\\ &= \left\langle e^{-\Lambda^\alpha t}|u|,|u|\right\rangle_{L^2(-T,T)}.\end{aligned}$$

Then we have for $t>0$ that

$$-\frac{\left\langle e^{-\Lambda^\alpha t}u,u\right\rangle_{L^2(-T,T)}-\langle u,u\rangle_{L^2(-T,T)}}{t}\ge-\frac{\left\langle e^{-\Lambda^\alpha t}|u|,|u|\right\rangle_{L^2(-T,T)}-\langle|u|,|u|\rangle_{L^2(-T,T)}}{t},$$

and taking $t\to 0^+$ yields

$$-\frac{d}{dt}\Big|_{t=0^+}\left\langle e^{-\Lambda^\alpha t}u,u\right\rangle_{L^2(-T,T)}\ge-\frac{d}{dt}\Big|_{t=0^+}\left\langle e^{-\Lambda^\alpha t}|u|,|u|\right\rangle_{L^2(-T,T)},$$

and it follows immediately by (B.2) that

$$\int_{-T}^{T}\left|\Lambda^{\alpha/2}u\right|^2dx\ge\int_{-T}^{T}\left|\Lambda^{\alpha/2}|u|\right|^2dx.$$

Then by $T$-antiperiodicity, we finally have

$$K(u)=\int_0^T\left|\Lambda^{\alpha/2}u\right|^2dx\ge\int_0^T\left|\Lambda^{\alpha/2}|u|\right|^2dx=K(|u|).$$

□

# Appendix C

# General Framework for Computing the Spectrum of a Bidirectional Whitham Model Linearization

In this appendix we seek to generalize the method for shown in Section 3.3.1 for setting up a bi-infinite matrix representation of a linearized operator, whose spectrum is suitably approximated by truncating to finite dimensions.

Recall that we are dealing with nonlinear traveling wave models of the form (3.8). To linearize the operator associated with such a model about an equilibrium solution

$$(u(x,t),\eta(x,t)) = (\phi(x),\psi(x)),$$

we first express solutions $u$ and $\eta$ as localized perturbations from equilibrium:

$$\begin{aligned} u(x,t) &= \phi(x)+\varepsilon v(x,t)+\mathcal{O}(\varepsilon^2) \\ \eta(x,t) &= \psi(x)+\varepsilon w(x,t)+\mathcal{O}(\varepsilon^2) \end{aligned} \tag{C.1}$$

with $v(\cdot,t), w(\cdot,t) \in L^2(\mathbb{R})$ for each $t > 0$ for which they are defined. Substituting (C.1) into (3.7), Taylor expanding, and taking $\varepsilon \to 0$ yields

$$\begin{cases} v_t &= \displaystyle\sum_{j=0}^{n} \left[ F_{\partial_x^j u}(\vec{\phi},\vec{\psi})\partial_x^j v + F_{\partial_x^j u}(\vec{\phi},\vec{\psi})\partial_x^j w \right] \\ w_t &= \displaystyle\sum_{j=0}^{n} \left[ G_{\partial_x^j u}(\vec{\phi},\vec{\psi})\partial_x^j v + G_{\partial_x^j u}(\vec{\phi},\vec{\psi})\partial_x^j w \right] \end{cases} \tag{C.2}$$

where

$$\vec{\phi} := (\phi, \phi', \phi'', \dots \phi^{(n)}), \quad \vec{\psi} := (\psi, \psi', \psi'', \dots \psi^{(n)}).$$

As was done in [60] for the Whitham equation, we will apply Bloch theory to study the $2\pi$-periodic spectrum of the linearization by writing

$$v(x,t) = e^{\lambda t} V(x) + c.c., \quad w(x,t) = e^{\lambda t} W(x) + c.c., \tag{C.3}$$

where $c.c.$ denotes complex conjugate of the preceding expression (in order to ensure the reality of the functions $v$ and $w$), and

$$V(x) = \sum_{l \in \mathbb{Z}} \widetilde{V}(l) e^{i\kappa(\mu+l)x}, \quad W(x) = \sum_{l \in \mathbb{Z}} \widetilde{W}(l) e^{i\kappa(\mu+l)x} \tag{C.4}$$

with *Bloch coefficients* $\widetilde{V}(l), \widetilde{W}(l)$ for $l \in \mathbb{Z}$ and *Bloch parameter* $\mu \in [0,1)$. We remark that the classical Floquet theorem that justifies these expansions only applies to differential operators. However, the theorem can be extended to the nonlocal setting: see [42, Proposition 3.1], for instance.

Per equations (C.2), we will need to understand how the operators $F_{\partial_x^j u}$, $F_{\partial_x^j \eta}$, $G_{\partial_x^j u}$, and $G_{\partial_x^j \eta}$ act on the Bloch decompositions (C.4). In the models of interest, these operators will be linear combinations of $2\pi$-periodic multiplication operators and the differen-

tial/pseudodifferential operators $\partial_x$, $\mathcal{K}$. We derive the Bloch transforms of such operators here.

If $f$ is a $2\pi/\kappa$-periodic function (multiplication operator), then we may represent $f$ in Fourier series as

$$f(x) = \sum_{m\in\mathbb{Z}} \widehat{f}(m) e^{im\kappa x}.$$

Then

$$\begin{aligned} f(x)V(x) &= \left(\sum_{m\in\mathbb{Z}} \widehat{f}(m)e^{im\kappa x}\right)\left(\sum_{l\in\mathbb{Z}} \widetilde{V}(l)e^{i\kappa(\mu+l)x}\right) \\ &= \sum_{m\in\mathbb{Z}}\sum_{l\in\mathbb{Z}} \widehat{f}(m)\widetilde{V}(l)e^{i\kappa(\mu+m+l)x} \\ &= \sum_{m\in\mathbb{Z}}\left(\sum_{l\in\mathbb{Z}} \widehat{f}(m-l)\widetilde{V}(l)\right)e^{i\kappa(\mu+m)x} \quad \text{by taking } m\mapsto m-l. \end{aligned}$$

Hence the Bloch transform of the product $fV$ is given by

$$\widetilde{fV}(m) = \sum_{l\in\mathbb{Z}} \widehat{f}(m-l)\widetilde{V}(l), \quad m\in\mathbb{Z}. \tag{C.5}$$

Moreover, the Bloch transform with parameter $\mu$ acts on the derivative operator $\partial_x$ as

$$\widetilde{\partial_x f}(m) = \widehat{\partial}_x(\kappa(\mu+m))\widetilde{f}(m) = i\kappa(\mu+m)\widetilde{f}(m), \quad m\in\mathbb{Z},$$

and, by analogy, the Bloch transform acts on the pseudodifferential operator $\mathcal{K}$ as

$$\widetilde{\mathcal{K}f}(m) := \widehat{\mathcal{K}}(\kappa(\mu+m))\widetilde{f}(m) = \frac{\tanh(\kappa(\mu+m))}{\kappa(\mu+m)}\widetilde{f}(m), \quad m\in\mathbb{Z}. \tag{C.6}$$

Substituting (C.3) into (C.2) and taking the Bloch transform of both sides, we have the simultaneous eigenvalue problems

$$\begin{aligned}\lambda\widetilde{V}(m) &= \sum_{j=0}^{n}\left(F_{\partial_x^j u}(\vec{\phi},\vec{\psi};c)V^{(j)} + F_{\partial_x^j \eta}(\vec{\phi},\vec{\psi};c)W^{(j)}\right)^{\sim}(m) \\ &=: \sum_{l\in\mathbb{Z}}\left[\widehat{A}^{\mu}(m,l)\widetilde{V}(l) + \widehat{B}^{\mu}(m,l)\widetilde{W}(l)\right] \qquad \text{(C.7)}\end{aligned}$$

$$\begin{aligned}\text{and}\quad \lambda\widetilde{W}(m) &= \sum_{j=0}^{n}\left(G_{\partial_x^j u}(\vec{\phi},\vec{\psi};c)V^{(j)} + G_{\partial_x^j \eta}(\vec{\phi},\vec{\psi};c)W^{(j)}\right)^{\sim}(m) \\ &=: \sum_{l\in\mathbb{Z}}\left[\widehat{C}^{\mu}(m,l)\widetilde{V}(l) + \widehat{D}^{\mu}(m,l)\widetilde{W}(l)\right], \qquad \text{(C.8)}\end{aligned}$$

where $\widehat{A}^{\mu}(m,l)$, $\widehat{B}^{\mu}(m,l)$, $\widehat{C}^{\mu}(m,l)$, and $\widehat{D}^{\mu}(m,l)$ are the coefficients of the Bloch coefficients upon expanding the Bloch transform. Define the following bi-infinite matrices entry-wise for row-$m$ and column-$l$ with $m,l\in\mathbb{Z}$ as

$$\begin{aligned}\widehat{A}^{\mu} &:= [\widehat{A}^{\mu}(m,l)]_{m,l\in\mathbb{Z}}, \qquad \widehat{B}^{\mu} := [\widehat{B}^{\mu}(m,l)]_{m,l\in\mathbb{Z}}, \\ \widehat{C}^{\mu} &:= [\widehat{C}^{\mu}(m,l)]_{m,l\in\mathbb{Z}}, \qquad \widehat{D}^{\mu} := [\widehat{D}^{\mu}(m,l)]_{m,l\in\mathbb{Z}}.\end{aligned}$$

Writing (C.7) and (C.8) jointly in block bi-infinte matrix form, we have

$$\lambda\begin{bmatrix}\widetilde{V}\\ \hline \widetilde{W}\end{bmatrix} = \left[\begin{array}{c|c}\widehat{A}^{\mu} & \widehat{B}^{\mu}\\ \hline \widehat{C}^{\mu} & \widehat{D}^{\mu}\end{array}\right]\begin{bmatrix}\widetilde{V}\\ \hline \widetilde{W}\end{bmatrix} =: \widehat{\mathcal{L}}^{\mu}\begin{bmatrix}\widetilde{V}\\ \hline \widetilde{W}\end{bmatrix} \qquad \text{(C.9)}$$

where

$$\begin{aligned}\widetilde{V} &:= \begin{bmatrix}\dots & \widetilde{V}(-2) & \widetilde{V}(-1) & \widetilde{V}(0) & \widetilde{V}(1) & \widetilde{V}(2) & \dots\end{bmatrix}^{T} \\ \widetilde{W} &:= \begin{bmatrix}\dots & \widetilde{W}(-2) & \widetilde{W}(-1) & \widetilde{W}(0) & \widetilde{W}(1) & \widetilde{W}(2) & \dots\end{bmatrix}^{T}.\end{aligned}$$

To numerically approximate the bi-infinite eigenvalue problem (C.9), we truncate each of the bi-infinite matrices $\widehat{A}^\mu$, $\widehat{B}^\mu$, $\widehat{C}^\mu$, and $\widehat{D}^\mu$ to have dimension $(2N+1)\times(2N+1)$, i.e.

$$\widehat{A}^\mu_N(m,l) := [\widehat{A}^\mu(m,l)]_{-N\le m,l\le N} \in \mathbb{C}^{(2N+1)\times(2N+1)}$$

and similarly define $\widehat{B}^\mu_N$, $\widehat{C}^\mu_N$, and $\widehat{D}^\mu_N$, which together form $\widehat{\mathcal{L}}^\mu_N \in \mathbb{C}^{(4N+2)\times(4N+2)}$ as shown in (C.10) below. Moreover, we also truncate $\widetilde{V}$ and $\widetilde{W}$ as

$$\widetilde{V}_N = \begin{bmatrix} \widetilde{V}(-N) & \dots & \widetilde{V}(0) & \dots & \widetilde{V}(N) \end{bmatrix}^T,$$
$$\widetilde{W}_N = \begin{bmatrix} \widetilde{W}(-N) & \dots & \widetilde{W}(0) & \dots & \widetilde{W}(N) \end{bmatrix}^T.$$

Then, using a standard matrix eigenvalue solver (e.g. Matlab's `eig` or Python's `numpy.linalg.eig` [43]), we solve for $\lambda^\mu_N \in \mathbb{C}$ such that

$$\lambda^\mu_N \left[\begin{array}{c} \widetilde{V}_N \\ \hline \widetilde{W}_N \end{array}\right] = \left[\begin{array}{c|c} \widehat{A}^\mu_N & \widehat{B}^\mu_N \\ \hline \widehat{C}^\mu_N & \widehat{D}^\mu_N \end{array}\right] \left[\begin{array}{c} \widetilde{V}_N \\ \hline \widetilde{W}_N \end{array}\right] =: \widehat{\mathcal{L}}^\mu_N \left[\begin{array}{c} \widetilde{V}_N \\ \hline \widetilde{W}_N \end{array}\right] \tag{C.10}$$

We solve this eigenvalue problem for $\mu$ in a discrete subset of $[0,1)$. For our computations, we used a uniform mesh $\{\mu_j = j\Delta\mu\}_j$ with subintervals of constant width $\Delta\mu$.

*Remark* C.0.1. The above method is inspired by the Fourier-Floquet-Hill Method (FFHM) given in [16], which is used to compute the spectrum of a linear, locally-acting operator having periodic coefficients. As was done in [16], we define convergence of the spectral approximation in the sense that any eigenvalue $\lambda^\mu_N$ of $\widehat{\mathcal{L}}^\mu_N$ above converges to some eigenvalue $\lambda$ of non-truncated linearization $\mathcal{L}$. Moreover, the incorporation of all Bloch

parameters $\mu \in [0,1)$ yields the entire spectrum, i.e.

$$\lim_{N\to\infty} \bigcup_{\mu\in[0,1)} \sigma(\widehat{\mathcal{L}}_N^{\mu}) = \sigma(\mathcal{L}).$$

To obtain the approximate Fourier coefficients $\widehat{\phi}$ and $\widehat{\psi}$ (in the exponential basis) needed to construct the bi-infinite matrix $\widehat{\mathcal{L}}_N^{\mu}$, for a given wave speed $c$, we use the approximate values of $\phi(x_m)$ at each collocation point $x_m = \frac{(2m-1)\pi}{2\kappa N}$ obtained in the numerical bifurcation (see Section 3.2) and compute the approximate coefficients via their integral definitions using the midpoint quadrature:

$$\begin{aligned}
\widehat{\phi}(n) &= \frac{\kappa}{2\pi}\int_{-\pi/\kappa}^{\pi/\kappa} \phi(x) e^{-in\kappa x}\, dx \\
&= \frac{\kappa}{\pi}\int_{0}^{\pi/\kappa} \phi(x)\cos(n\kappa x)\, dx \quad \text{since } \phi \text{ is even} \\
&\approx \frac{1}{N}\sum_{m=1}^{N} \phi(x_m)\cos(n\kappa x_m) \quad \text{by (3.13)}.
\end{aligned}$$

Similarly,

$$\widehat{\psi}(n) \approx \frac{1}{N}\sum_{m=1}^{N} \psi(x_m)\cos(n\kappa x_m).$$

*Remark* C.0.2. The approximation of $\widehat{\psi}(n)$ above requires that $\psi$ be an even function. This is always the case since we are considering models for which $\psi$ can be resolved in terms of $\phi$, hence $\psi = \psi(\phi(x))$ is also an even function.

As an example, here we show the relevant calculations in detail for the model (3.22) as a concrete demonstration of the more abstract framework established in this appendix.

Recall that this model is given by

$$\begin{cases} u_t &= cu_x - \eta_x - uu_x =: F(u, u_x, \eta, \eta_x) \\ \eta_t &= c\eta_x - \mathcal{K}u_x - (\eta u)_x =: G(u, u_x, \eta, \eta_x), \end{cases}$$

with equilibrium solutions $u(x,t) = \phi(x)$, $\eta(x,t) = \psi(x)$. Beginning with (3.32), we first compute

$$F_u(\phi, \phi', \psi, \psi') = -\phi', \qquad F_{u_x}(\phi, \phi', \psi, \psi') = c - \phi,$$
$$F_\eta(\phi, \phi', \psi, \psi') = 0, \qquad F_{\eta_x}(\phi, \phi', \psi, \psi') = -1.$$

All of the above are $2\pi/\kappa$-periodic multiplication operators, hence we apply (C.5) in (C.7), here with $n = 1$, to achieve the following formulas for $m \in \mathbb{Z}$:

$$\widetilde{F_u V}(m) = \sum_{l\in\mathbb{Z}} \widehat{-\phi'}(m-l)\widetilde{V}(l) = \sum_{l\in\mathbb{Z}} -i\kappa(m-l)\widehat{\phi}(m-l)\widetilde{V}(l)$$
$$\widetilde{F_{u_x} V'}(m) = \sum_{l\in\mathbb{Z}} \widehat{(c-\phi)}(m-l)\ \widetilde{\partial_x V}(l) = \sum_{l\in\mathbb{Z}} \Big(c\delta_{m,l} - \widehat{\phi}(m-l)\Big) \cdot i\kappa(\mu+l)\widetilde{V}(l)$$
$$\widetilde{F_\eta W}(m) = \sum_{l\in\mathbb{Z}} 0\,\widetilde{W}(l)$$
$$\widetilde{F_{\eta_x} W'}(m) = \sum_{l\in\mathbb{Z}} \widehat{(-1)}(m-l)\ \widetilde{\partial_x W}(l) = \sum_{l\in\mathbb{Z}} -\delta_{m,l} \cdot i\kappa(\mu+l)\widetilde{W}(l),$$

where $\delta_{m,l}$ is the Kronecker delta. Summing the above expressions and grouping terms involving $\widetilde{V}(l)$ and $\widetilde{W}(l)$ per (C.7), we obtain

$$\begin{aligned} \widehat{A}^\mu(m,l) &= -i\kappa(m-l)\widehat{\phi}(m-l) + \Big(c\delta_{m,l} - \widehat{\phi}(m-l)\Big) \cdot i\kappa(\mu+l) \\ &= ic\kappa(\mu+l)\delta_{m,l} - i\kappa(\mu+m)\widehat{\phi}(m-l) \qquad \text{(C.11)} \\ \widehat{B}^\mu(m,l) &= -i\kappa(\mu+l)\delta_{m,l}, \qquad \text{(C.12)} \end{aligned}$$

Similarly, per (C.8), we compute

$$G_u(\phi,\phi',\psi,\psi') = -\psi', \quad G_{u_x}(\phi,\phi',\psi,\psi') = -\mathcal{K}-\psi,$$
$$G_\eta(\phi,\phi',\psi,\psi') = -\phi', \quad G_{\eta_x}(\phi,\phi',\psi,\psi') = c-\phi.$$

Then

$$\begin{aligned}
\widetilde{G_u V}(m) &= \sum_{l\in\mathbb{Z}} \widehat{-\psi'}(m-l)\widetilde{V}(l) = -i\kappa(m-l)\widehat{\psi}(m-l)\widetilde{V}(l) \\
\widetilde{G_{u_x} V'}(m) &= [(-\mathcal{K}-\psi)\partial_x V]^{\sim}(m) \\
&= -\widetilde{\mathcal{K}\partial_x V}(m) - \widetilde{\psi\,\partial_x V}(m) \\
&= -i\kappa(\mu+m)\widehat{\mathcal{K}}(\kappa(\mu+m))\widetilde{V}(m) - \sum_{l\in\mathbb{Z}} \widehat{\psi}(m-l)\, i\kappa(\mu+l)\widetilde{V}(l) \\
&= \sum_{l\in\mathbb{Z}} -i\kappa(\mu+l)\left[\widehat{\mathcal{K}}(\kappa(\mu+l))\delta_{m,l} + \widehat{\psi}(m-l)\right]\widetilde{V}(l) \\
\widetilde{G_\eta W}(m) &= \sum_{l\in\mathbb{Z}} \widehat{-\phi'}(m-l)\widetilde{W}(l) = \sum_{l\in\mathbb{Z}} -i\kappa(m-l)\widehat{\phi}(m-l)\widetilde{W}(l) \\
\widetilde{G_{\eta_x} W'}(m) &= \sum_{l\in\mathbb{Z}} \widehat{(c-\phi)}(m-l)\ \widetilde{\partial_x W}(l) = \sum_{l\in\mathbb{Z}} \Big(c\delta_{m,l} - \widehat{\phi}(m-l)\Big)\cdot i\kappa(\mu+l)\widetilde{W}(l).
\end{aligned}$$

Summing the above expressions and grouping terms involving $\widetilde{V}(l)$ and $\widetilde{W}(l)$ per (C.8), we obtain

$$\widehat{C}^\mu(m,l) = -i\kappa(\mu+l)\widehat{\mathcal{K}}(\kappa(\mu+l))\delta_{m,l} - i\kappa(\mu+m)\widehat{\psi}(m-l) \tag{C.13}$$
$$\widehat{D}^\mu(m,l) = ic\kappa(\mu+l)\delta_{m,l} - i\kappa(\mu+m)\widehat{\phi}(m-l). \tag{C.14}$$

Note that the formulas for $\widehat{A}^\mu(m,l)$, $\widehat{B}^\mu(m,l)$, $\widehat{C}^\mu(m,l)$, $\widehat{D}^\mu(m,l)$ given above in (C.11), (C.12), (C.13), and (C.14) agree with those found in Section 3.3.1 circa (3.32), (3.33) by manipulating Fourier series.

# Appendix D

# Bidirectional Whitham Numerical Parameters

## D.1 Bifurcation and Spectral Figures

In Table D.1, we provide the numerical parameters used to compute bifurcations via the pseudo-arclength method and spectra via the Fourier-Floquet-Hill-Method (FFHM). A brief reminder of the symbols involved:

Pseudo-arclength Parameters:

- $\kappa$ is the wavenumber, which yields waves of period $2\pi/\kappa$.
- $N$ is the number of collocation points $x_i = \frac{(2i-1)\pi}{2\kappa N}$, $i = 1, \ldots, N$ on the half-period cell $[0, \pi/\kappa]$, as well as the number of modes used in the profile's truncated series $\phi(x) = \sum_{n=0}^{N-1} \widehat{\phi}(n) \cos(n\kappa x)$. See Section 3.2.1.
- $h$ is the length of a step along the tangent direction in each iteration of the pseudo-arclength method. See Figure 3.1 and the surrounding discussion.
- $\varepsilon_0$ determines a suitable starting point (see (3.21)) near the global bifurcation curve based on the model's local bifurcation formulas (e.g. (3.26), (3.27)).

FFHM Parameters:

- $\Delta\mu$ is the width of a subinterval in the uniform mesh $\{\mu_j = j\Delta\mu\}_j \subset [0,1)$ of Bloch parameters used to discretize the $L^2(\mathbb{R})$ spectrum. See (C.4) and Remark C.0.1.
- $N$ determines the dimension of the truncated bi-infinite matrix $\widehat{\mathcal{L}}_N^\mu \in \mathbb{C}^{(4N+2)\times(4N+2)}$. See (C.10) and the surrounding discussion.

## D.2 Time Evolution by Operator Splitting

Consider the time-evolution of a nonlinear initial-value problem

$$\begin{cases} u_t(x,t) &= (A+B)u(x,t) \\ u(x,0) &= u_0(x), \end{cases} \tag{D.1}$$

where $A$ and $B$ are, respectively, linear and nonlinear operators. Abstractly, the solution at time $t$ is given in terms of the operator exponential as

$$u(x,t) = e^{(A+B)t}u_0(x).$$

An *operator-splitting method* allows one to solve the above IVP by successively solving the linear and nonlinear parts separately. For example, it is easy to verify that

$$e^{(A+B)t} = e^{\frac{1}{2}tA}e^{tB}e^{\frac{1}{2}tA} + \mathcal{O}(t^3). \tag{D.2}$$

That is, to second order in the time step $t$, the IVP (D.1) can be evolved forward by time step $t$ as follows:

1. Solve the linear equation $u_t = Au$ with initial data $u_0$ forward by time step $\frac{1}{2}t$.

2. Then solve the nonlinear equation $u_t = Bu$ forward by time step $t$ using initial data $e^{\frac{1}{2}tA}u_0$ (the output of Step 1).

3. Then again solve the linear equation $u_t = Au$ forward by time step $\frac{1}{2}t$ using initial data $e^{tB}e^{\frac{1}{2}tA}u_0$ (the output of Step 2).

Iterating the above method allows one to time-evolve the system to arbitrary time. A big advantage of this method in solving periodic problems is that solutions of the linear equation can be performed very efficiently using spectral (i.e. Fourier transform) methods, while the nonlinear part can be solved using a method that is well-suited to the given nonlinearity (the standard fourth-order Runge-Kutta method is often a good choice). For the time evolution here, we use a sixth-order pseudospectral operator splitting method as described above, where the details of the method and the analogous form of (D.2) for sixth-order accuracy can be found in [67].

The linear part of (3.2) is

$$\begin{cases} u_t &= -\eta_x \\ \eta_t &= -\mathcal{K}u_x, \end{cases}$$

which can be transformed into decoupled wave-like second-order in time IVPs

$$\begin{cases} \eta_{tt}(x,t) &= \mathcal{K}\eta_{xx}(x,t) \\ \eta(x,0) &= \psi(x) \\ \eta_t(x,0) &= -\mathcal{K}\phi'(x) \end{cases} \qquad \begin{cases} u_{tt}(x,t) &= \mathcal{K}u_{xx}(x,t) \\ u(x,0) &= \phi(x) \\ u_t(x,0) &= -\psi'(x), \end{cases}$$

where $\psi(x)$, $\phi(x)$ are equilibria as discussed in Section 3.3.1. Taking the Fourier transform of the above equations in $x$ yields ODE IVPs in $t$ for each fixed $n \in \mathbb{Z}$:

$$\begin{cases} \widehat{\eta}_{tt}(n,t) &= -\kappa^2 n^2 \widehat{\mathcal{K}}(n)\widehat{\eta}(n,t) \\ \widehat{\eta}(n,0) &= \widehat{\psi}(n) \\ \widehat{\eta}_t(n,0) &= -in\widehat{\mathcal{K}}(n)\widehat{\phi}(n) \end{cases} \qquad \begin{cases} \widehat{u}_{tt}(n,t) &= -\kappa^2 n^2 \widehat{\mathcal{K}}(n)\widehat{u}(n,t) \\ \widehat{u}(n,0) &= \widehat{\phi}(n) \\ \widehat{u}_t(n,0) &= -in\widehat{\psi}(n). \end{cases} \tag{D.3}$$

The equations in (D.3) are well-known to model simple harmonic motion and can be solved explicitly. For the nonlinear part of (3.2), the typical fourth-order Runge-Kutta scheme (RK4) is used.

- In Figure 3.7, a small $2\pi$-periodic wave of height $\max\psi - \min\psi \approx 0.00109$ generated by the pseudo-arclength method with parameters $\kappa = 1$, $h = 0.01$, $\varepsilon_0 = 1 \times 10^{-5}$, and $N = 2048$ collocation points on the half-periodic cell $[0, \pi]$ ($\Delta x = \frac{\pi}{2048} \approx 0.00153$) is used as initial data in (D.3). A time step of $\Delta t = 0.001$ is used in each iteration of the 6th-order operator splitting method to integrate to time $t = 2.55$, which is about 35.4% of a temporal period for this wave.

- In Figure 3.10, a large $2\pi$-periodic *positive* wave of height $\max\psi - \min\psi \approx 0.387$ generated by the pseudo-arclength method with parameters $\kappa = 1$, $h = 0.01$, $\varepsilon_0 = 1 \times 10^{-5}$, and $N = 2048$ collocation points on the half-periodic cell $[0, \pi]$ ($\Delta x = \frac{\pi}{2048} \approx 0.00153$) is used as initial data in (D.3). A time step of $\Delta t = 0.001$ was used to integrate for 15 temporal periods (to time $t \approx 80.5706$).

The ease of time-evolving large positive waves (which are proven to be locally well-posed; see [22]), as opposed to the difficulty of evolving non-positive waves in the same model with the same $\Delta t/\Delta x \approx 0.6536$ suggests that the non-positive waves are not locally well-posed in time.

Table D.1: Parameters for figures generated by the pseudo-arclength method (bifurcation) and Fourier-Floquet-Hill method (spectrum).

| Figure(s) | Pseudo-arclength Parameters | FFHM Parameters |
|---|---|---|
| 3.2 (a) | $\kappa = 1$, $N = 256$, $h = 10^{-3}$, $\varepsilon_0 = 10^{-5}$ | |
| 3.2 (b) | $\kappa \in \{0.8, 1.0, 1.3, 1.6\}$, $N = 256$, $h = 10^{-3}$, $\varepsilon_0 = 10^{-5}$ | |
| 3.3 (a), (b) | $\kappa = 1$, $N = 256$, $h = 10^{-3}$, $\varepsilon_0 = 10^{-5}$ | |
| 3.4 (a) | $\kappa = 1$, $N = 256$, $h = 10^{-3}$, $\varepsilon_0 = 10^{-5}$ | $N = 50$, $\Delta\mu = 1/10000$ |
| 3.4 (b), (c) | $\kappa = 1$, $N = 256$, $h = 10^{-3}$, $\varepsilon_0 = 10^{-5}$ | $N = 50$, $\Delta\mu = 1/5000$ |
| 3.4 (d), (e) | $\kappa = 1$, $N = 256$, $h = 10^{-3}$, $\varepsilon_0 = 10^{-5}$ | $N = 128$, $\Delta\mu = 1/5000$ |
| 3.5 (a)-(e) | Same data as Figure 3.4 (a)-(e) | Same data as Figure 3.4 (a)-(e) |
| 3.6 (a) | $\kappa = 1.005$, $N = 64$, $h = 10^{-3}$, $\varepsilon_0 = 10^{-5}$ | $N = 50$, $\Delta\mu = 1/15000$ |
| 3.6 (b) | $\kappa = 1.008$, $N = 64$, $h = 10^{-3}$, $\varepsilon_0 = 10^{-5}$ | $N = 64$, $\Delta\mu = 1/15000$ |
| 3.8 (b) | $\kappa \in \{0.5, 1.0, 1.3, 1.6\}$, $N = 256$, $h = 10^{-3}$, $\varepsilon_0 = 10^{-5}$ | |
| 3.9 (a), (b) | $\kappa = 1$, $N = 2048$, $h = 10^{-3}$, $\varepsilon_0 = 10^{-5}$ | |
| 3.11 (a) | $\kappa = 1$, $N = 2048$, $h = 10^{-3}$, $\varepsilon_0 = 10^{-5}$ | $N = 50$, $\Delta\mu = 1/50000$ |
| 3.11 (b) | $\kappa = 1$, $N = 2048$, $h = 10^{-3}$, $\varepsilon_0 = 10^{-5}$ | $N = 50$, $\Delta\mu = 1/10000$ |
| 3.11 (c) | $\kappa = 1$, $N = 2048$, $h = 10^{-3}$, $\varepsilon_0 = 10^{-5}$ | $N = 128$, $\Delta\mu = 1/5000$ |
| 3.12 (a)-(c) | $\kappa = 1.611$, $N = 256$, $h = 10^{-3}$, $\varepsilon_0 = 10^{-5}$ | |
| 3.12 (d) | $\kappa \in \{0.8, 1, 1.3, 1.6\}$, $N = 256$, $h = 10^{-3}$, $\varepsilon_0 = 10^{-5}$ | |
| 3.13 | $\kappa = 1$, $N \in \{64, 128, 256, 512\}$, $h = 10^{-3}$, $\varepsilon_0 = 10^{-5}$ | |
| 3.14 (a), (b) | $\kappa = 1.611$, $N = 256$, $h = 10^{-3}$, $\varepsilon_0 = 10^{-5}$ | $N = 50$, $\Delta\mu = 1/10000$ |
| 3.14 (c), (d) | $\kappa = 1.611$, $N = 256$, $h = 10^{-3}$, $\varepsilon_0 = 10^{-5}$ | $N = 50$, $\Delta\mu = 1/5000$ |
| 3.14 (e) | $\kappa = 1.611$, $N = 256$, $h = 10^{-3}$, $\varepsilon_0 = 10^{-5}$ | $N = 128$, $\Delta\mu = 1/5000$ |
| 3.15 (a), (b) | $\kappa = 1.609$, $N = 256$, $h = 10^{-3}$, $\varepsilon_0 = 10^{-5}$ | $N = 50$, $\Delta\mu = 1/10000$ |
| 3.16 (a)-(e) | Same data as Figure 3.14 | Same data as Figure 3.14 |
| 3.17 (a)-(c) | $\kappa = 1$, $N = 256$, $h = 10^{-3}$, $\varepsilon_0 = 10^{-5}$ | |
| 3.17 (d) | $\kappa \in \{0.8, 1.0, 1.3, 1.6\}$, $N = 256$, $h = 10^{-3}$, $\varepsilon_0 = 10^{-5}$ | |
| 3.18 (a)-(d) | $\kappa = 1$, $N = 256$, $h = 10^{-3}$, $\varepsilon_0 = 10^{-5}$ | $N = 50$, $\Delta\mu = 1/10000$ |
| 3.18 (e) | $\kappa = 1$, $N = 256$, $h = 10^{-3}$, $\varepsilon_0 = 10^{-5}$ | $N = 128$, $\Delta\mu = 1/10000$ |
| 3.19 | Same data as Figure 3.18 | Same data as Figure 3.18 |

# Bibliography


[1] Herbert Amann. Compact embeddings of vector-valued Sobolev and Besov spaces. *Glas. Mat. Ser. III*, 35(55)(1):161–177, 2000. Dedicated to the memory of Branko Najman. Cited on 7

[2] Daniel Andersson. Estimates of the Spherical and Ultraspherical Heat Kernel. Master's thesis, Chalmers University of Technology, Gothenburg, Sweden, 2013. Cited on 57

[3] Jaime Angulo Pava. Nonlinear stability of periodic traveling wave solutions to the Schrödinger and the modified Korteweg-de Vries equations. *J. Differential Equations*, 2007. Cited on 12, 25

[4] Albert Baernstein, II and B. A. Taylor. Spherical rearrangements, subharmonic functions, and $*$-functions in $n$-space. *Duke Math. J.*, 43(2):245–268, 1976. Cited on 137

[5] Fabrice Béthuel, Philippe Gravejat, Jean-Claude Saut, and Didier Smets. Orbital stability of the black soliton for the Gross-Pitaevskii equation. *Indiana Univ. Math. J.*, 57(6):2611–2642, 2008. Cited on 24

[6] Nate Bottman and Bernard Deconinck. KdV cnoidal waves are spectrally stable. *Discrete Contin. Dyn. Syst.*, 25(4):1163–1180, 2009. Cited on 15

[7] Nathaniel Bottman, Bernard Deconinck, and Michael Nivala. Elliptic solutions of the defocusing NLS equation are stable. *J. Phys. A*, 44(28):285201, 24, 2011. Cited on 25

[8] Jared C. Bronski, Vera Mikyoung Hur, and Mathew A. Johnson. Modulational instability in equations of KdV type. In *New approaches to nonlinear waves*, volume 908 of *Lecture Notes in Phys.*, pages 83–133. Springer, Cham, 2016. Cited on 105

[9] C. Bucur and E. Valdinoci. Nonlocal diffusion and applications. *preprint*, 2015. arXiv:1504.08292. Cited on 24

[10] Luis Caffarelli and Luis Silvestre. An extension problem related to the fractional Laplacian. *Comm. Partial Differential Equations*, 32(7-9):1245–1260, 2007. Cited on 64

[11] P. Cardaliaguet, F. Da Lio, N. Forcadel, and R. Monneau. Dislocation dynamics: a non-local moving boundary. In *Free boundary problems*, volume 154 of *Internat. Ser. Numer. Math.*, pages 125–135. Birkhäuser, Basel, 2007. Cited on 24

[12] J. D. Carter. Bidirectional Whitham Equations as Models of Waves on Shallow Water. *ArXiv e-prints*, May 2017. Cited on 88

[13] T. Cazenave and P.-L. Lions. Orbital stability of standing waves for some nonlinear Schrödinger equations. *Comm. Math. Phys.*, 85(4):549–561, 1982. Cited on 24

[14] F. M. Christ and M. I. Weinstein. Dispersion of small amplitude solutions of the generalized Korteweg-de Vries equation. *J. Funct. Anal.*, 100(1):87–109, 1991. Cited on 41

[15] B. Deconinck and B. L. Segal. The stability spectrum for elliptic solutions to the focusing NLS equation. *Physica D Nonlinear Phenomena*, 346:1–19, May 2017. Cited on 25

[16] Bernard Deconinck and J. Nathan Kutz. Computing spectra of linear operators using the floquetfourierhill method. *Journal of Computational Physics*, 219(1):296 – 321, 2006. Cited on 21, 99, 145

[17] Bernard Deconinck and Katie Oliveras. The instability of periodic surface gravity waves. *J. Fluid Mech.*, 675:141–167, 2011. Cited on 88, 91

[18] Bernard Deconinck and Olga Trichtchenko. High-frequency instabilities of small-amplitude solutions of Hamiltonian PDEs. *Discrete Contin. Dyn. Syst.*, 37(3):1323–1358, 2017. Cited on 88, 90, 121, 122

[19] Tomáš Dohnal, Michael Plum, and Wolfgang Reichel. Localized modes of the linear periodic Schrödinger operator with a nonlocal perturbation. *SIAM J. Math. Anal.*, 41(5):1967–1993, 2009. Cited on 62, 63

[20] M. Ehrnström, M. A. Johnson, and K. M. Claassen. Existence of a highest wave in a fully dispersive two-way shallow water model. *ArXiv e-prints*, October 2016. arXiv:1610.02603. Cited on 87, 88, 89, 101, 102, 103, 109, 111

[21] M. Ehrnström and H. Kalisch. Global bifurcation for the Whitham equation. *Math. Model. Nat. Phenom.*, 8(5):13–30, 2013. Cited on 87

[22] M. Ehrnström, L. Pei, and Y. Wang. A conditional well-posedness result for the bidirectional Whitham equation. *ArXiv e-prints*, August 2017. Cited on 88, 89, 93, 111, 128, 152

[23] M. Ehrnström and E. Wahlén. On whithams conjecture of a highest cusped wave for a nonlocal dispersive shallow water wave equation. *Preprint*, 2015. arXiv:1602.05384, 2015. Cited on 88

[24] Mats Ehrnström and Henrik Kalisch. Traveling waves for the Whitham equation. *Differential Integral Equations*, 22(11-12):1193–1210, 2009. Cited on 87

[25] Rupert L. Frank and Enno Lenzmann. Uniqueness of non-linear ground states for fractional Laplacians in $\mathbb{R}$. *Acta Math.*, 210(2):261–318, 2013. Cited on 24, 27, 28, 51, 54, 55, 56, 63, 64, 65

[26] T. Gallay and M. Hărăgus. Orbital stability of periodic waves for the nonlinear Schrödinger equation. *Journal of Dynamics and Differential Equations*, 2007. Cited on 26, 27, 28, 51, 83

[27] Thierry Gallay and Mariana Hărăguş. Stability of small periodic waves for the nonlinear Schrödinger equation. *J. Differential Equations*, 234(2):544–581, 2007. Cited on 25

[28] Thierry Gallay and Dmitry Pelinovsky. Orbital stability in the cubic defocusing NLS equation: II. The black soliton. *J. Differential Equations*, 258(10):3639–3660, 2015. Cited on 24

[29] Philippe Gravejat and Didier Smets. Asymptotic stability of the black soliton for the Gross–Pitaevskii equation. *Proc. Lond. Math. Soc. (3)*, 111(2):305–353, 2015. Cited on 24

[30] Manoussos Grillakis, Jalal Shatah, and Walter Strauss. Stability theory of solitary waves in the presence of symmetry. I. *J. Funct. Anal.*, 74(1):160–197, 1987. Cited on 26

[31] Manoussos Grillakis, Jalal Shatah, and Walter Strauss. Stability theory of solitary waves in the presence of symmetry. II. *J. Funct. Anal.*, 94(2):308–348, 1990. Cited on 26

[32] Boling Guo and Daiwen Huang. Existence and stability of standing waves for nonlinear fractional Schrödinger equations. *J. Math. Phys.*, 53(8):083702, 15, 2012. Cited on 24

[33] S. Gustafson, S. Le Coz, and T.-P. Tsai. Stability of periodic waves of 1D cubic nonlinear Schr{\"o}dinger equations. *ArXiv e-prints*, June 2016. arXiv:1606.04215. Cited on 25

[34] Y. Hong and Y. Sire. On Fractional Schrodinger Equations in sobolev spaces. *ArXiv e-prints*, January 2015. arXiv:1501.01414. Cited on 41

[35] V. Mikyoung Hur and A. K. Pandey. Modulational instability in a full-dispersion shallow water model. *ArXiv e-prints*, August 2016. arXiv:1608.04685. Cited on 88, 90, 91, 93, 108, 117, 121

[36] Vera Mikyoung Hur. Wave breaking in the Whitham equation. *Adv. Math.*, 317:410–437, 2017. Cited on 88

[37] Vera Mikyoung Hur and Mathew A. Johnson. Modulational instability in the Whitham equation for water waves. *Stud. Appl. Math.*, 134(1):120–143, 2015. Cited on 87, 88

[38] Vera Mikyoung Hur and Mathew A. Johnson. Modulational instability in the Whitham equation with surface tension and vorticity. *Nonlinear Anal.*, 129:104–118, 2015. Cited on 88

[39] Vera Mikyoung Hur and Mathew A. Johnson. Stability of Periodic Traveling Waves for Nonlinear Dispersive Equations. *SIAM Journal on Mathematical Analysis*, 47(5):3528–3554, 2015. Cited on 27, 28, 51, 63, 64, 65, 83

[40] Vera Mikyoung Hur, Mathew A. Johnson, and Jeremy L. Martin. Oscillation estimates of eigenfunctions via the combinatorics of noncrossing partitions. *Discrete Analysis*, to appear. Cited on 65

[41] Alexandru D. Ionescu and Fabio Pusateri. Nonlinear fractional Schrödinger equations in one dimension. *J. Funct. Anal.*, 266(1):139–176, 2014. Cited on 24

[42] Mathew A. Johnson. Stability of small periodic waves in fractional kdv-type equations. *SIAM Journal on Mathematical Analysis*, 45(5):3168–3193, 2013. Cited on 22, 142

[43] Eric Jones, Travis Oliphant, Pearu Peterson, et al. SciPy: Open source scientific tools for Python, 2001–. Cited on 21, 145

[44] Bernhard Kawohl. *Rearrangements and convexity of level sets in PDE*, volume 1150 of *Lecture Notes in Mathematics*. Springer-Verlag, Berlin, 1985. Cited on 135

[45] C. E. Kenig, Y. Martel, and L. Robbiano. Local well-posedness and blow-up in the energy space for a class of $L^2$ critical dispersion generalized Benjamin-Ono equations. *Ann. Inst. H. Poincaré Anal. Non Linéaire*, 28(6):853–887, 2011. Cited on 27

[46] Kay Kirkpatrick, Enno Lenzmann, and Gigliola Staffilani. On the continuum limit for discrete NLS with long-range lattice interactions. *Comm. Math. Phys.*, 317(3):563–591, 2013. Cited on 24

[47] Elliott H. Lieb and Michael Loss. *Analysis*, volume 14 of *Graduate Studies in Mathematics*. American Mathematical Society, Providence, RI, second edition, 2001. Cited on 135, 138

[48] Zhiwu Lin. Instability of nonlinear dispersive solitary waves. *J. Funct. Anal.*, 255(5):1191–1224, 2008. Cited on 26

[49] Wilhelm Magnus and Stanley Winkler. *Hill's equation*. Dover Publications, Inc., New York, 1979. Corrected reprint of the 1966 edition. Cited on 12, 27

[50] John W. McLean. Instabilities of finite-amplitude gravity waves on water of finite depth. *J. Fluid Mech.*, 114:331–341, 1982. Cited on 91

[51] S. Mingaleev, P. Christiansen, Y. Gaididei, M. Johannson, and K. Rasmussen. Models for energy and charge transport and storage in biomolecules. *J. Biol. Phys.*, 25:41–63, 1999. Cited on 24

[52] Daulet Moldabayev, Henrik Kalisch, and Denys Dutykh. The Whitham equation as a model for surface water waves. *Phys. D*, 309:99–107, 2015. Cited on 88

[53] Diego Noja, Dmitry Pelinovsky, and Gaukhar Shaikhova. Bifurcations and stability of standing waves in the nonlinear Schrödinger equation on the tadpole graph. *Nonlinearity*, 28(7):2343–2378, 2015. Cited on 62

[54] A. K. Pandey. Comparison of modulational instabilities in full-dispersion shallow water models. *ArXiv e-prints*, August 2017. Cited on 88, 90

[55] M. Reed and B. Simon. *Analysis of operators*. Methods of Modern Mathematical Physics. Academic Press, 1978. Cited on 52, 62

[56] Michael Reed and Barry Simon. *Methods of modern mathematical physics. IV. Analysis of operators*. Academic Press [Harcourt Brace Jovanovich, Publishers], New York-London, 1978. Cited on 105

[57] Filippo Remonato and Henrik Kalisch. Numerical bifurcation for the capillary Whitham equation. *Phys. D*, 343:51–62, 2017. Cited on 87

[58] Luz Roncal and Pablo Raúl Stinga. Fractional laplacian on the torus. *Commun. Comtemp. Math.*, 2015. DOI: 10.1142/S0219199715500339. Cited on 64

[59] G. Rowlands. On the stability of solutions of the Non-linear Schrödinger equation. *IMA J Appl Math*, 1974. Cited on 25

[60] Nathan Sanford, Keri Kodama, John D. Carter, and Henrik Kalisch. Stability of traveling wave solutions to the whitham equation. *Physics Letters A*, 378(3031):2100 – 2107, 2014. Cited on 15, 87, 142

[61] Catherine Sulem and Pierre-Louis Sulem. *The nonlinear Schrödinger equation*, volume 139 of *Applied Mathematical Sciences*. Springer-Verlag, New York, 1999. Self-focusing and wave collapse. Cited on 24, 27

[62] Thomas L. Szabo. Time domain wave equations for lossy media obeying a frequency power law. *The Journal of the Acoustical Society of America*, 96(1):491–500, 1994. Cited on 24

[63] Gerald Teschl. *Ordinary differential equations and dynamical systems*, volume 140 of *Graduate Studies in Mathematics*. American Mathematical Society, Providence, RI, 2012. Cited on 12

[64] Michael I. Weinstein. Modulational stability of ground states of nonlinear Schrödinger equations. *SIAM J. Math. Anal.*, 16(3):472–491, 1985. Cited on 24

[65] Michael I. Weinstein. Lyapunov stability of ground states of nonlinear dispersive evolution equations. *Comm. Pure Appl. Math.*, 39(1):51–67, 1986. Cited on 24, 26

[66] G. B. Whitham. *Linear and nonlinear waves*. Wiley-Interscience [John Wiley & Sons], New York-London-Sydney, 1974. Pure and Applied Mathematics. Cited on 13, 14, 15, 87

[67] Haruo Yoshida. Construction of higher order symplectic integrators. *Phys. Lett. A*, 150(5-7):262–268, 1990. Cited on 109, 151